Th-PM-Sym-1

FORCES FOR A BETTER PHYSICS OF BIO-MOLECULAR ORGANIZATION
Adrian Parsegian, National Institutes of Health, Bethesda, MD 20892 and Princeton University, Princeton, NJ 08544-0708

Imagine. With all the frenetic theorizing and speculating on macromolecular folding, packing and dynamics, people are still largely using ideas of physical forces from the 1940's and '50's. Yet these assumed forces look very little or not at all like those that have been measured over the past fifteen years. With the recently reported direct measurement of forces between polysaccharide molecules (Science 249:1278, '90), we now have good information on all four major categories of bio-materials: saccharides, proteins, lipids, nucleic acids. Hydration of the molecular surface insistently appears to be the dominant and generally neglected feature of molecular interaction at those distances, <20 Angstroms, where molecules get serious with each other.

So what? For example, consider Hemoglobin with its famous cooperativity in oxygen binding, a phenomenon that has motivated virtuoso achievements in structure determination as well as a non-convergent series of speculative models. Osmotic stress measurements show that some 70 water molecules come on to the Hb tetramer when it goes from its "T" deoxy to its "R" oxy form (Colombo, Rau, & Parsegian, this meeting). One might think of the replacement of a "salt bridge" between monomers in the Tight or Tense state by waters of solvation around charged groups. The pull toward a link of a bridge is opposite to the spreading stress that goes with solvation. Given force-measurement information on the energy of solvation, one can think then of enormous changes in lateral stress on the surface of the molecule. It appears that the energies involved can be large enough to effect the packing changes at heme groups thought to increase the binding energy of oxygen to Relaxed Hb.

Similar ideas are being developed for other materials where the power of measured forces is finally being recognized.

Th-PM-Sym-2

THE ROLE OF TRANSMEMBRANE HELICES IN MEMBRANE PROTEIN FOLDING AND OLIGOMERIZATION.
Authors: D.M. Engelman, A.T. Brunger, J.M. Flanagan, J.F. Hunt, T.W. Kahn, M.A. Lemmon, H. Treutlein, Department of Molecular Biophysics and Biochemistry, Yale University.

Transmembrane helices appear to be present in many membrane proteins, and their side-to-side interactions are a major factor in the folding and stability of bacteriorhodopsin and photosynthetic reaction centers. Interestingly, the helices are well predicted from predominant hydrophobicity of regions in the amino acid sequence of a protein, suggesting that they may be stable as individual entities. It follows that a folded protein having many spans of the bilayer can often be well described as a set of independently stable helices in the membrane, permitting a separation of energy terms dictating helix formation from those driving association of helices. The result may be a great simplification in understanding membrane protein folding.

Studies with bacteriorhodopsin show that many of the helices are, in fact, stable as independent entities and that the molecule can be assembled from several fragments, for example from Helix A plus Helix B plus a fragment containing the remaining five helices. This observation provides a test for the idea of separable energy terms, but also suggests a role for helix-helix interactions in oligomerization.

Glycophorin is a dimeric protein in the erythrocyte membrane, and the stability of the dimer is largely due to the interactions of the transmembrane helices. We have devised a chimeric protein construct of the transmembrane helix fused with staphylococcal nuclease to study the interactions. Random mutagenesis of single sites clearly suggests a surface for helix-helix interactions. Theoretical studies using molecular dynamics approaches show that the same surface would be near an energy minimum in a coiled coil conformation. Therefore, we are nearing a point at which the idea of two separable stages in folding and oligomerization is supported by experimental data and the simplest case of a parallel dimer of helices may be understood in theoretical energetic terms. In the future, it may prove possible to predict oligomeric associations and folding.

Th-PM-Sym-3

PROTEIN GLYCOSYLATION IN THE ENDOPLASMIC RETICULUM, W. J. Lennarz, Dept. of Biochemistry and Cell Biology, State University of New York at Stony Brook, Stony Brook, NY 11794-5215.

The synthesis of N-linked glycoproteins is a complex, multi-step process that involves passage of nascent polypeptide chains through the lipid bilayer of the endoplasmic reticulum, as well as N-glycosylation of these chains. The N-glycosylation process itself involves multiple steps. It is initiated in the cytoplasm where sugar nucleotides are assembled; subsequently a series of glycosyl transferase-mediated reactions occur on or within the membrane of the endoplasmic reticulum. In these steps sugar residues are added sequentially to dolichyl phosphate, culminating in formation of $Glc_3Man_9GlcNAc_2$-PP-dolichol. Near or at the lumenal face of the membrane of the endoplasmic reticulum this oligosaccharide chain is transferred to an Asn residue contained within the sequence -Asn-X-Ser/Thr- in the growing polypeptide chain. The existence of this sequential assembly process raises a number of interesting questions about 1.) the topology and the potential transmembrane movement of the various dolichyl-linked intermediates and 2.) the properties and organization of oligosaccharyl transferase, the enzyme that catalyzes the transfer to the polypeptide. These questions will be the subject of this talk. Supported by NIH grant GM33184.

Th-PM-Sym-4

CELL SIGNALLING AND THE METABOLISM OF MEMBRANE LIPIDS IN BACTERIAL SYSTEMS. Eugene P. Kennedy, Dept. of Biol. Chem. and Mol. Pharmacol., Harvard Medical School, Boston MA 02115.

The turnover of membrane phospholipids in the enteric bacteria and in the Rhizobiaceae is linked to the transfer of their polar head groups to the periplasmic glucans, including the membrane-derived oligosaccharides (MDO) of Escherichia coli and the cyclic glucans of the Rhizobiaceae. The periplasmic glucans are cell-signalling substances that play an important but poorly understood role in osmotic adaptation and in the case of species of Rhizobium, interaction with specific plant hosts leading to symbiotic nitrogen fixation, a process of great biological and economic importance. The function of membrane lipids in these Gram-negative bacteria offers a striking parallel to the similar roles of inositol phosphatides and other phospholipids in animal cells.

Evidence that the biosynthesis of MDO in E. coli requires not only a suprising function of acyl carrier protein, but also polyprenyl-P will be presented, as well as current work on mechanisms of osmotic regulation of MDO biosynthesis and on its genetic regulation. Levels of enzymes of MDO biosynthesis have been found to be little affected by the osmolarity of the growth medium; their activity appears to be autonomously regulated by the ionic strength of the cytosol, consistent with a model of a hierarchy of osmotic regulation in which other systems detect and respond to the level of MDO in the periplasm.

Th-PM-A1

CAN A SINGLE KINESIN *HEAD* DRIVE MICROTUBULE MOVEMENT?

Bruce J. Schnapp*, Steven M. Block+§, Lawrence S.B. Goldstein+, Russell J. Stewart+ and Christopher P. Godek*. *Department of Physiology, Boston University Medical School, Boston MA 02192; +Department of Cellular and Developmental Biology, Harvard University, Cambridge MA 02138; §Rowland Institute for Science, Cambridge MA 02142.

Single molecules of kinesin can drive microtubule gliding (Howard, *et al.*, ***Nature*** 342:154-158, 1989) or bead movement along microtubules (Block *et al.*, ***Nature***, *in press*). Although native kinesin has two globular heads, a chimeric form of kinesin, consisting of a single globular head (comprising ~450 amino acids of the amino-terminal domain of *Drosophila* kinesin) fused to a spectrin tail (comprising a 1280 amino-acid sequence of *Drosophila* α-spectrin) was recently expressed in *E. Coli* and shown to drive microtubule gliding *in vitro* (Yang, *et al.*, ***Science*** 249:42-47, 1990). It is likely that the construct generates a single-headed species. We examined the ability of this protein to drive microtubule gliding at limiting dilutions, below which no movement is seen. Under these conditions, microtubules attach at single points to a glass surface coated with chimeric kinesin molecules and are driven through a fraction of their own length, usually until the trailing edge of the microtubule reaches the point of attachment, whereupon the microtubule dissociates from the surface. This result is identical to that seen with two-headed bovine brain kinesin (Howard, *et al.* ,1989), and to two-headed squid kinesin. In a quantitative analysis, histogram plots of the number of microtubules moving through a given fraction, *L*, of their length, are essentially flat for $L<1$, consistent with movement driven by single "units." The histogram shape is diagnostic of the numbers of such units: if two molecules are required to bind independently along the microtubule, one expects a straight line decreasing to 0 as *L* goes to 1; for *n* such molecules, one expects a monotonically decreasing polynomial of degree (*n*-1). For purified squid optic lobe kinesin, the limiting dilution occurs at a surface density of less than ten molecules/μm²; while for single-headed chimeric kinesin, it occurs at several hundred molecules/μm². Otherwise, the behavior of the two preparations was identical. This difference may lie in the relative purity, stability, or surface-binding characteristics of the respective preparations. Our results may be explained by single kinesin heads acting independently to drive the movement, but our analysis cannot yet rigorously exclude the possibility that the movement was generated by aggregates of two or more heads at discrete, unitary loci, thereby mimicing the action of a double-headed molecule.

Th-PM-A2

KINESIN-MICROTUBULE SYSTEM: A MECHANISTIC STUDY. Annamma Sadhu and Edwin W. Taylor. Dept. of Molecular Genetics and Cell Biology, University of Chicago, Chicago, Illinois 60637.

Kinesin was isolated from bovine brain by modification of the method of Kuznetsov and Gelfand (PNAS 83, 8530, 1986) including a microtubule binding step in the presence of AMPPNP or tripolyphosphate. The composition was approximately one heavy chain (116 kDa) to one lighter chain (LC-1, 68 kDa plus LC-2, 60 kDa). The kinesin bound one mole of nucleotide per heavy chain and gave a phosphate burst approaching one mole per mole as shown previously by Hackney et al. [J. Biol. Chem. 264, 15943 (1989)]. The rate of dissociation of methyl anthraniloyl ADP (MAND) measured by a 30% change in fluorescence was approximately equal to the steady state rate of hydrolysis. The rate constant of nucleotide dissociation was increased at least 40-fold by the binding of microtubules. The association constant of kinesin with microtubules in the presence of nucleotides varied in the order ATP ≤ ADP < no nucleotide ≤ AMPPNP. The microtubule activation of the ATPase was at least 300 fold, V_{max} = 1 S^{-1} and K_M for ATP = 5 μM (20°C). AMPPNP appears to be a competitive inhibitor of the ATPase (K_i = 50 nM) over a moderate range of concentrations, but the rate did not approach zero at high AMPPNP concentrations. The kinesin prepared by the standard procedure is heterogeneous. In the presence of ATP about 20-30% of the kinesin is bound to microtubules at infinite microtubule concentrations when prepared by an AMPPNP-microtubule binding step while 50-60% is bound when prepared using a tripolyphosphate-microtubule binding step. The kinesin which was competent to bind to microtubules in the presence of ATP was essentially completely bound in a second binding experiment. The competent fraction was both depleted in light chains (LC/HC approximately 0.5 to 0.6) and enriched in LC-1 (LC-1/LC-2 approximately 0.5 in initial samples, LC-1/LC-2 ≥ 1 in competent fraction). The kinetic behaviour of the kinesin-microtubule system shows similarities to the myosin-actin system.

Th-PM-A3

PHOTOLYSIS OF CAGED ATP INITIATES DYNEIN-MEDIATED TRANSLOCATION OF MICROTUBULES.
M.G. Bell*, K. Barkalow+, T. Hamasaki+, and P. Satir+, Intro. by Y.E. Goldman, *Dept. of Biochemistry and Biophysics, University of Pennsylvania, and +Dept. of Anatomy and Structural Biology, Albert Einstein College of Medicine.

We have photolyzed caged ATP (C-ATP) to initiate the active translocation of taxol-stabilized microtubules of bovine brain over a glass slide coated with 22S dynein from *Paramecium*. Translocation was observed with a SIT camera under dark-field illumination. C-ATP (5 mM initially) was photolyzed by 350 nm light from a xenon flash lamp which was focused through the microscope's epifluorescence port.

During control experiments in which ATP was perfused into the chamber, 1-2 minutes elapsed before translocation was observed. Activation via flash photolysis of C-ATP in the field of observation pre-empted this delay, eliciting microtubule gliding in less than 1 second after the flash. Observable gliding persisted for as long as 30-40 seconds, at which time ATP was presumably lost to hydrolysis and diffusion.

We were able to test the effects of photolysis with multiple flashes in the same field of view and solution, since each flash could photolyze only a small fraction of the C-ATP in the chamber. Translocation was initiated by repeated flashes and also by subsequent perfusion with ATP buffer, implying that the proteins were not appreciably affected by the 350 nm irradiation, the C-ATP, or its by-products.

Our findings demonstrate the feasibility of experiments which employ caged compounds within these types of motility assays, paving the way for further exploration into the mechano-chemistry of microtubule-based motility.

Supported by grants from the USPHS and the American Heart Association.

Th-PM-A4

CYCLIC AMP-DEPENDENT PHOSPHORYLATION OF DYNEIN ALPHA-HEAVY CHAINS IN MYTILUS EDULIS SPERM FLAGELLA. R. E. Stephens and G. Prior, Marine Biological Laboratory, Woods Hole, MA.

Because Mytilus edulis sperm are reported to be serotonin-activated, we investigated whether dynein is phosphorylated via cAMP. Sperm, released from minced ripe testes, were decapitated by homogenization. Flagella were recovered by differential centrifugation, permeabilized with 0.012% NP-40, and then incubated with γ-^{32}-P-labeled ATP, either with or without added cAMP. The reaction was stopped and the membranes were removed by extraction with 0.25% NP-40. Outer arm dynein was produced by extracting the 9+2 axonemes with 0.6 M NaCl at pH 7 for 15 minutes on ice, while inner arm dynein was obtained by a second extraction with 0.6 M NaCl containing 0.25% NP-40. The former showed a 2-3-fold NP-40-activated latency and, at lowered ionic strength, rebound with high efficiency to axonemes stripped of dynein by high salt plus detergent. The dynein fractions were analyzed by SDS-PAGE, autoradiography, and sucrose gradient centrifugation. Each fraction represented >45% of the total ATPase, measured after detergent activation, and contained a proportionate amount of dynein heavy chains. The dynein sedimented at 18-21S and consisted of equimolar α and β heavy chains, intermediate chains of 95 kDa and 80 kDa, and 2-3 light chains. Accounting for most of the total 9+2 phosphorylation, the α heavy chains of both the outer and the inner dynein arm fractions were labeled to a level of 1 phosphate per chain. The phosphorylation was rapid, highly stable, and Ca^{++}-independent, maximizing at cAMP levels >1 μM. Cyclic GMP was effective at >10-fold higher levels. Neither the K_m nor the salt- and pH-profiles of the enzyme was influenced by α heavy chain phosphorylation. Photocleavage at 360 nm in the presence of vanadate and Mg-ATP yielded 250/240 kDa (HUV1 α/β) and 200/190 kDa (LUV1 α/β) fragments while photocleavage in the presence of vanadate and Mn^{++} yielded 270/250 kDa (HUV2 α/β) and 180/170 kDa (LUV2 β/α) fragments. Phosphorylation occurred exclusively on the 200 kDa LUV1 and the 270 kDa HUV2 fragments, suggesting that the phosphorylated site is beyond the ATP binding region, toward the C-terminus. Supported by USPHS GM 20,644.

Th-PM-A5

MODELLING MICROTUBULE INTERACTIONS IN THE AXONEME. M.E.J. HOLWILL[1] AND P. SATIR[2].
[1]Physics Department, Kings College, London, and [2]Department of Anatomy and Structural Biology, Albert Einstein College of Medicine, Bronx, N.Y.

Using the considerable body of data available from electron microscopic studies, we have developed a structural representation of the ciliary axoneme as the first stage in the formulation of a computer-generated functional model. Modelling is effected through a Fortran softwave package SURREAL (SURface REndering ALgorithms), which generates a scene of solid, opaque objects, fully shaded and with hidden lines removed, illuminated by a point source at infinity. For comparisons with structural data, models can be viewed from any direction. Axonemal microtubules are built of 4 nm diameter spheres, simplified representations of α- and β-tubulin. Dynein arms, interdoublet links, spokes and the central complex are modelled appropriately at ~ 4 nm resolution. This computer-generated axoneme is the only current model which has a consistent three-dimensional representation of all the major structural features. The model can be used to resolve ambiquities of interpretation of structural detail due to superposition. For example, the model indicates how different structural intepretations of the dynein arms may be reconciled. By modelling the shape of the dynein arms under different conditions, we are able to propose a possible structural cycle for the arms. Since the force generated by an individual arm is known, the first steps in the translation of the structural to the functional model can be taken. The functional model is limited by our lack of information concerning the mechanical properties of the structures (interdoublet links and spokes?) which transform sliding into bending. In an initial study to gather this information, we have examined the influence of the circumferential interdoublet links, spokes and arm activity on disintegration of the axoneme by sliding. Many of the disintegration patterns observed during polarized sliding can be predicted. One conclusion, consistent with experiment, is that link breakage will tend to occur between doublets N and N+1, if the arms on doublet N are inactive, while those on either doublet N-1 or doublet N+1 are active.

Th-PM-A6

A PROPOSAL FOR A NEW TYPE OF POSITIVE COOPERATIVITY IN AXONEMAL MOTION: A STEADY-STATE KINETIC ANALYSIS. C.K. Omoto, Program in Genetics and Cell Biology, Washington State University, Pullman, WA 99164-4234.

Eukaryotic flagellar beat frequency exhibits an unusual positive cooperativity with respect to ATP concentration with Hill coefficient greater than one at the lowest concentration of substrate. One interpretation of this unusual behavior of apparent positive cooperativity in axonemal motion may be a requirement for ATP to bind to each active site in a multimeric dynein in order to produce oscillatory motion. Such an interpretation of beat frequency data prompted the examination of a steady-state kinetic model of dynein that uses multiple active sites. A steady state kinetic model for axonemal motion based upon a 4-state mechanochemical cycle of dynein with two active sites is described. This model analysis determines the steady-state concentrations of enzyme species for specified rate constants, most which are empirically derived, with given substrate and product concentrations. Concentration of enzyme species with both active sites detached from microtubules in the model appears to be proportional to beat frequency and exhibits an apparent positive cooperativity at low substrate concentrations. Furthermore, this correlation between 'Both Detached' enzyme species and beat frequency mimicked experimental observations with a nucleotide analog and with product inhibition.
Supported by NSF grant DCB 8918108.

Th-PM-A7

CALCIUM CONTROL OF SCALLOP SPERM MOTILITY. T. Otter and B.F.C. Galgoci, Dept. of Zoology, Univ. of Vermont, Burlington, VT (Intro. by B.B. Hamrell).

Male sea scallops (*Placopecten magellanicus*) provide an excellent source of sperm flagella for biochemical studies. Near the peak of development, the testis may constitute >30% of total tissue wet weight, yielding (by mincing, filtration, centrifugation) up to 10g of packed sperm (ca. 10^{11} sperm) from a single animal. In the course of our studies on axonemal calcium-binding proteins (CaBPs) that control sperm motility, we have applied biochemical fractionation techniques similar to those developed for sea urchin sperm to obtain excellent yields of highly pure scallop sperm flagella and axonemes. Analyzed on SDS-PAGE gradient gels (4-16% acrylamide, 1-8M urea) the protein composition of the flagella, axonemes, and detergent-soluble membrane+matrix fractions appear virtually invariant from preparation to preparation. The axonemes contain one major CaBP that approximately comigrates with calmodulin. Biochemical characterization of this CaBP is in progress. This CaBP remains associated with axonemes after washing them (by centrifugation) with buffer containing 1mM EGTA (pH 8.0), suggesting that it is bound to the axoneme in a Ca^{2+}-independent manner. When scallop sperm are extracted with Triton X-100 (0.04%; 4°C) in the presence of Ca^{2+} (in mM: 2 Ca, 150 KCl, 1 DTT, 0.1 EGTA, 10 Tris-HCl, pH 8) and then reactivated with ATP (in mM: 150 KAcetate, 2 $MgSO_4$, 1 DTT, 20 Tris-HCl, pH 8, 2% PEG, var. Ca, EGTA, EDTA, ATP), the symmetry of flagellar beat depends on the pCa of the reactivation buffer. [Ca^{2+}] less than about 100nM induces symmetric beat, while increasing [Ca^{2+}] to 1μM or above progressively increases the asymmetry of flagellar bending, independent of the [ATP] in the range of 2 -20μM ATP. Thus, the motility of scallop sperm flagella in vivo is apparently controlled by intraflagellar calcium, perhaps via the tightly-bound axonemal calmodulin. Supported by NSF DCB 8812081 (T.O.) and the L.P. Markey Charitable Trust.

Th-PM-A8

MEASURING THE ISOMETRIC FORCE OF SINGLE KINESIN MOLECULES USING THE LASER OPTICAL TRAP

Scot C. Kuo and Michael P. Sheetz
Department of Cell Biology, Box 3709, Duke University Medical Center, Durham, NC 27710

Microtubules can be translocated by a single kinesin molecule (Howard *et al.*, 1989 *Nature 342*, 154) when limiting dilutions of kinesin is adsorbed to glass in the presence of carrier proteins. By attaching latex beads as "handles" to translocating microtubules, we can reversibly stop the movement of these microtubules by a single-beam optical trap, also called laser tweezers. The optical trap uses the radiation pressure of near-infrared laser illumination to trap microscopic particles (Ashkin *et al.*, 1987 *Science 235*, 1517; *Nature 330*, 769). The force of the optical trap was calibrated by viscous drag on latex beads and the trapping force is linear with the amount of laser illumination. Preliminary measurements indicate that the maximum force (i.e. isometric force) of a single kinesin attachment site is between 2.0 and 2.3 piconewtons (10^{-7} dyne). Stalling kinesin with the laser tweezers is reversible; when trapping forces are decreased, microtubule translocation resumes. Further measurements are required for statistical analysis and would determine the cooperativity, if present, of force generation as additional kinesin molecules drive the same microtubule filament. A videotape demonstrating the technique will be shown.

Th-PM-B1

MOLECULAR DYNAMICS STUDIES OF A SELF-SPLICING RNA AND SOME NUCLEOTIDE FRAGMENTS

Lennart Nilsson, Arne Elofsson, Jan Norberg, Department of medical biophysics, Karolinska Institutet, S-104 01 STOCKHOLM, Sweden, Agneta Åhgren-Stålhandske, Ann-Sofie Sjögren, Solveig Hahne and Britt-Marie Sjöberg, Department of molecular biology, University of Stockholm, S-106 91 STOCKHOLM, Sweden.

The active site of the self splicing intron in the bacteriophage T4 *nrdB* messenger RNA has been modelled[1] on a graphics workstation on the basis of suggested 3-D[2] arrangement of the *Tetrahymena* intervening sequence. This structure was then subjected to energy minimization and molecular dynamics simulation to relax tensions. In this process the energy decreased considerably, and gave a final structure that deviated by 3Å root mean square from the model built initial structure. The cofactor guanosine was docked to a proposed[3] binding site where it was found to fit well; a minor modification of the proposed binding mode easily brought the 03'-end of the guanosine within 2Å of the phosphodiester bond where the primary cleavage in this group 1A intron occurs. Results from a series of force field test calculations on nucleotides and nucleotide fragments will also be presented.

[1] Nilsson, L. *et al.* (1990) Biochemistry, in press.
[2] Kim, S.H. & Cech, T.R. (1987) Proc. Natl. Acad. Sci. USA 84, 8788.
[3] Michel, F. *et al.* (1989) Nature 342, 391.

Th-PM-B2

Determination of the Stereoselective Binding of Peptide Inhibitors to the HIV-1 Protease

David M. Ferguson, Randall J. Radmer, and Peter A. Kollman
(Intro. by Fred E. Cohen)
University of California, San Francisco

The HIV-1 protease is a prime target for drug design. The enzyme is required to cleave specific amide bonds of a peptide precursor to form proteins that are essential to viral infection and activity (Krausslich and Wimmer *Ann. Rev. Biochem., 57,* 701, 1988). The protein is an aspartyl protease, containing two catalytic aspartates intimately involved in the hydrolytic cleavage of the peptide. Transition-state analogs that mimic the tetrahedral intermediate of hydrolysis have been used as inhibitors of the protease. Recently, an inhibitor was reported (Rich *et al. J. Med. Chem., 33,* 1285, 1990) that effectively bound the HIV protease with impressive efficacy. The hydroxyethylamine inhibitor described contains a chiral center to which a crucial hydroxyl group is connected, however, the preferred stereo-isomer (R or S-hydroxyl) was not determined. Free energy perturbation calculations were performed to predict the free energy difference of binding for the R and S hydroxylethylamine inhibitors. The results were compared to experimental values that were determined independently and showed reasonable agreement. The model was then applied to calculate the relative binding affinity of an inhibitor that did not contain the hydroxyl group that is thought to stabilize the intermediate. This change in the inhibitor was found to decrease the binding affinity, in accord with previous suggestions regarding the optimal structure of HIV-1 inhibitors. Insight was also afforded as to the protonation state of the aspartates directed toward the hydroxyl stereo-center. Our results suggest that the active site is singly protonated at the aspartate that is not interacting with the quaternary amine of the inhibitor.

Th-PM-B3

THE IN SITU DRAMATIC REVERSIBLE MOLECULAR DYNAMICS OF THE TRANSMEMBRANE PROTON-TRANSPORT PROTEIN BACTERIORHODOPSIN.

Nicholas J. Gibson, James E. Draheim and Joseph Y. Cassim, Department of Microbiology and Program in Biophysics, The Ohio State University, Columbus, OH 43210.

The bacteriorhodopsin is a chromoprotein with a Schiff-base bound retinylidine prosthetic group. It is presently the best-characterized example of a membrane protein and considered by many to be the paradigm of transmembrane transport proteins. It is the sole protein in the purple membrane, consisting of a single 26,866-D, 80% α-helical-20% aperiodic polypeptide chain. The purple membrane functions as a light-driven proton pump in the photosynthesis of the *Halobacterium halobium*. The α-helix of the bacteriorhodopsin contains equally on the average both α_I and α_{II} structural characteristics.

In situ in the purple membrane the bacteriorhodopsin is enfolded into the membrane bilayer forming seven transmembrane helical segments oriented parallel to the membrane normal. The molecular dynamics of the bacteriorhodopsin can be studied by determination of the changes of the net segmental tilt angle (the angle between the segments and the membrane normal) in response to structural perturbations of the purple membrane.

The reversible process of light bleaching of the purple membrane in the presence of hydroxylamine results in the hydrolysis of the Schiff-base bond of the bacteriorhodopsin and the formation of retinaloxime. Two independent spectral methods, oriented far ultraviolet circular dichroism and mid-infrared linear dichroism, have shown that this process also results in a net change in this tilt angle from 0° to 20-24° with no change in the protein secondary structure. This bleach-induced reversible tilt angle change can be further enhanced up to 34-35° again with no change in the protein secondary structure with dimethyl adipimidate cross-linking or papain digestion of the purple membrane which by themselves do not alter the native segmental orientations.

These results pose an intriguing question: Is this dramatic molecular dynamics of the bacteriorhodopsin a unique characteristic solely of the bacteriorhodopsin or an inherent characteristic of transmembrane transport proteins in general?

Th-PM-B4

STRUCTURE ELUCIDATION OF SELECTED GENE PROMOTER REGION OLIGONUCLEOTIDE SEQUENCES USING NMR-BASED DISTANCE AND TORSION ANGLE RESTRAINTS WITH MOLECULAR DYNAMICS

Schmitz U., Sethson I., and James T.L.
Department of Pharmaceutical Chemistry
University of California, San Francisco, CA 94143-0446

Solution structures of DNA oligomers $[d(GTATATAC)]_2$ and d(GTATAATG)·d(CATATTAC) were determined by restrained molecular dynamics (AMBER) utilizing interproton distance restraints obtained from 2D NOE experiments. Accurate upper and lower bounds distance restraints were calculated with the complete relaxation matrix analysis program MARDIGRAS[1] on the basis of different NOE datasets. For $[d(GTATATAC)]_2$ convergent structures were obtained from three starting models (A-, B-, and wrinkled D-DNA), where two of them were very similar. The similarities among the rMD structures were independent of starting models. The NMR spectra of both oligomers showed evidence of dynamic processes including limited conformational averaging. Comparison of several rMD structures obtained from the same starting model showed different degrees of randomization for some of the structural parameters, suggesting conformational flexibility in terminal residues and some sugar moieties. Independent analysis[2] of sugar pucker in $[d(GTATATAC)]_2$ on the basis DQF-COSY coupling constants was in agreement with deoxyribose conformation obtained using restrained molecular dynamics despite some conformational flexibility.
Interstrand distance restraints were found to be extremely important in defining helical parameters accurately.

(1) Borgias B.A. and James T.L., *J. Magn. Reson.*, 87, 475 (1990)
(2) Schmitz U., Zon G., and James T.L., *Biochemistry*, 29, 2357 (1990)

Th-PM-B5

GLOBAL ANALYSIS OF TWO-DIMENSIONAL NMR SPECTRA OF POLYPEPTIDES. Yuan Xu, Istvan P. Sugar. Departments of Biomathematical Sciences and Physiology & Biophysics, Mount Sinai Medical Center, New York, N.Y. 10029

Nuclear Overhauser Enhancement Spectroscopy (NOESY) is the most powerful way to determine the structure of biological macromolecules in solution. In this work a global analysis of the NOESY spectra of polypeptides has been developed, comparing computer simulated spectra with entire experimental spectra taken at different mixing times. To calculate the NOESY spectra, the full matrix method has been applied without assuming low or high field approximations. The calculated spectrum has been fitted to the experimental one in the following four steps: i) determination of the proton distance constraints from the experimental NOESY spectrum; ii) calculation of a rough three-dimensional molecular structure by applying a distance geometry algorithm (DISGEO); iii) refinement of the three-dimensional molecular structure by systematically changing the dihedral angles of the molecule; iv) adjustment of the correlation time of the overall tumbling motion of the molecule. The method of the analysis has been demonstrated on the NOESY spectrum of the proline pentapeptide.

Th-PM-B6

USE OF DISULFIDE BOND FORMATION TO DETECT PROTEIN BACKBONE MOTIONS. Claire L. Careaga and Joseph J. Falke, Department of Chemistry and Biochemistry, University of Colorado, Boulder CO 80309-0215

All proteins are constantly undergoing thermally induced structural fluctuations about an average structure. Ligand induced conformational changes require concerted thermal fluctuations. Thus, understanding internal motions on a biologically relevant timescale is central to the understanding of protein function.

The relative motions of two alpha helices in the *E. coli* galactose and glucose receptor, GGR, ± D-glucose have been investigated using disulfide bond formation to detect contact between two cysteine residues that collide during a motion. Using oligonucleotide directed mutagenesis, a series of di-cysteine substitutions have been engineered into GGR. One helix is engineered to contain a fixed cysteine, the other helix is engineered to contain a second cysteine at varying distances from the fixed site. The cysteine positions chosen are on the surface (from the 1.9Å crystal structure determined by F. Quiocho et.al.) and are not conserved in the homologous periplasmic binding proteins. The substituted proteins are tested for retention of native structure by determining the glucose KD, $\tau 1/2$ for terbium dissociation from the Ca(II) site, $\Delta\Delta Gu$ for unfolding in urea and chemical shifts of the 5-fluorotryptophan labeled receptors.

Known structures of disulfide bonds in proteins indicate that backbone motions must occur for disulfide bond formation between two cysteine residues whose alpha carbons are >7.4Å apart. The alpha carbon distances between the two engineered cysteine residues are 9.5Å, 12.5Å, and 19.5Å for GGR Q26C / K263C, Q26C / D267C, and Q26C / D274C respectively. Therefore, backbone fluctuations must occur to bring the thiols into proximity for the copper phenanthroline catalyzed disulfide bond to form. Chemical environment of the thiol, side chain torsion angles, pH and temperature also contribute to reactivity.

All of the di-cysteine mutants show significant rates of disulfide bond formation (+) glucose at 37°C on the second to minute timescale. The highest amplitude motion detected is 19.5-7.4=12.1Å, assuming that this collision is not caused by a partial or complete unfolding of the protein. Each of the measured disulfide reaction rates gives a lower limit for the frequency of that backbone motion. The rates of disulfide bond formaiton were significantly greater in the unliganded than in the liganded receptors. Kinetics of disulfide bond formation and the interpretation of these results will be discussed.

Th-PM-B7

CROSS RELAXATION AND THE SOURCE OF TISSUE-SPECIFIC CONTRAST IN MAGNETIC RESONANCE IMAGING (MRI) Seymour H. Koenig, IBM T. J. Watson Research Center, Yorktown Heights, NY 10598, USA;

The clinical success of MRI relates to the existence of tissue-specific values of the nuclear magnetic relaxation rates $1/T_1$ and $1/T_2$ of the protons of mobile water molecules of tissue. Evidence is accumulating that the majority of this relaxation arises from cross relaxation: transfer of magnetization across the multitude of macromolecular-water interfaces in the cells of tissue. We argue that transfer is between protons of water molecules hydrogen bonded at the interface to protons within a depth ~10 Å below the surface. The lifetime of the hydrogen bonds, $\sim 10^{-10}$ s, is the correlation time for the interaction. The efficacy of the transfer relates to the temperature and field dependent values of $1/T_1$ of the macromolecular protons, namely, how good a magnetization sink they are. This conveys a field dependence to $1/T_1$ of tissue even when the field (Larmor frequency) is less than the of the correlation time for the cross-relaxation interaction. As a rule, the heavier the proteins, the more rigid the membranes, and the lower the temperature or field, the better the sink. By applying these ideas – developed from a reexamination of published data on the field and temperature dependence of $1/T_1$ of tissue and protein solutions – it is possible to: predict the functional form of the field dependence of $1/T_1$ of tissue as a fixed temperature from the temperature dependence at a fixed field; account for the unique contribution of myelin to $1/T_1$ of white matter; and explain why the ratio T_1/T_2 of most tissues at typical imaging fields is about the same (~10). In a broad sense, it is the dynamics of the surface layers of macromolecular structures of tissue that is the major determinant of the appearance of a tissue in MRI.

Th-PM-B8

TIME RESOLVED CIRCULAR DICHROISM STUDIES OF BIOLOGICAL SYSTEMS

John D. Simon, Xiaoliang Xie and Robert Dunn, Department of Chemistry, University of California at San Diego, La Jolla, California 92093-0341

This paper examines new experimental approaches for studying ultrafast relaxation processes in biological systems -- picosecond time resolved circular dichroism and magnetic circular dichroism spectroscopy. The technical details and optical theory of the experimental apparatus will be discussed. Extension of this approach to femtosecond time resolution will also be examined.

Applications of this technique to both photodissociation reactions of heme proteins and photosynthetic reaction centers will be presented. In particular, time resolved circular dichroism and magnetic circular dichroism studies of the photodissociation of CO from carbonmonoxymyoglobin reveal a protein relaxation process which occurs on the hundred picosecond time scale. This process is attributed to the structural rearrangement of the protein matrix in the vicinity of the heme ring following bond cleavage. The time dependent magnetic circular dichroism data suggest that the spin state change of the coordinated iron occurs in less than 20 picoseconds.

This new transient spectroscopy has also been used to examine the evolution of the CD spectrum of the monomer bacteriochlorophyll during the initial electron transfer events in photosynthetic bacterial reaction centers. The CD spectrum is found to be insensitive to the first two step of the charge separation process. In addition, the transient CD spectrum is not conservative, arguing that it does not arise from excitonic interactions between the pigments. The transient spectrum enable the absolute assignment of the high energy exciton band of the special pair of bacteriochlorophylls.

This work is supported by the National Institute of Health, Grant GM-41942.

Th-PM-C1

REVERSIBLE MONOVALENT CATION DEPENDENT TRANSITION BETWEEN THE QUADRUPLEX AND WATSON-CRICK HAIRPIN FORMS OF d(CGC G_3 GCG). Charles C. Hardin *, Thomas Watson, Matthew Corregan and Charles Bailey, Department of Biochemistry, North Carolina State University, Raleigh, NC 27695.

The DNA molecule d(CGC G_3 GCG) can potentially form either : i) a Watson-Crick (WC) hairpin that has a stem containing three C-G base pairs and a loop composed of three guanine residues, ii) an antiparallel four-stranded 'quadruplex' containing three G-G base paired guanine 'quartet' assemblies and four sets of duplex stems composed of three C-G base pairs, or iii) a quadruplex structure, in which the strands are in a parallel configuration, containing four contiguous G-quartets flanked by cytidine residues then two additional G-quartets. Based on circular dichroism (CD) results, it was concluded that a peak at 264 nm can be used to monitor the quadruplex complex and a peak at 286 nm represents the hairpin species. It was found that the quadruplex is stable in the presence of 40 mM K^+ and can be kinetically trapped as a metastable form when prepared at high DNA concentration then diluted into buffer containing 40 mM Na^+. However, when the temperature is raised above *ca.* 60°, the quadruplex is converted to the WC hairpin. Since the quadruplex is composed of four strands, the single-strand to quadruplex equilibrium should be strongly dependent on the DNA concentration. It was found that the concentration of K^+ required to convert the WC hairpin to the quadruplex decreases dramatically as the DNA concentration is increased. CD and imino proton NMR results verified the assignment of the 264 nm and 286 nm CD bands to quadruplex and WC hairpin species, respectively. The NMR results indicate that the parallel-stranded quadruplex is adopted. It was found that cations stabilize the quadruplex in the order : $K^+ > Ca^{2+} > Na^+ > Mg^{2+} > Li^+$, indicating that both ionic radius and charge affect the extent of stabilization induced by the ion. In contrast, the stability of the WC hairpin conformation is essentially independent of the type of cation. The effect of pH on the WC hairpin and quadruplex structures was assessed by CD. These results showed that both structures are deprotonated with a pK_a of *ca.* 8.8, resulting in destabilization. However, the quadruplex is very different from the WC hairpin in having a second pK_a of *ca.* 6.7.

Th-PM-C2

STRUCTURAL STUDIES ON DNA HAIRPINS IN SOLUTION, Goutam Gupta and Angel E. Garcia, Theoretical Biology and Biophysics Group, T-10, MS K710, Los Alamos National Laboratory, Los Alamos 87545

Solution NMR and theoretical studies reveal that introduction of mismatched (A.C, G.T, or T.T) pairs in a self-complementary DNA duplex results in the mismatched duplex⇐⇒hairpin equilibrium. The nature of this equilibrium depends upon the type of the mismatch and the solution conditions (i.e., DNA concentration, salt, temperature, etc.) A DNA oligomer under appropriate solution conditions can display either the hairpin or the mismatched duplex conformation. Therefore, NOESY experiments at various mixing times under such conditions, allow determination of a set of average inter-proton distances characteristic of the hairpin or the mismatched duplex for a given oligomer. Energetically stable structures of the hairpin or the mismatched duplex for a given oligomer are, then, derived using inter-proton distances as structural constraints. Stability and biological implications of these structures will be discussed.

Th-PM-C3

THE STRUCTURE OF DNA IN CANINE PARVOVIRUS. Michael S. Chapman, Jun Tsao, Mavis Agbandje, Hao Wu, Walter Keller, Kathy Smith and Michael G. Rossmann

Canine parvovirus (CPV) is a single-stranded DNA icosahedral virus which has an external diameter of around 260 Å. Its total molecular weight is about 6×10^6 D of which about 1×10^6 D represents DNA. The genome contains are 5124 bases and codes for the capsid protein and one or possibly two non-structural proteins.

The three-dimensional structure of CPV has been solved to 3.2 Å resolution by X-ray crystallographic methods. The structure of DNA can be seen where it conforms to the 60-fold icosahedral symmetry of the protein shell. The symmetry equivalent oligonucleotides, each being composed of up to 11 nucleotides, together represent about 13% of the total genome. The built DNA structure conforms with allowed conformational angles, van der Waal contacts and the observed electron density. It contains ribose rings in both C_2-*endo* and C_3-*endo* conformations. Each of the 60 oligonucleotides consists of a seven-residue loop nestled in a pocket on the internal surface of the protein shell.

On the 3' side of the loop, four bases are stacked in a manner reminiscent of other nucleic acid structures. Surprisingly, within this stacking interaction, nucleotides #8 and #10 are neighbors because nucleotide 9 is "flipped" so that its base points in the opposite direction to those that are stacked. This "flipped" base joins another stacking interaction involving a protein phenylalanine and nucleotide #3, the first of the loop. Two metal ions, chelated between DNA phosphates, also help to stabilize the loop. One lies at the center of the seven-nucleotide loop. Four of the phosphates lie in a plane, chelating to the central metal ion. An asparagine forms a fifth ligand. The second has just two phosphate ligands from the beginning and end of the loop.

No base pairing is observed, but rather bases point outwards toward the internal pocket of the protein. There are only a few protein-DNA hydrogen bonds. Presumably van der Waal's contacts are sufficient to endow some sequence specificity. Although the electron density represents the average of 60 oligonucleotides within the genome, at some positions the distinction between purine and pyrimidine is clear. Such specificity may play a role in the selective incorporation of viral nucleic acid within the protein shell, a problem which must be particularly severe for viruses that assemble in the nucleus.

Th-PM-C4

EVIDENCE FOR GENERAL, SEQUENCE-DEPENDENT CURVATURE IN DNA CONTAINING NO POLY A TRACTS: IMPLICATIONS FOR PROTEIN BINDING

Peter T. McNamara and Rodney E. Harrington, *Department of Biochemistry, University of Nevada Reno, Reno, NV 89557 USA*

Sequence-directed DNA curvature is most commonly associated with AA dinucleotides in the form of poly adenine runs. We demonstrate inherent curvature in DNA which lacks poly A regions using the criteria of polyacrylamide gel mobility and circularization probability. Evidence is based upon studies of several 21 bp synthetic DNA fragments designed to exhibit fixed curvature according to wedge angle deflections made to the helical axis by all dinucleotides in the sequences. Wedge deflections are obtained from our recent determination of the full set of 16 DNA wedge angles (A.Bolshoy, P.T.McNamara, R.E.Harrington and E.N.Trifonov, submitted). Repeats of these sequences display anomalously slow migration in polyacrylamide gels typical of curved DNA. Analysis of circular products formed by self-ligation shows substantial inherent curvature compared to (non curved) control sequences. In circularization probability determinations, ligated repeats of these sequences typically form circles as small as 126 bp. In addition, chemical cleavage with hydroxyl radical is consistent with local variation in helical conformation at specific dinucleotide stacks. Results from all these types of study are generally consistent with molecular modelling of the DNA fragments using the calculated wedge angles. Curved DNA is increasingly becoming implicated in the binding of specific proteins associated with transcriptional control and other site-specific processes, and in the formation of large nucleoprotein complexes. Biological implications of the present experimental findings are discussed in terms of specific protein binding sites.

Th-PM-C5

INTRINSIC BENDING OF DNA CONTAINING A_n:T_n BLOCKS. A MONTE CARLO STUDY.

V.B. Zhurkin, N.B. Ulyanov, A.A. Gorin, and R.L. Jernigan
Laboratory of Mathematical Biology, NCI, National Institutes of Health, Bg 10, Rm 4B56, Bethesda, MD 20892 USA

To investigate the influence of thermal fluctuations on the DNA curvature the Metropolis procedure at 300K was applied to decamers A_5T_5, A_5TCTCT, A_5CTCTC, A_5GAGAG, GA_4T_4C and CT_4A_4G. Generalized coordinates of bases and sugar rings were chosen as independent variables (in all, 160 parameters). Geometry of the sugar-phosphate backbone was found using the chain-closure algorithm.

Monte Carlo simulations have confirmed the DNA bending anisotropy, revealed earlier by energy minimization: B-DNA bends in groove directions (roll) more easily than in perpendicular direction (tilt). The A_5T_5 block is more rigid than the other sequences; the *pyr-pur* sequences are found to be the most flexible. For A_5TCTCT, A_5CTCTC and A_5GAGAG the average bending angle per decamer was 20-25°, in agreement with the estimates based on ring closure probabilities. Their bending occurs toward the minor groove in the center of A_5:T_5 block, which is consistent with the *junction* and *wedge AA models*. However, in A_5T_5, GA_4T_4C and CT_4A_4G bending is directed into the grooves at the 5' and 3' ends of purine tracks as in the *pyr-pur model* of DNA bending. Thus, directionality of bending caused by A_n:T_n blocks, strongly depends on the neighboring sequences.

The decamer structures were generated under the periodic boundary conditions, so they could be used to produce longer pieces of DNA (up to 200 bp). Afterwards, the effect of fluctuations on the overall shape of curved DNA fragments was estimated. For sequences withe strong curvature, the static model and Monte Carlo ensemble give similar results; however in the case of moderately and slightly curved sequences (A_5T_5, CT_4A_4G) the two representations are significantly different. This is important for quantitative interpretation of the PAGE-measurements of DNA curvature.

Th-PM-C6

PROBING THE STRUCTURE OF B-Z DNA JUNCTIONS. Stephen A. Winkle, Maria Aloyo, Tatiana Lee-Chee, Department of Chemistry, Florida International University, Miami, FL 33199. David E. Graves, Department of Chemistry, University of Mississippi, Oxford, MS, Richard D. Sheardy, Department of Chemistry, Seton Hall University, South Orange, NJ, 07079.

The structure of the B-Z DNA junctions formed when the following oligonucleotides (or ligated polymers of combinations of these oligomers) were placed in 50 uM cobalt hexamine were examined using nuclease digestion studies:

BZ I 5' CGCGCGCGACTGACTG

BZ III 5' ATCGCGCGCGATCAGTCAGT

(NOTE C* are 5-methyl C; only top strands as shown, proposed BZ Junction bases underlined)
In contrast to the expected and observed inhibition of the restruction endonuclease HhaI (which cuts GCGC), the cleavage of BZIII or polymers of BZ I + III by MboI (cleavage site GATC, at the junction) is enhanced when the (CG) segments are in the Z form relative to cleavage under B conditions. Exonuclease III cleavage is inhibited to either side of the indicated junction. The nuclease Bal 31 also stops at the junctions. These results suggest that the junction differs in structure from either the B or Z segments and suggestions that the junction occupies circa 3 base pairs. Nuclease digestions were also conducted in the presence of ethidium, ethiduim azide, actinomycin D or amentantrone. In cobalt, these agents inhibit cleavage by MboI and alter the cleavage patterns of Bal 31 and exonuclease III. Preferential binding of these drugs to junction regions could account for these results. These studies support previous gel mobility and spectroscopic data suggesting that junctions have an enhanced flexibility relative to surrounding sequences.

Th-PM-C7

GEL MOBILITY, SPECTROSCOPIC, AND ENZYMATIC DIGESTION STUDIES OF A PROTO-B-Z-JUNCTION. Stephen A. Winkle, Maria Aloyo, Tamara Infante, Nelida Morales, Department of Chemistry, Florida International University, Miami, FL and Richard D. Sheardy, Department of Chemistry, Seton Hall University, South Orange, NJ.

Ligation polymers of the oligomer shown below were examined in the absence and presence of 50 uM cobalt hexamine, using gel mobility, nuclease digestion assays and circular dichroism studies. Note that the C's in the potential Z-forming CG segment are NOT methylated. Circular dichroism results indicate that in the presence of 50 uM cobalt, these segments do not flip to a Z-type structure-although there is a structural change. (50 uM cobalt does convert DNAs containing 5-methyl C to the Z-form.) The molecules in this study are cleaved by the endonuclease HhaI (cleavage site GCGC) but this cleavage is inhibited by actinomycin D- further indications of non-Z structure. Cleavage by MboI (site GATC) is enhanced in the presence of cobalt, as was observed in molecules with a B-Z junction and gel mobilities of the ligation products give the same enhancements shown by molecules with B-Z junctions. Cleavage of the potential junction region by Bal 31, Endonuclease III and MboI is affected by the presence of actinomycin D, ethidium and ametantrone - suggesting that these may bind near this region. These results suggest that the underlined region is a proto-junction- a structure different from the flanking sequences (even when the molecule is non-Z) and a structure that could, under appropriate inducements, be transformed to a junction.

TCGACGCGCGCGATCAGTCA

GCGCGCGCTAGTCAGTAGCT

Th-PM-C8

STUDIES OF THE STRUCTURE OF SUPERCOILED AND CATENATED DNA.

S.D. Levene[1], A.V. Vologodskii[2], K. Klenin[2], C. Donohue[1], and N.R. Cozzarelli[1].
[1]Department of Molecular and Cell Biology, University of California, Berkeley and [2]Institute of Molecular Genetics, USSR Academy of Sciences, Moscow, USSR.

Most of the DNA in the cell is supercoiled, and DNA supercoiling is either required for or introduced by a large number of biological processes. A detailed model for the structure of supercoiled DNA in solution has been difficult to obtain, however, because the gross dimensions of supercoiled circular DNAs as measured by many physical techniques are relatively insensitive to changes in parameters that determine the state of supercoiling, namely the linking number deficit. We have studied the coiling of DNA in supercoiled plasmids and in multiply-linked dimeric DNA catenanes. Dimeric DNA catenanes are products of a large class of site-specific recombination reactions involving closed-circular DNA. The complexity of catenane products generated in these reactions is directly related to the structure of supercoils present prior to recombination.

We present studies of the structure of supercoiled and catenated DNA using electron microscopy and site-specific recombination in conjunction with Monte Carlo simulations of polymer models of these topological forms. Extremely good agreement is obtained between the simulation results and experimentally measured parameters such as superhelix dimensions and the distribution of catenane interlinks determined by recombination. We discuss the implications of the results for protein-DNA interactions and the higher-order organization of DNA.

Th-PM-C9

FLUCTUATIONAL BASE PAIR OPENING PROBABILITY PREDICTED BY MSPA CALCULATIONS

Y.Z. Chen, Y. Feng and E.W. Prohofsky,
Dept. of Physics, Purdue University, West Lafayette, IN 47907

Modified Selfconsistent Phonon Theory (MSPA) has been used to incorporate temperature dependence into theoretical vibrational mode calculations in DNA polymers. The calculations show anomalous behavior above critical temperatures which correlate with DNA thermal denaturation temperatures. This correlation has led to the development of MSPA into an indicator of interbase h-bond melting or disruption. Since MSPA retains the atom-atom dimensionality of the helix one can probe the thermal behavior of the individual interbase h-bonds. We define a probability in the premelted region for the disruption of the amino h-bond in poly(dA)·poly(dT) by thermal fluctuations. We then correlate this particular state with that associated with the "open state" of amino hydrogen exchange. We find a fluctuational probability for the disruption of both interbase h-bonds in poly(dA)·poly(dT) which we correlate with the state associated with imino proton exchange. Our temperature dependent probabilities are in agreement with some experimental observations.

Th-Pos1

THIN FILAMENTS OF RABBIT SKELETAL MUSCLE ARE IN ROTATIONAL REGISTER. Raúl Padrón[1], Lorenzo Alamo[1], Jose Reinaldo Guerrero[1] and Roger Craig[2]. [1]IVIC-Biofísica, Apdo 21827, Caracas 1020A, Venezuela; [2]Dept. of Cell Biology, U. Mass. Medical School, Worcester, MA 01655.

Squire (J. Mol. Biol. 90, 153, 1974) has proposed two models to explain the arrangement of the thin filaments in vertebrate skeletal muscle: I. All thin filaments have the same rotational orientation in each half of the sarcomere; II. Adjacent filaments are rotated by 90° relative to each other. A third possibility is that the thin filaments have no fixed orientation relative to each other. We have tested these models by electron microscopy of rapidly frozen, freeze substituted, skinned rabbit psoas muscle in rigor. Thin longitudinal sections showed good preservation, revealing periodic transverse striations running across the overlap zones of the A-bands. Fourier transforms of these areas showed a strong first layer line corresponding to the 36 nm crossover repeat of the actin filaments. The alignment of attached crossbridges in adjacent filaments revealed by the presence of the stripes suggested that the crossovers in the actin filaments were in register, indicating that the thin filaments in the overlap zone have the same rotational orientation. This conclusion was supported by the Fourier transforms. The first layer line in the transform was strongly sampled, which argues against the third model. A strong meridional reflection on this layer line supported model I and argued against model II. These results support the conclusions of Hirose and Wakabayashi (J. Mol. Biol. 204, 797, 1988), who used exogenous S1 to reveal the thin filament orientation, that the thin filaments in the overlap zone have the same rotational orientation (Model I). Supported by grants from NIH, MDA, NSF and CONICIT.

Th-Pos2

2-D X-RAY STUDY OF RELAXED, TRITON SKINNED RABBIT PSOAS MUSCLE AT LOW IONIC STRENGTH AND HIGH TEMPERATURE. Brian Collett, NIAMS/LPB, NIH, Bethesda, MD and Physics Dept., Hamilton College, Clinton, NY & Richard Podolsky, NIAMS/LPB, NIH, Bethesda, MD

Recently, it has been shown that the myosin based reflections in the the 2-D X-ray diffraction pattern from relaxed rabbit muscle is very much clearer at high temperature (18-20°C) than at the conventional low temperature (J. Wray, J. Muscle Res. Cell Motil. 8,62,1987). We have found that this is true for both skinned and intact rabbit muscle and that the pattern from high temperature, Triton skinned, relaxed psoas muscle is essentially indistinguishable from that of high temperature intact muscle. The difference between relaxed and rigor patterns in rabbit is similar to that seen at low temperatures with frog muscle—a dramatic loss of myosin based layer line lines and an enhancement of the actin based reflections, especially those far from the meridian (except the 59Å actin layer line). We have used this improved preparation and a 2-D photon-counting X-ray detector (c.v. R.S.I. 59,1122,1988) to study the effects of low ionic strength on relaxed muscle at high temperatures. We find that the equatorial X-ray pattern from small bundles (<0.5mm thick) of relaxed rabbit psoas muscle at 20°C and 120mM ionic strength is rather more relaxed than at low temperature (lower I_{11}/I_{10}) (c.v. Wakabayashi et. al. in Mol.Mech.Musc.Contr. ed. Sugi & Pollack 1988) and that at 40mM ionic strength there is a doubling of I_{11} without a fall in I_{10} similar to the result in single fibres at low temperature (Brenner et. al. Biophys. J. 46,299,1984). In addition, the rapid stiffness of a relaxed muscle rises at 40mM ionic strength to a similar degree at both 20°C and 4°C (V. Barnett personal communication). Thus we believe that low salt bridges are being formed at room temperature as well as in the cold. The stiffness measurements indicate that at least 50% of all possible bridges are present at 40mM salt and 20°C. The 2-D pattern shows little change going from 120mM to 40mM ionic strength. At least 5 orders of myosin layer line are present at 40mM and there is little sign of enhancement on the actin reflections. There may be a small reduction in the myosin layer lines but the basic 2-D pattern is little changed by an ionic strength change which causes dramatic changes in the stiffness and equatorial intensity distribution. This result is in complete agreement with the findings of Matsuda and Podolsky (PNAS 81,2364,1984) at low temperature but the results are much clearer due to the improved preparation.

Th-Pos3

CHARACTERIZATION OF NEM-S1 BINDING TO THE THIN FILAMENT IN SINGLE SKINNED RABBIT PSOAS FIBERS. S. Schnekenbühl*, Th. Kraft*, L.C. Yu+, J. Chalovich#, B. Brenner+. *Univ. of Ulm, FRG; +NIH; #E. Carolina Univ., N.C.

The ATPase activity of myosin, in the presence of actin-tropomyosin-troponin, can be activated by either Ca^{2+} or by the binding of rigor crossbridges to regulated actin (Bremel et al., 1972). In solution, NEM modified S1 has been used to study the role of strong binding S1 in activating actomyosin ATPase (Pemrick & Weber, 1976; Nagashima & Asakura, 1982; Williams, et al., 1988). However, the effect of rigor crossbridges on activation in muscle fibers has not yet been studied in detail. As a first step in investigating the role of strong binding crossbridges in the regulation of muscle contraction, we have characterized the binding of NEM-S1 to the thin filament in single skinned fibers. S1 is sequentially modified with iodoacetamide and N-ethylmaleimide. In solution, the resulting S1 is shown to bind tightly to actin-troponin-tropomyosin. It has very low ATPase activity both in the presence and absence of actin but it potentiates the actin activated ATP hydrolysis of unmodified S1 as described by others. The binding of the added NEM-S1 to thin filaments in muscle fibers is monitored by the increase of the equatorial X-ray intensity ratio I_{11}/I_{10}. The diffusion of the modified S1 into the skinned fiber (diameter ~60 - 80 μm) is shown to take 3-4 hours to reach equilibrium. In the presence of ATPγS, the binding of NEM-S1 was studied as a function of ionic strength. The results indicate that in ATPγS the affinity of the modified S1 is stronger than that of the unmodified native crossbridges in muscle fibers. The effect of NEM-S1 on activation of contraction will be discussed.

Th-Pos4

EFFECT OF STRETCH ON EQUATORIAL X-RAY DIFFRACTION PATTERN OF RABBIT SKELETAL MUSCLE FIBERS CROSSLINKED WITH ZERO-LENGTH CROSSLINKER EDC H. Iwamoto and R.J. Podolsky
Laboratory of Physical Biology, NIAMS, NIH, Bethesda, MD 20892

Changes in the equatorial X-ray reflection intensities upon stretch of skinned skeletal muscle fibers of rabbit psoas were studied before and after crosslinking of myosin heads to actin using the zero-length crosslinker ethyldimethylaminopropylcarbodiimide (EDC). About 40% of the myosin heads were crosslinked in rigor solution. The bundles were placed in various ligands and repeatedly stretched and released by 1% of their length at 5°C while time-resolved X-ray patterns were collected.

Before crosslinking, the bundles showed little change in equatorial reflections upon stretch in any solution. After crosslinking, the 1,1 reflection intensity ($I_{1,1}$) dropped by about 10% upon stretch in 4mM MgATP, while $I_{1,0}$ stayed almost unchanged. The drop of $I_{1,1}$ was complete within the first 20ms of stretch and persistent for at least 100s. Replacing ATP with ligands with weaker dissociating action on the actomyosin complex (4mM MgPPi or 1mM MgAMPPNP) resulted in slower drop of $I_{1,1}$ upon stretch. In rigor it took 100s to obtain 5% drop of $I_{1,1}$. Thus the rate of $I_{1,1}$ drop was strongly correlated with the detachment rate of myosin heads in each ligand.

The results suggest that chemically 'detached' but mechanically 'tethered' myosin heads can rotate so as to affect the equatorial reflection intensities. Calculations showed that rotation of myosin heads in a 3-dimensional manner could explain the apparently non-reciprocal changes in equatorial reflection intensities.

Th-Pos5

HIGH RESOLUTION EQUATORIAL X-RAY DIFFRACTION PATTERNS FROM SINGLE MUSCLE FIBERS IN THE PRESENCE OF ATPγS.

Sengen Xu and L.C. Yu, NIAMS, NIH, Bethesda, MD.

Two dimensional electron density maps reconstructed from the first five equatorial X-ray diffraction intensities indicated that the configurations of the attached crossbridges in the relaxed and rigor states are distinct from each other (Yu and Brenner, Biophys. J. 55, 441, 1989). However, in reconstructing the density maps it was assumed that the phases of the X-ray reflections were the same in the two states. If there are changes in the phases, the difference in the density maps would be even more prominent. One way to test the assumption of phases being unchanged is to modulate the fraction of attached crossbridges in the relaxed state vs. in the rigor state by varying the concentration of ATP in the bathing solution. The corresponding changes in the reflection intensities could indicate whether phase changes take place. However, at low ATP concentration the muscle fiber is likely to be activated. Thus we have used the analog ATPγS in place of ATP, since it has been shown that crossbridges with bound ATPγS behave as weak binding crossbridges (Kraft, et al., Biophys. J., 57, 410a, 1990). Concentration of ATPγS varied from 0 to 1 mM at ionic strength of 64 mM. The changes in [1,0], [1,1], [2,0] and [2,1] are monotonic, but changes in [3,0] appear to be biphasic. In addition, change in [3,0] is steeper at $\leq 20\mu$M compared to those in I_{10} and I_{11}. This raises the possibility of a phase change in [3,0] as the population of the attached crossbridges shifts from the relaxed to rigor configuration. The findings, if supported by further experiments, suggest that the differences in the configurations of the attached crossbridges in those two states are more profound than previously proposed.

Th-Pos6

A CHANGE IN AEQUORIN TRANSIENTS UNRELATED TO Ca^{2+} CAUSED BY ACTIVE FORCE AND VOLUME CHANGES DURING ISOMETRIC CONTRACTION OF FROG MUSCLE FIBERS.

J. Rafael Lopez*, V. Arlene Morris, Laura A. Quesenberry, Ian R. Neering*, and Stuart R. Taylor*, Department of Pharmacology, Mayo Foundation, Rochester, MN 55905.

While studying volume changes in skeletal muscle (Morris et al., this meeting) we confirmed with isolated fibers that the initial change in an isometric twitch is a volume increase (Abbott & Baskin. 1962. J. Physiol.161:379). This suggested that changes in shape or cross-sectional area during contraction might distort an optical signal. Twitches and tetani of isolated, intact frog fibers injected with aequorin were monitored at regular intervals (every 300 seconds at 15° C). We recorded a cell's image during rest intervals. The addition of glycerol to normal Ringer (200mM final concentration) rapidly shrunk cells and abolished twitch force but not the aequorin signal which was increased. Twitch aequorin signals then decreased progressively as twitch force and cell volume spontaneously recovered. In contrast, tetanic aequorin signals did not increase when cells shrunk. Tetanic stimulation slowed and decreased force but did not abolish it. Tetanic aequorin signals also decreased progressively as force and volume spontaneously recovered. These changes are consistent with the idea that vigorous, active contraction produces radial as well as axial forces and the radial forces reversibly increase volume during contraction. Perhaps the normal twitch aequorin response is inversely related to the peak twitch force in glycerol Ringer because the radiant flux per unit area is depressed during contraction compared with shrunken fibers initially paralyzed by the hypertonic solution. The apparent increase in the Ca^{2+} transient of a twitch in hypertonic solution (Taylor et al., 1975. Fed. Proc. 34:1379) may be due to the great reduction in both the axial and radial components of a normal twitch.

Supported by CONICIT of Venezuela (JRL), the Australian NH & MRC (IRN), the NIH NS 22369, NSF DMB-85034964 and Pittsburgh Supercomputer Center DCB-890009P (SRT).

Th-Pos7

X-RAY DIFFRACTION MEASUREMENTS ON THE EFFECT OF RAPID LENGTH CHANGES ON RIGOR CROSS-BRIDGES IN SKINNED RABBIT PSOAS FIBRES

K. J. V. Poole & G. Rapp, Max Planck Inst. Med. Forschung, Heidelberg, Germany & EMBL, DESY, Hamburg, Germany.

We have measured the intensity and widths of the equatorial 10 and 11, and the meridional 143Å reflections after stretching and releasing bundles of 10 detergent skinned rabbit psoas fibres in the relaxed and rigor states. The sarcomere length was originally set at 2.7μm, the temperature to 20°C, and the fibre orientation to be perpendicular to the synchrotron x-ray beam by rotating the fibres so as to maximize the intensity in the 143 Å meridional reflections. The relaxed 143Å reflection is broad, i.e. not well sampled as it is in relaxed living frog muscle (Huxley et. al. J. Mol. Biol. 158, 637, 1982). On washing out ATP the 143Å reflection increases in intensity (between 50 & 120%) and width (ca 100%). These observations may be explained if rigor bridges adopt, on average, a more perpendicular attitude to the fibre axis with some disturbance in their axial ordering due to the influence of the thin filament geometry. Rapid (1ms), 0.3% stretches and releases had no measurable effect on the equatorial intensities as previously shown by Naylor & Podolsky (Proc. Natl. Acad. Sci. USA 78, 5559, 1981), but had very large effects on the 143Å intensity without any measurable change in its width, suggesting that the effect is not due simply to a change in the sampling or general ordering of the thick filament lattice. Stretches caused up to 100% increase in intensity, complete within the first 100ms time frame, which then remained high for the 1s period of stretch. Releases produced the opposite effect; a 50-70% reduction in intensity. No effect was seen on perturbing relaxed fibres in this way, even when much larger length changes were used. These data suggest that small, rapid length changes may cause the rotation of rigor cross-bridges.

This work was supported by a grant from the European Community.

Th-Pos8

X-RAY DIFFRACTION EVIDENCE FOR TWO ATTACHED STATES OF MYOSIN IN ACTIVE FISH MUSCLE

Jeff Harford, John Squire, Michael Chew & Liz Towns-Andrews*
Biophysics Section, Blackett Laboratory, Imperial College, London SW7 & *SERC Daresbury Laboratory, Warrington.

Time-resolved X-ray diffraction experiments have been carried out on contracting fin muscles of bony fish in which the A-bands have regular 3-dimensional order [Harford, J.J. & Squire, J.M. (1986) Biophys. J. 50, 145-155]. The low-angle diffraction patterns from both resting and active turbot fin muscle are regularly sampled, and the time-courses of change in the equatorial 100, 110, 200, 210 and 300 reflections and the (42.9 nm) myosin layer-line 111 and 201 reflections have been followed on a 5 or 10 ms timescale during typical tetanic contractions [Harford, J.J. & Squire, J.M. (1990) In "Molecular Mechanisms in Muscular Contraction" (Squire, J.M. ed.) pp. 287-320. Macmillan Press, Basingstoke]. The 100 and 110 equatorial reflections have quite different time-courses with the 110 change preceding tension at the level of 50% change by about 15 to 20 ms. The 100 reflection change is more similar to that of tension. Computed electron density maps from the first five equatorial reflections show the redistribution of mass during tension development. It can be concluded (independent of phase choice: 1,1,-1,1,1 or 1,1,-1,-1,1) that, at the level of 50% change, the time-course of mass arrival at actin precedes tension generation by about 15 to 20 ms. Electron density maps from the early (weak-binding?) period and the tension plateau show the difference between the mass distributions in the two actin-attached states; the difference is a change in radial distribution of mass around the actin filaments consistent with axial swinging of actin-attached crossbridges.

The uniquely informative diffraction data from bony fish muscle are now being solved directly by model-building, phase refinement and phase extension to yield a 3-dimensional image at 5 to 7 nm resolution of the myosin and actin filaments in the bony fish muscle A-band. [Work supported by the MRC]

Th-Pos9

EQUATORIAL X-RAY DIFFRACTION INTENSITIES FROM SINGLE INTACT MUSCLE FIBRES DURING SHORTENING. P.J. Griffiths*, C.C. Ashley, G. Cecchi‡, Y. Maeda & M.A. Bagni‡. EMBL Outstation, DESY, Hamburg, FGR; Univ. Lab. of Physiol., Oxford, UK; ‡ Dptm. di Scienze Fisiol., Uni. degli Studi, Florence, Italy.

Tetanised, intact single fibres from tibialis anterior muscles of Rana temporaria were allowed to shorten at constant velocity at the tetanus plateau (P_o). Equatorial intensities of the fibre diffraction pattern produced by exposure to synchrotron radiation were recorded during shortening (sampling rate 10ms, averaged over 20-50 tetani). Sarcomere length (2.15um initially) was continuously monitored using a HeNe laser diffractometer. Fibre stiffness was calculated from force responses to 4kHz sinusoidal length oscillations (<0.2% fibre length peak to peak amplitude). All experiments were performed at 4°C. Changes in fibre stiffness and equatorial intensity are thought to indicate the formation of crossbridges upon activation, but during shortening these parameters were not in agreement. During shortening at Vmax, the change in equatorial signals which accompanied activation was reversed by 50%, while stiffness fell to 30% of its plateau value. At shortening velocities which reduced force to $0.3P_o$ appreciable changes in stiffness occurred but equatorial signals were unaffected. Steady-state levels of the equatorial signals were reached at shorter times for higher shortening velocities, and were always reached more slowly than steady-state force. Comparison with the 1957 model of A.F. Huxley shows that stiffness data accords better with the predicted number of attached crossbridges than does the intensity data. We conclude that equatorial intensities indicate a mass transfer from thick to thin filaments during shortening which is not detected by stiffness measurements. If attached, such bridges are either unable to bear strain or are in rapid equilibrium with detached bridges in comparison to the time domain (4kHz) of the stiffness measurements.

Th-Pos10

RADIAL CROSSBRIDGE FORCES AT DIFFERENT MYOFILAMENT LATTICE SPACING IN INTACT SINGLE MUSCLE FIBRES. M.A. Bagni*, C.C. Ashley, G. Cecchi‡, Y. Maeda & P.J. Griffiths. EMBL Outstation, DESY, Hamburg, FGR; Univ. Lab. of Physiol., Oxford, UK; ‡ Dptm. di Scienze Fisiol., Uni. degli Studi, Florence, Italy.

Single intact muscle fibres from tibialis anterior muscles of Rana temporaria were exposed to synchrotron radiation (=0.15nm) during tetani. Myofilament lattice spacing (centre to centre distance between adjacent myosin filaments) was calculated from 10 or 11 reflection separation on the fibre's x-ray diffraction pattern. Sarcomere length was recorded using a HeNe laser diffractometer and adjusted to 2.15um prior to stimulation. Spacing was varied by exposure to Ringer's solution rendered hypo- (0.8x) or hypertonic (1.4x) by changes in [NaCl]. In unmodified Ringer's, spacing was 41.8nm; 44.0nm in 0.8x tonicity; 38.8nm in 1.4x tonicity. Force was reduced by 25% in hypertonic conditions, increased by 5% in hypotonic. Fibre shortening at a velocity sufficient to reduce tension to below $0.1P_o$ in unmodified Ringer's caused lattice expansion. Isometric tension recovery on termination of shortening was accompanied by a lattice compression of 1.03nm. Under hypotonic conditions compression during recovery was increased to 2.70nm, under hypertonic conditions reduced to 0.34nm. We believe this compression arises from a radial component of crossbridge force. If transmission of force between thick and thin filaments occurs through an element (S2) whose angle of contact with the thick filament (projected onto the plane containing both the thick and thin filaments) decreases as lattice spacing is reduced, one would expect a reduction of the radial force component at reduced lattice spacing. Our findings are consistent with such a model, and would therefore place constraints on the possible geometrical arrangement of the S1 and S2 components of the crossbridge in the force-generating configuration.

Th-Pos11

LATTICE STRUCTURE OF FROG SKELETAL MUSCLE DURING CONTRACTION.

Barry M. Millman, Rasika Rajapakshe and Quanning Li, Biophysics Interdepartmental Group, Physics Department, University of Guelph, Guelph, Ontario, Canada, N1G 2W1.

We have used small-angle X-ray diffraction to obtain equatorial diffraction patterns from intact muscle. The X-ray source was a GX6 Elliott rotating-anode X-ray generator with either double- or single-mirror focusing cameras and patterns were recorded with a TV-based area detector (K.Kalata, 1985: Methods in Enzymology, 114:486). X-ray diffraction patterns were from frog sartorius muscles at rest and during contraction (tetanic) in Ringer's solution where the osmolarity was varied from 25% to 200% of that of normal Ringer's solution. Lattice spacings and reflection intensities were measured and analysed by procedures outlined in Irving & Millman (1989: J. Mus. Res. Cell Motility, 10:385). Electron density reconstructions for the lattice from contracting muscle were obtained using the same phases as used for relaxed muscle, which were verified by modelling procedures similar to those used by Irving & Millman (1989). There was either no change in lattice spacing (found in vivo conditions) or a small increase in spacing; the latter could be because of a change in radial lattice forces. The electron density diagrams showed a shift in mass from a position along the 1,0 planes at rest (i.e. in the region between adjacent thick filaments) to the 1,1 planes during contraction (i.e. in the region between thick and thin filaments).

This research was supported by the Natural Sciences and Engineering Research Council of Canada.

Th-Pos12

LIMULUS THICK FILAMENTS SHORTEN BY FRAGMENTING

R.J.C. Levine & J.L. Woodhead, Department of Anatomy & Neurobiology, Medical College of Pennsylvania, Philadelphia, PA 19129

The decrease in A-band length during isotonic contraction of *Limulus* telson muscle reflects, in part, a 25-30% decrease in thick filament length, from >4 to ca. 3 μm[1]. This is due to a loss of filament proteins, rather than their rearrangement, since short filaments, recovered from either intact fibers, stimulated by brief exposure to high K^+ or Ca^{2+}-activated, skinned fibers, have helical arrangements of surface subunits and diameters identical to those of long filaments recovered from unstimulated fibers, either intact or skinned[2].

Our recent finding of numerous end-fragments of thick filaments on EM grids of preparations made from Ca^{2+}-activated, skinned fibers and similar structures, penetrating the I-bands in sections of skinned fibers, stretched beyond overlap prior to Ca^{2+} activation, led us to reexamine micrographs of filament preparations from intact, K^+-stimulated muscle and preparations where intact long filaments were exposed to myosin light chain kinase. In all cases where activation occurred, whether at the level of the sarcolemma, by introduction of Ca^{2+}, or by direct phosphorylation of the two regulatory myosin light chains on isolated filaments, both short thick filaments and filament end-fragments abound. The latter are absent in filament preparations from unstimulated muscle, and from the I-bands in sections of non-overlap, skinned, unstimulated fibers. Gels show no evidence of activation-induced proteolysis.

"Gap" filaments, seen in muscle stretched beyond overlap, attach to the thick filaments in unstimulated fibers. End-fragments within the I-bands of stimulated fibers are surrounded and held by "gap" filaments. 5% SDS-PAGE shows a band with the mobility of titin.

From these findings, we suggest that *Limulus* thick filaments may shorten by end-fragmentation resulting from phosphorylation of one or both RLCs at a defined region along each thick filament arm. In fibers operating over their normal length range, titin-like molecules may keep the fragments within the A-bands, where they can easily re-anneal to the rest of the filament. In highly stretched fibers, fragments may be translocated into the I-bands by elastic recoil of the "gap" filaments.

[1] Dewey et al. J. Cell Biol. 58:573, '73
[2] Levine & Kensler. J. Mol. Biol. 182:347, '85

Supported by HHS grants: AR33302 & HL15835 (Penna Mus. Inst.)

Th-Pos13

TESTING THE HARRINGTON MODEL FROM TIME-RESOLVED X-RAY DIFFRACTION OF FLATFISH FIN MUSCLE

M.W.K.Chew, J.J.Harford & J.M.Squire
The Blackett Laboratory, Imperial College, London, U.K.

The widely accepted model for force generation in muscle involves the rotation of myosin heads while transiently attached to actin filaments. An alternative model by Harrington (*PNAS* 76, 5066-5070, 1979) suggested that part of the helical S2 may melt during the contractile cycle and that this helix-coil transition could give rise to muscular force. Much circumstantial evidence has been produced in support of this model, but it has not been directly tested. With advanced synchrotron X-ray facilities it is now possible to test the Harrington model by studying the characteristic α-helical coiled-coil 5.1Å meridional reflection during force production. However, interpretation of any changes in this region is complicated by non-myosin proteins that also contribute to this reflection. Notable contributors could be tropomyosin and troponin-T in actin filaments, nebulin in the I-band and possibly any axially oriented coiled-coil helical domains in globular proteins. It is possible to model the transforms of these various structures in order to assess their likely relative contributions to the observed reflections. Our analysis suggests that by far the major contributor to this 5.1Å reflection is the myosin rod. Results from time-resolved X-ray diffraction studies using flatfish fin muscle showed only very small changes in shape and integrated intensity over the 5.1Å reflection when the muscle is undergoing isometric contraction.

[We thank the staff of the SRS, Daresbury Laboratory, UK for their help. Work supported by a project grant from MRC (UK)]

Th-Pos14

FLASH AND SMASH: ULTRASTRUCTURE OF RABBIT MUSCLE FIBERS RAPIDLY FROZEN FOLLOWING PHOTOLYSIS OF CAGED ATP. Keiko Hirose, Thomas D. Lenart, Clara Franzini-Armstrong and Yale E. Goldman. Univ. of Pennsylvania, Philadelphia, PA. 19104

We observed thin sections of rabbit psoas muscle fibers rapidly frozen at 20 to 300 ms after activation by laser photolysis of caged ATP. The glycerinated fibers were immersed in a Ca^{2+}-rigor solution with 10 mM caged ATP. The samples were frozen (see figure) on a helium-cooled metal block in a Heuser-Reese cryopress, with added tension transducer. Samples were freeze substituted in OsO_4 in acetone, warmed to room temperature and embedded in araldite. In longitudinal sections, the rigor crossbridges are wide near the actin filament and point away from the Z-lines. At 50 and 300 ms following photolysis, very few of the crossbridges are rigor-like, appearing thinner near the actin filaments and more variable in the angle of the main portion of the head. The average angle is approximately 90° to the fiber axis. Though force increases, the images change very little between 50 ms and 300 ms. At 20 ms, some rigor-type crossbridges are evident, and optical diffraction patterns of the overlap-regions show a 37 nm actin layer line. By 50 ms, the 37 nm layer line is weak. These results show that crossbridges in active fibers have structures distinct from rigor crossbridges. The structural changes of crossbridges during final tension development are subtle. Supported by NIH HL15835 to the PMI.

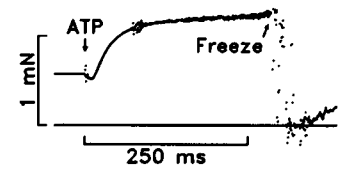

Th-Pos15

A QUICK-FREEZE APPARATUS FOR STUDYING SINGLE MUSCLE FIBERS DURING CONTRACTION Pieter H.W.W. Baatsen and Gerald H. Pollack. Center for Bioengineering, University of Washington WD-12, Seattle WA 98195.

It is generally accepted that thick filaments do not change length during muscle contraction. Nevertheless, structural studies have yielded conflicting results. Therefore, we set out to reinvestigate thick filament behavior in intact single fibers. Since it can be expected that chemical fixation methods for electron microscopy interfere with activation phenomena, quick-freezing was selected as preparatory method. To this end, we had originally built a quick-freeze apparatus (Baatsen et al., Biophys. J. 55:466a, 1989), but because of problems that arose (artifactual fiber stretch, suboptimal cryopreservation) we made several modifications in the apparatus, which are presented here.

In the modified version, the fiber is frozen by liquid-nitrogen-cooled copper cryopliers, which are moved pneumatically upward toward the fiber. The advantage over the previous freezing device is that the fiber is now cooled from two sides, improving cryopreservation. Further, a stop halts the cryopliers after clamping, averting stretch of the fiber due to vertical deflection. The fiber is mounted horizontally between two hooks, the right one of which is connected to a force transducer. Stimulation (100 Hz) takes place through the hooks. Isotonic releases are performed by removing the stop that holds the left hook in fixed position. In this way, the fiber is allowed to pull the hook in the axial direction, thereby lifting a weight that is suspended from a beam connected to the hook. Instants of shortening and freezing are precisely timed. Sarcomere length is measured by laser diffraction during test contractions.

In a previous study we found that measurements of thick filament length were complicated by uncertainty in determining the filament ends when freeze-fracture was used (Baatsen et al., Biophys. J. 51:474a, 1987). Therefore, fibers are now freeze-substituted in a methanol-glutaraldehyde-osmium tetroxide-uranyl acetate mixture. Specimens are embedded in araldite, sectioned, and poststained with lead citrate and saturated uranyl acetate in methanol.

Preliminary results show good preservation of the ultrastructure with no detectable freeze damage in both intact and skinned fibers. A systematic study in which fibers will be frozen during isotonic shortening under different loads and over different shortening ranges is underway.

Th-Pos16

DIRECT DETERMINATION OF SCALLOP MYOSIN FILAMENT SYMMETRY BY RAPID FREEZING. Roger Craig[1], Raúl Padrón[2] and Lorenzo Alamo[2]. [1]Dept. of Cell Biology, U. Mass. Medical School, Worcester, MA 01655, and [2]IVIC-Biofísica, Apdo 21827, Caracas 1020A, Venezuela.

We have used cryo-electron microscopy to observe directly the rotational symmetry and helix hand of the myosin filaments of scallop (Placopecten magellanicus) striated adductor muscle. Strips of muscle were chemically skinned in relaxing conditions, rapidly frozen against a copper block cooled with liquid helium, and freeze substituted in osmium/acetone. Electron micrographs of ultra-thin transverse sections of the A-band often showed clear projections protruding in a regular arrangement from the thick filament backbone: in the majority of cases the number of projections was directly observed to be seven. Correlation analysis of filament images supported this value without any assumption of helicity or rotational symmetry. The averaged image of 26 filaments clearly showed 7 crossbridges regularly spaced and slewed slightly around the filament axis, as observed in the original images, and the rotational power spectrum of the average had a strong peak at N=7. Tilting of thick sections in the electron microscope showed that the long-pitch (48 nm) crossbridge helices were right-handed. These results directly confirm some of the essential features of the low resolution 3-dimensional helical reconstruction of negatively stained scallop filaments calculated previously (Vibert and Craig, J. Mol. Biol. 165: 303, 1983). Supported by grants from NIH, MDA, NSF and CONICIT.

Th-Pos17

AN ULTRASTRUCTURAL STUDY OF ISOLATED RABBIT PSOAS MUSCLE THICK FILAMENTS. Robert W. Kensler, School of Basic Life Sciences, University of Missouri at Kansas City, and Murray Stewart, Medical Research Council Laboratory of Molecular Biology, Hills Road, Cambridge, England

Thick Filaments isolated from rabbit psoas muscle by a modification of our previously published procedure (Kensler and Stewart. 1989. J. Cell Sci. 94:391) have been examined by electron microscopy of negatively-stained and platinum-shadowed preparations, and by computer image analysis of the micrographs. Images of the negatively-stained filaments show a clear periodicity associated with the crossbridges, with a repeat every third crossbridge level (42.9 nm). Optical diffraction patterns and computed Fourier transforms of the filament images show a series of layer lines confirming the periodicity (42.9 nm), and often extend to the sixth layer line. These patterns appear relatively similar to those previously published for isolated frog thick filaments (Kensler and Stewart. 1983. J. Cell Biol. 96:1797) and show a similar tendency for the meridional reflection on the 3rd layer to be more variable in intensity than seen for isolated fish thick filaments (Kensler and Stewart. 1989. J. Cell Sci. 94:391). Computer filtrations of images of the negatively-stained rabbit filaments show the repeat every 3rd level of crossbridges and appear consistent with a 3-stranded arrangement of the crossbridges. Unidirectional shadowing of the filaments with platinum demonstrates that the crossbridges lie along a series of right-handed helical or near-helical strands as previously found for other vertebrate thick filaments. Work supported in part by NIH Grant AR30442.

Th-Pos18

ION DEPENDENT CHANGES IN TITIN EPITOPE POSITION DURING MYOFIBRIL PREPARATION. J. D. Fritz and M. L. Greaser. Muscle Biology Laboratory, University of Wisconsin, Madison, WI 53706.

Rabbit psoas muscle strips were soaked for 18 hours in rigor solution (75mM KCl/2mM $MgCl_2$/ 2mM EGTA/2mM NaN_3/0.1mM PMSF, pH 7.2) containing either 10mM Tris or 5mM phosphate. The muscle strips were then frozen in liquid nitrogen cooled isopentane or used to prepare myofibrils. Longitudinal frozen sections and myofibrils were placed on coverslips, fixed with 3.7% formaldehyde, and then incubated with monoclonal anti-titin 9D10 plus Texas Red conjugated secondary antibody. The center-to-center distances between titin stained zones within a sarcomere (titin spacing) and the sarcomere lengths (SL) were measured. Plots of titin spacing versus SL gave slopes of 0.50 and 0.48 for frozen sections of muscle soaked in Tris or phosphate respectively. Myofibrils prepared from companion strips had slopes of 0.22 and 0.004 (sarcomere lengths in the range of 2.0 to 3.5μm). Preparations of myofibrils from muscle previously soaked in 50% glycerol with Tris or phosphate solutions for two weeks at -20°C had slopes of 0.32 and 0.19. Inclusion of formaldehyde in the Tris or phosphate soaks increased the slopes to 0.36 and 0.38. Fixation of myofibrils with 0.2% glutaraldehyde instead of formaldehyde gave similar results. No differences were evident between the Tris and phosphate myofibrils on SDS gels (amounts of titin or nebulin relative to the myosin heavy chain or total protein), the ratios of titins T1 to T2, or the levels of breakdown products of titin or nebulin observed on Western blots. Thus there appears to be a structural rearrangement of titin during myofibril preparation which is accentuated by prior soaking in a phosphate containing buffer.

Th-Pos19

INTERACTION OF TITIN AND THE A-BAND PROTEINS. S.-M. Wang and C.-J. Jeng. Department of Anatomy, College of Medicine, National Taiwan University, Taipei, Taiwan, ROC.

The interaction of titin with the structure and proteins of the A-band was examined in this study. We obtained three monoclonal anti-titin antibodies (A12, A2 and E2) which recognize distinct epitopes on the titin in the A-band. The position of titin bands stained by these antibodies remained the same in long sarcomeres where the A-band was translocated from the center to the side of the sarcomere or in isolated A-bands produced by formamide extraction of the myofibrils. These results suggest a close association of titin and the A-band structure. In addition, biotinylated titin could be added to the outer A-band and Z-bands in intact myofibrils, thus confirming the in situ binding of titin to the A-band. In order to analyse the domain of myosin contributing to the binding for titin, we conducted a solid phase binding assay. Myosin (heavy and light chains, and myosin fragments) and its associated proteins were coated on the microtiter wells and then reacted with biotinylated titin. The binding of biotinylated titin was detected by the avidin-biotin-peroxidase method. The results demonstrated that light meromyosin and subfragment 1 are the major domains for the binding of thick filaments to titin. Light chains, C-protein, and M-line proteins also bound to the titin. The present studies have shown that titin domain in the A-band has little extensibility which might be due to its strong binding to the myosin rod, myosin head and C-protein.

Th-Pos20

BUNDLING OF F-ACTIN BY CLONED NEBULIN FRAGMENTS.

T. C. Irving, J.-P. Jin and K. Wang. Dept. of Chemistry and Biochemistry, Clayton Foundation Biochemical Institute, University of Texas at Austin, Austin, TX., 78712.

Nebulin is a giant (600-800 kD) myofibrillar protein that has been proposed to constitute a set of inextensible longitudinal filaments anchored at the Z-line and co-extensive with the thin filaments in the sarcomere (Wang & Wright, 1988. J. Cell Biol. 107:2199). Molecular cloning and sequence studies of human nebulin cDNA have shown a well-conserved ~ 35 residue repeat throughout the molecule (Wang et al., 1990. Biophys. J., 57:555a). Each repeating unit ("module") may represent the structural domain which binds to one actin monomer.

Our group has recently expressed several human nebulin fragments in E. coli. We have examined three different fragments of different lengths: one (ND8) contains 2 of the 35 amino acid modules, another (NA4) has 6-7 modules, and the third, NA3 has 7-8 modules. All three fragments bind specifically to F-actin in co-sedimentation assays (Jin & Wang, submitted). We have examined, using epifluorescence microscopy, the effects of adding nebulin fragments to F-actin fluorescently labeled by rhodamine/phalloidin. Incubation with NA3 and NA4 yielded large, bright bundles, with dramatically reduced numbers of free actin filaments in solution. ND8, however, did not produce such bundles, despite the fact that its actin binding behavior is similar to that of NA3 and NA4 in ELISA assays. The F-actin bundles frequently showed large loops, kinks, or spiral structures. These data suggest that the cross-linking of F-actin by nebulin requires a minimal number of modules in the nebulin fragment. The lack of bundling by ND8 suggests that a two module fragment is too short to engage in such interactions. The presence of curvature in F-actin bundles suggests that nebulin fragments may bind to actin in an asymmetric fashion. The ability of nebulin to cross-link actin raises the possibility that nebulin might produce inter- thin filament cross-linkages in the sarcomere.

Th-Pos21

FIXATION OF VERTEBRATE MUSCLE WITH TANNIC ACID CAN PRESERVE FINE STRUCTURAL DETAILS. David Popp, Hernando Sosa and Hugh E. Huxley, Rosenstiel Center, Brandeis University, Waltham, MA 02254.

Small bundles (2-20 fibers) of skinned rabbit psoas muscle were incubated in appropriate buffer (relaxed or rigor), in the presence of 0.2% Tannic Acid (TA) (Galloylglucose), pH 7.0 for up to 24 hours at 4 C. After washing out excess TA, the muscles were incubated in 1% uranyl acetate or osmium tetroxide, which led to an immediate chemical reaction between the TA and the heavy metal as indicated by the blackening of the muscle. The muscle was dehydrated in either ethanol or acetone and embedded in araldite. Parts of the preparations were sectioned and examined by electron microscopy after further staining with uranyl acetate and lead citrate. Other parts were used to obtain X-ray diffraction patterns using a GX-13 rotating anode and either a double mirror or a mirror-monochromator setup.

As revealed by the X-ray diffraction pattern, the rigor structure is well preserved and all actin based layer lines including the 6th (5.1 nm) are intensified as in unfixed specimens of rigor muscle, indicating good preservation of the crossbridge structure. The thin filament structure is well preserved as indicated by the strong troponin reflexions at 38.5 and 19.2 nm and the presence of the second layer line (18 nm axial and 4.5 nm radial spacing).

Optical transforms of thin sections compare well with the X-ray diffraction pattern, showing strong sampling of the prominent 1st (36 nm) actin layer-line and of the 14.5 nm layer line. The ~24 nm layer line is also visible. In the EM the crossbridges in rigor are clearly revealed as arrowheads. In comparison with the commonly used fixation glutaraldehyde which gives EM preparation showing only weak diffraction in the 36 nm and 14.5 nm region and nothing beyond, tannic acid is able to preserve the relatively robustly ordered rigor structure and give strong diffraction at the longest spacings and visible reflections out to 5.1Å in some cases. More labile crossbridge configurations such as those in relaxed muscle are more difficult to preserve, because of structural changes induced by TA itself. Very similar results were obtained with rapidly-frozen muscles which were freeze-substituted in acetone containing 0.2% tannic acid at –80° C.

Supported by NIH AR38899, by a NATO postdoctoral fellowship from DAAD (D.P.) and by a grant from the Lucille P. Markey Charitable Trust (H.E.H.)

Th-Pos22

FIXATION OF INSECT FLIGHT MUSCLE (IFM) BY "TAOS" AND "TAURAC" TANNIC-ACID-METAL PROCEDURES. Michael K. Reedy*, Carmen Lucaveche* & David Popp#, *Cell Biology, Duke Univ., Durham, NC, & #Rosenstiel Center, Brandeis Univ., Waltham, MA.

When fixed for EM in mixtures of glutaraldehyde with tannic acid (TA), even as single fibers, thin-sectioned glycerinated insect flight muscle (IFM) often shows a gradient in fixation quality, as if the benefits of TA reached deeper structures too late to prevent slight degradative actions of the quicker-penetrating aldehyde. So we explored TA->metal sequences without aldehyde, encouraged by Nielson & Griffith (*J. Histochem. Cytochem.* 26:138) that a primary supportive TA impregnation could be secondarily crosslinked and stabilized by certain metal reagents. We adapted TA followed by uranyl acetate (TAURAC) from Fujiwara & Tilney (*Ann. N. Y. Acad. Sci.* 253:27), and TA followed by OsO_4 (TAOS) from Hirose & Wakabayashi (J. Mol. Biol. 204:797). Fibers were fixed in 0.2% TA in rigor, relaxing, etc. buffer for 0.5 h (1-3 fibers) to 24 h (10-60 fibers), rinsed, then metal-treated before epoxy embedding. Slight negative staining is more common with TAOS than TAURAC, but both preserve excellent order by EM and diffraction criteria (Fe^{3+} and many others do not). Rigor IFM EMs appear and diffract as nicely as the best aldehyde-TA fixation, and post-embedding X-ray patterns retain more actin layer lines, and clearer tropomyosin reflections at 39 nm. Relaxed IFM EMs differ 4 ways from aldehyde-TA fixation, preserving better thick filament order (better 14.5 nm repeat; clear helical surface lattice on thick filaments in H-bands of stretched sarcomeres), but altered thin filament order as shown by striking enhancement of crossbridge features (possibly trapped myosin-troponin contacts) that intensify 39 nm lattice order, and stronger 5.1 nm than 5.9 nm actin layer lines in ODs. TAURAC works well in acetone for freeze substitution (as did TAOS for Hirose and Wakabayashi) and this approach overcomes in relaxed IFM the non-native 39 nm enhancement of cross-bridging seen after aqueous TAURAC at 0-20°C and seen also to a lesser extent after aldehyde fixation (Reedy et al., J. Musc Res. 4:25). Turning from *Lethocerus* to glycerinated Dipteran relaxed IFM, TAURAC fixation preserves unprecedented though weak 14.5 nm thick filament periods, and has several times "extracted" the actin core of thin filaments while leaving in place a strikingly ordered 39 nm repeat of paired troponins. In general, the TAURAC procedure is a useful alternative fixation for thin section EM of permeabilized or freeze-substituted cells, lower in cost, toxicity, and negative-staining tendency than TAOS.
Supported by NIH, MDA (M.K.R.) & NATO (D.P.)

Th-Pos23

ELASTIC BEHAVIOR AND ARRANGEMENT OF TITIN FILAMENTS IN THE I-BAND. Károly Trombitás*†, Gerald H. Pollack†, John Wright*, and Kuan Wang.* *Clayton Foundation, Univ. of Texas, Austin TX 78712. †Center for Bioengineering, University of Washington, Seattle WA 98195

Although immunoelectron microscopic studies have revealed that the titin filament's I-band domain behaves elastically, the relation between the titin filament and the actin filament is unclear. We report experiments that suggest that except near the Z-line, the two filaments are independent of one another.

Freshly prepared bundles of rabbit psoas fibers were quickly frozen, and then broken into small pieces. The rationale was to create fracture planes in different zones along the sarcomere. During subsequent fixation with paraformaldehyde in PBS, the still-frozen pieces were permitted to thaw, thereby allowing elastic filaments to retract. The pieces were then labelled with monoclonal anti-titin (RT13, or Sigma T11). In sarcomeres in which no fracture was present, I-bands were labelled symmetrically. In sarcomeres fractured across the A-band, the titin epitope did not translate relative to other sarcomeric structures; thus, there was no filament retraction. In sarcomeres fractured along the Z-line, the epitope translated to the edge of the A-band; thus, titin filaments in the broken half-sarcomere retracted to the ends of the thick filaments. The unbroken half-sarcomere was not affected. In sarcomeres broken at the A-I junction, thin filament remnants remained in their original position relative to the Z-line, but titin filaments retracted, independently of the thin filament remnants, forming a dense band near the Z-line. The retracted density appeared at the so-called N_1 line, a short distance from the Z-line. Thus, in the vicinity of the Z-line, the titin filament either associates firmly with the actin filament, or is inelastic. In the remainder of the I-band region, the retraction phenomena demonstrate that the titin filament is elastic, and independent of the actin filament.

Th-Pos24

NATURE AND ORIGIN OF GAP FILAMENTS IN FROG SEMITENDINOSUS MUSCLE.
K. Trombitás, P.H.W.W. Baatsen, M.S.Z. Kellermayer, and G.H. Pollack, Bioengineering WD-12, University of Washington, Seattle WA 98195

When fibers are stretched beyond filament overlap, a gap appears between thick and thin filaments. The gap is filled with fine longitudinal filaments, which have long-ago been called "gap filaments." It now appears that the gap filament may be a segment of titin strand (which runs between M-line and Z-line). To test this, we used a monoclonal anti-titin antibody (T-11, Sigma), which, at physiological sarcomere length, binds to an epitope just beyond the tapered end of the thick filament (Fürst et al., 1988). We labelled single mechanically skinned fibers in the sarcomere-length range 2.5 - 6.0 μm. At the shorter sarcomere lengths, the epitope was found about 0.9 μm from the M-line, just barely in the I-band. Unexpectedly, the span between M-line and epitope did not change perceptibly with increasing sarcomere length, up to 3.6 μm. Above 3.6 μm, the span abruptly increased, and the label could be seen in the gap. The label remained aligned across the myofibril, even with this high degree of stretch. Presumably, a segment of titin came free of its thick filament bonds, allowing the epitope to be pulled well into the gap. Thus, gap filaments appear to be recruited from both the I- and A-band domains of the titin strand. Apparently, both domains are intrinsically elastic. The data confirm that the gap filament is indeed a part of the titin strand.

Th-Pos25

A THEORETICAL ANALYSIS OF FINE STRUCTURE FROM STRIATED MUSCLE LIGHT DIFFRACTION PATTERNS

Kenneth P. Roos and Alfred F. Leung*
*Cardiovascular Research Lab, UCLA School of Medicine, Los Angeles, CA. 90024-1760 & *Department of Physics-Astronomy, California State University, Long Beach, CA 90840.*

Light diffraction patterns are generated by numerical methods from data arrays of sarcomere striation positions obtained from real isolated cardiac myocytes or computer generated models. (Roos & Leung, Biophys. J. 52:329, 1987). Model cells containing one, two, or three physically distinct domains of sarcomeres with different average sarcomere lengths (SL) and variable amounts of 3-D position randomization generated diffraction patterns indistinguishable from real patterns in terms of layer line intensity, position and fine structure. Fine structure is present in patterns from all configurations of striation ordering containing at least a 3% randomization of SL. The exact pattern of fine structure depends upon the 3-D ordering and orientation of the entire diffracting structure. Any internal reordering of the 3-D organization of diffractors changes the specific pattern of fine structure but not the layer line centroid position used to calculate SL. Patterns from double or triple domain models demonstrate multiple columns of diffracted light within each layer line if the difference in domain SLs is > 3% of the average SL. The average column positions do, but the specific fine structures do not, correspond to the domain's SL. Thus, 1) diffraction fine structures arise from the interference of light waves scattered by randomly positioned sarcomeres of different lengths, and 2) it is unlikely that there is a one-to-one correspondence between a specific fine structure and a sarcomere domain.

Supported by NIH HL-29671 (KPR) & Pittsburgh Supercomputing Center grant DMB880009P (S.R. Taylor & KPR).

Th-Pos26

COMPLETE CODING SEQUENCES OF cDNAS OF FOUR VARIANTS OF RABBIT SKELETAL MUSCLE TROPONIN-T.

Setsuko Fujita, Kayo Maeda# and Yuichiro Maéda*.
European Molecular Biology Laboratory at DESY, Notkestraße 85, W-2000 Hamburg 52, and # Abteilung Biophysik, Max-Planck-Institut für medizinische Forschung, Jahnstr. 29, W-6900 Heidelberg, Germany.

cDNAs encoding sequences of four isoforms of troponin-T derived from eleven-day-old rabbit skeletal muscle have been isolated and sequenced. One variant (TnT-1) contains the complete coding sequence, while in three variants the coding sequences are truncated at the 5' termini. Comparison of amino acid sequences derived from these variants with each other and with the published (Pearlstone *et al.* (1977) *J.Biol.Chem.* **252**, 983-989) amino acid sequence, TnT-P, of the protein (prepared from adult rabbit skeletal muscle) reveal : (A) In the amino-terminal region none of two variants have the same sequence nor any of them is the same as TnT-P. The sequence differences in this region corresponds to the finding on the rat skeletal muscle troponin T gene that exons 4 through 8 are alternatively spliced in an interchangable but not mutually exclusive manner. (B) A sequence is observed corresponding to an extra exon or exons between exon 5 and 6. This sequence is shorter than that of chicken skeletal muscle gene and not detected in the rat skeletal muscle gene. (C) In the region near the carboxyl-termini, all the four cDNAs express exon 17 (β-type), not exon 16 (α-type) which is present in the previously published peptide sequence. This difference corresponds to the alternative splicing of these two exons in mutually exclusive manner in the rat gene. This is also consistent with the finding in chicken skeletal muscle that in new-born animals β-type is predominantly expressed while α-type is dominant in adult muscles. (D) Apart from the differences originating from the alternative splicing, the previously published amino acid sequence differs from the present cDNA-derived sequences at three locations. At least two, possibly the all, of them are likely accounted for by errors in peptide sequencing. The longest of these four variants, TnT-1, may be the complete (β-type) transcript of the fast skeletal muscle TnT gene; every exon 4 through 8 is expressed in TnT-1 while exon 4 is absent in TnT-P.

Th-Pos27

POLARITY OF TROPONIN T IN TROPOMYOSIN/TROPONIN T COCRYSTALS. D. Cabral-Lilly, L.S. Tobacman*, J.P. Mehegan* and C. Cohen. Rosenstiel Center, Brandeis University, Waltham, MA 02254. *Dept. of Internal Medicine, The University of Iowa College of Medicine, Iowa City, IA 52242.

Tropomyosin, complexed with troponin T, forms an ordered crystalline structure called the "double diamond" mesh consisting of a network of large and small diamonds formed by straight, cross-connected tropomyosin filaments (Cohen et al., Cold Spring Harbor Symp. Quant. Biol. 1972, 37:287). In this lattice, pairs of tropomyosin filaments are linked by one end of pairs of the troponin T subunits at the acute vertex of the large diamond; the rest of each troponin T then spans more than half an arm of the mesh. The polarity of both troponin T and tropomyosin in the lattice was determined by electron microscopy of negatively stained complexes of rabbit α_7 tropomyosin and a cloned rat troponin T fragment lacking the N-terminus (amino acids 70-259). Cocrystals of the double diamond form were produced, indicating that the C-terminal region of troponin T must be at the vertex of the large diamond with the N-terminal region extending into the arm. X-ray diffraction studies have shown that the N-terminus of troponin T spans the head-to-tail joint of the tropomyosin filaments (White et al., Nature 1987, 325:826). This joint between tropomyosin molecules must therefore lie roughly midway along the arm of the double diamond mesh. Knowledge of this polarity is essential to interpret cryo-electron micrographs of double diamonds embedded in vitreous ice. Such cocrystals made from bovine cardiac troponin T and rabbit α_7 tropomyosin are strikingly clear and diffract to 15 Å resolution. Preliminary image processing suggests the presence of substructure in the troponin T molecule that may be related to function: binding to the tropomyosin filament joint at the N-terminus of troponin T, and binding to troponins C and I at the C-terminus.

Th-Pos28

THE EFFECT OF AMINO TERMINAL DELETIONS ON TROPONIN T FUNCTION. J.P. Mehegan, P.S. Ro, and L.S. Tobacman, The University of Iowa College of Medicine, Iowa City, Iowa 52242.

Alternative RNA processing regulates the amino acid sequence of the amino terminal region of troponin T (TnT). This portion of the protein spans the overlap between adjacent tropomyosins and is thought to be involved in the regulation of thin filament function. To evaluate the importance of this region, a full length rat skeletal muscle cDNA was constructed from partial length clones obtained from Dr. R. Breitbart. From this, a sequence encoding a shortened TnT was constructed and ligated into pET3d. This bacterial expression vector was used to transform E. coli DE3 cells and express a TnT missing the initial 69 amino acids (TnT-70-259). The mutant protein was purified to homogeneity by precipitation at low ionic strength and by hydroxylapatite chromatography in the presence of 5M urea. Yield was 5-8 mg of purified protein per liter of bacterial culture. The amino acid composition was confirmed by N-terminal sequencing. The molecule differs from the corresponding region of rabbit skeletal muscle TnT by three conservative amino acid substitutions. TnT-70-159 and rabbit skeletal muscle TnI and TnC were used to reconstitute troponin. This resulted in a molecule that inhibited MgATPase activation of the myosin S-1-actin-tropomyosin complex in the absence of Ca^{2+} and promoted activation in the presence of Ca^{2+}. These results imply that the region of TnT spanning the tropomyosin-tropomyosin joint is not essential for thin filament regulation by Ca^{2+}. A second cDNA for a protein including amino acids 151-259 has also been constructed. Further studies on thin filament assembly and regulation will be performed using these molecules.

Th-Pos29

REMOVAL OF THE FIRST 45 NH_2-TERMINAL RESIDUES OF RABBIT SKELETAL TROPONIN T STRENGTHENS BINDING OF RECONSTITUTED TROPONIN TO TROPOMYOSIN. B. Pan,+* A.M. Gordon+ and J.D. Potter*, +Dept. of Physiology & Biophysics, Univ. of Washington, Seattle WA 98195 & *Dept. of Molecular & Cellular Pharmacology, Univ. of Miami, Sch. of Med. Miami FL 33101

The NH_2-terminal region of troponin T (TnT) is thought to constitute a pivotal link between troponin (Tn) and tropomyosin (Tm) (e.g. White et al Nature 325:826-828). To further explore the structural role of the NH_2-terminal region of TnT, we studied the binding of a 26K TnT fragment (residues 46-259) (Ohtsuki et al J. Biochem. 95:1337-1342;) to α-tropomyosin using immobilized α-Tm. 26K-TnT and TnT_{2b}, the major TnT isoform in rabbit back muscle, were purified respectively by a method developed by us (Chin et al Biophys. J. 57:147a) and the procedure of Briggs et al (J. Biol. Chem. 259:10369-10375). The protein samples were loaded on an α-Tm-Sepharose 4B column equilibrated with 150 mM NaCl, 1 mM Mg^{2+}, 1 mM DTT, pH 7.0. The proteins bound to the column were eluted with NaCl gradients, and subsequently identified and semi-quantitated by SDS-polyacrylamide gel electrophoresis, silver staining and densitometry. In the absence of troponin I (TnI) and troponin C (TnC), 26K-TnT was eluted at a higher ionic strength than was TnT_{2f}, indicating that 26K-TnT bound more strongly to Tm than did TnT_{2f}. When the binary complex of TnI-TnC was applied alone, it was eluted in the void volume. However, when excess TnI-TnC was applied subsequently to TnT_{2f} and/or 26K-TnT, a portion of TnI-TnC was retained by the column and eluted together with TnT_{2f} or 26K-TnT, in a molar ratio suggesting formation of the ternary troponin complex. In such experiments 26K-TnT was again eluted at higher ionic strength than was TnT_{2f} whether Ca^{2+} was present or not. Earlier studies of TnT fragments (e.g. Pearlstone and Smillie, J. Biol. Chem. 257:10587-10592) found that the CB3 region (residues 1-70) of TnT is important for attachment of NH_2-terminal 3/5 of TnT to Tm. Our new results imply that the first 45 NH_2-terminal residues in TnT_{2b} which encompass the variable region of TnT (Briggs and Schachat, J. Mol. Biol. 206:245-249), are not essential for anchoring the troponin complex to tropomyosin. (Supported by NIH Grants NS07097, HL31962, NS08384 and AR37701).

Th-Pos30

Ca^{2+} MODULATES TROPONIN-T BINDING TO TROPONIN-C. T.-I Lin, M. Mayadevi, and R.M. Dowben*. Baylor Research Foundation, Baylor University Medical Center, 3500 Gaston Avenue, Dallas, Texas 75246 and *Department of Neurology, University of Texas Southwestern Medical Center, Dallas, Texas 75235.

The effect of Ca^{2+} on the binding interaction between troponin-C (TnC) and troponin-T (TnT) was studied in the binary complex as well as in the presence of troponin-I (TnI) and/or tropomyosin (Tm). Rabbit skeletal TnC was labeled with 7-dimethylamino-4-methyl-3-*N*-meleimido-coumarin (DACM). IEF gel electrophoresis, HPLC, and HPCE studies of CNBr fragments of DACM-labeled TnC showed that Cys-98 was the only labeling site. Fluorescence titration curve of the labeled TnC with Ca^{2+} showed a biphasic response --- fluorescence was quenched (by 31%) initially but rose (by 64%) in the second phase. The biphasic fluorescence changes correspond presumably to the binding of Ca^{2+} to the two high affinity Ca^{2+}-Mg^{2+} binding sites (pCa = 7.35 and 6.6). A second order rate constant of $1.33 \times 10^6 M^{-1}s^{-1}$ was obtained from the transient kinetic study. Additional Ca^{2+} binding to the Ca^{2+}-specific sites did not cause further fluorescence change. Binding isotherm of TnT to TnC was obtained by titrating labeled TnC with TnT under various conditions and monitoring the fluorescence enhancement (40%) of DACM by TnT. The binding curve was analyzed by diagnostic plots and binding constant was obtained by a nonlinear regression curve-fitting technique. In the absence of Ca^{2+}, TnT bound very weakly to TnC ($K_a < 10^3 M^{-1}$) whereas in the presence of Ca^{2+}, TnT-TnC binding increased almost three orders of magnitude ($K_a = 0.34 \pm 0.15 \times 10^6 M^{-1}$). A rate constant of 1.6-2.3 $10^7 M^{-1}s^{-1}$ was obtained for TnT binding to TnC in the presence of 3 mM $CaCl_2$. Adding Tm to the system weakened the binding of TnT to TnC by at least 50 to 60%. In contrast, adding TnI to the binary system greatly increased the binding affinity of TnT to TnC ($K_a = 1.8 \pm 0.15 \times 10^6 M^{-1}$). It is proposed that the changes in binding affinity between TnC and TnT, as modulated by the binding of Ca^{2+} to TnC, may play an important role in the regulation mechanism of muscle contraction by Ca^{+2}.

This work was supported in part by U.S. Contract N0014-90-C-0034 and Baylor Medical Cell Biology Fund.

Th-Pos31

MUTANT OF SKELETAL TROPONIN C CONTAINING A DISULFIDE BOND IN THE C-TERMINAL DOMAIN. Z. Grabarek, N. Gusev, R.-Y. Tan, and J. Gergely. Department of Muscle Research, Boston Biomedical Research Institute, Boston MA 02114

Restriction of the Ca^{2+}-induced movement of α-helical segments in the N-terminal domain of a mutant of rabbit skeletal troponin C (TnC) by a disulfide bond leads to a decrease in Ca^{2+}-affinity and a loss of Ca^{2+}-sensitizing activity (Grabarek et al. Nature 345, 132, 1990). To test the importance of the segmental mobility in the C-terminal domain we have obtained a mutant containing, in addition to the indigeneous Cys-98, a second Cys substituted for Ser-122 (TnC98/122). A disulfide bond between the two Cys is readily formed leading to alteration of several properties as compared to rabbit skeletal TnC and to TnC98/122 in which disulfide formation is prevented by blocking Cys residues with iodoacetamide (CAMTnC98/122). The oxidized mutant (oxTnC98/122) has a higher α-helix content in the absence of Ca^{2+} reflected in the more negative ellipticity at 222 nm. The affinity for Ca^{2+} at sites III and IV is reduced as shown by a 0.45 pCa shift in Ca^{2+}-titration of circular dichroism at 222 nm and of the fluorescence of Tyr-108. CD measurements in the presence of Ca^{2+} show a higher melting temperature indicating that the disulfide bond increases the stability of the C-terminal domain. At micromolar concentrations oxTnC98/122 does not confer Ca^{2+}-sensitivity on TnC-deficient myofibrils owing to a several-hundred-fold decrease in affinity for TnI and failure to associate with reconstituted thin filaments. Partial regulation can be obtained at sufficiently higher concentrations. Thus the C-terminal domain of TnC appears to serve primarily as a binding domain while the N-terminal domain has a regulatory function. In both domains the mechanism of interaction with TnI appears to be similar in that it utilizes the interhelical interfaces accessible in the Ca^{2+}-bound form. Supported by NIH, AHA, MDA.

Th-Pos32

MAPPING OF INTERACTION SITES IN TROPONIN-C BY SITE-DIRECTED MUTAGENESIS, PHOTOCROSSLINKING AND FLUORESCENCE. I. Boldogh, J. Wang, J. Gergely & T. Tao (Intro. by A.M. Garcia). Dept. of Muscle Research, Boston Biomedical Research Institute, 20 Staniford St., Boston, MA 02114.

We have used a combination of site-directed mutagenesis, photocrosslinking, and fluorescence techniques to map sites in troponin-C (TnC) that interact with troponin-I (TnI) and Troponin-T (TnT). We synthesized in *E. coli* a series of mutant rabbit skeletal TnC's, each containing a single Cys residue at positions 12, 45, 49, 57 and 89 (the endogenous Cys98 in natural TnC was replaced by Leu). Each mutant was then labeled with the photocrosslinker BP-Mal (benzophenone-4-maleimide), reconstituted with either TnI alone or both TnI and TnT, and crosslinking initiated by ultraviolet irradiation. Each mutant was also labeled with the fluorescence probe 1,5-IAEDANS and the effects of Ca^{2+}, TnI, TnI and TnT binding on the fluorescence lifetime of the probe were examined. The results obtained here in combination with previous results are summarized below: 1) All the Cys's, including Cys98 in natural TnC can be crosslinked to TnI via BP-Mal. 2) Residues 89 and 98 can be crosslinked to TnT as well as to TnI. 3) For all the residues, the fluorescence lifetime of the attached AEDANS probe is enhanced by TnI. 4) For residues 12, 49, 89 and 98, the fluorescence lifetime of the attached AEDANS moiety is insensitive to Ca^{2+} binding at the low affinity "triggering sites". This is true regardless of whether the TnC is uncomplexed, complexed with TnI, or complexed with both TnI and TnT. 5) For residues 45 and 57, Ca^{2+}-binding to the low affinity sites caused the fluorescence lifetime of the attached AEDANS probe to decrease in uncomplexed TnC, and increase in either the TnC-TnI binary complex or the TnC-TnI-TnT ternary complex. Based on these results we tentatively conclude as follows: 1) Whereas TnI makes extensive contact with all parts of TnC, TnT only contacts the C-terminal half. 2) Only the region comprising the B- and C-helices in the N-terminal domain of TnC undergoes extensive conformational changes in response to Ca^{2+} binding at the low affinity sites. These changes are consistent with the hypothesis that binding of Ca^{2+} to the low affinity sites results in the movement of the B- and C-helices away from the central helix. (Supported by NIH and MDA).

Th-Pos33

BOTH Ca^{2+}-SPECIFIC SITES OF SKELETAL MUSCLE TnC ARE REQUIRED FOR FULL ACTIVITY. James D. Potter, Zelin Sheng, Todd Miller and William Strauss, Dept. of Molecular and Cellular Pharmacology, Univ. of Miami School of Medicine, Miami, FL 33101.

Troponin C, the Ca^{2+} binding subunit of troponin, contains four Ca^{2+} binding sites. Two Ca^{2+} specific binding sites are thought to be directly involved in switching on muscle contraction, whereas two Ca^{2+}-Mg^{2+} sites probably play a structural role. To investigate the role of the Ca^{2+}-specific (I and II) sites of fast skeletal muscle troponin C (TnC) in the regulation of contraction, we have produced two TnC mutants which have lost the ability to bind Ca^{2+} at either site I (VG1) or at site II (VG2). Both mutants were able to partially restore force to TnC depleted skinned muscle fibers (~25% for VG1 and ~50% for VG2). In contrast, bovine cardiac TnC (BCTnC), which like VG1 binds Ca^{2+} at only site II, could fully reactivate the contraction of TnC depleted fibers. Higher concentrations of both mutants were required to restore force to the TnC depleted fibers than with wild type TnC (WTnC) or BCTnC. VG1 and VG2 substituted fibers could not bind additional WTnC, indicating that all of the TnC binding sites were saturated with the mutant TnC's. The Ca^{2+} concentration required for force activation was much higher for VG1 and VG2 substituted fibers than for WTnC of BCTnC substituted fibers. Also, the steepness of force activation was much less in VG1 and VG2 vs. WTnC and BCTnC substituted fibers. These results suggest cooperative interactions between sites I and II in WTnC. In contrast, BCTnC has essentially the same apparent Ca^{2+} affinity and steepness of force activation as does WTnC. Thus, CTnC must have structural differences from WTnC which compensate for the lack of site I, while in WTnC, both Ca^{2+} specific sites are probably crucial for full functional activity. We are currently investigating the kinetics of Ca^{2+} binding to the proteins and their conformation by physical approaches. To confirm and extend these results, we have also mutated the X-coordinating aspartate residue to alanine in all 4 binding sites. Mutants having 1 or combinations of these changes are being prepared for assay in the skinned fiber system. This work are supported by a grant from the MDA.

Th-Pos34

COMPARITIVE NMR STUDIES OF CARDIAC TROPONIN C AND A MUTANT INCAPABLE OF BINDING CALCIUM AT SITE II. Rui Brito, John A. Putkey, George Krudy and Paul R. Rosevear. Dept. Biochem. and Mol. Biol., Univ. Texas Med. School, Houston.

A mutant of cTnC called CBM-IIA, which cannot bind Ca^{2+} at site II was generated by changing Asp-65 to Ala. CBM-IIA was previously shown to be incapable of regulating contraction in fast and slow skeletal muscle fibers. Analysis of the ^1H NMR spectrum for both CBM-IIA and cTnC by DQF-COSY, NOESY and ^{13}C-editing using [*mcthyl* -^{13}C]Met allowed identification of all aromatic spin system and all 10 Met methyl chemical shifts. All 3 Tyr residues and 2 of the 9 Phe residues were sequence specific assigned. In addition, 4 of the 9 Phe spin systems could be assigned to the N-terminal half and 2 to the C-terminal half of cTnC. A comparison of either the apo or Mg^{2+} bound forms of cTnC and CBM-IIA show very similar ^1H NMR spectra, which suggests that inactivation of Ca^{2+} binding site II by a single mutation, does not greatly alter the tertiary structure of the protein. Cardiac TnC and CBM-IIA were titrated with Ca^{2+} while comparing DQF-COSY spectra to monitor Tyr, Phe and Met methyl protons. Addition of Ca^{2+} sufficient to fill to sites III and IV induced similar spectral changes in both proteins. However, the addition Ca^{2+} sufficient to fill site II induced further changes in the spectra of only cTnC. Differences between the Ca^{2+}-saturated forms of the mutant and wild type protein represent conformational changes specific to binding Ca^{2+} site II and are important for triggering muscle contraction. These differences are confined to the N-terminal half of the cTnC, but the N-terminal helix is not affected. To obtain the total sequence specific assignment of the peptide backbone, the wild type protein was uniformly labeled with ^{15}N. At at least 158 of the expected 171 ^{15}N-H correlations have been detected. Selective ^{15}N-labeling with [^{15}N]Gly permitted identification of the 12 Gly and 4 Ser residues.

Th-Pos35

EVIDENCE FOR THE MECHANISM OF INHIBITION OF TnC REGULATION OF MUSCLE CONTRACTION BY A CALMODULIN BINDING PEPTIDE. Z. Sheng*, B. Pan*, J-M. Francois*, J.T. Penniston*, and J.D. Potter*. *Dept. of Molecular & Cellular Pharmacology, U. of Miami Sch. of Med., Miami, FL 33101, *Mayo Clinic, Rochester, MN. 55905

We have previously reported that a synthetic peptide, C28R2, which corresponds to the calmodulin-binding domain of the rat plasma membrane Ca^{2+} pump, inhibited reversibly the force development of skinned skeletal muscle fibers (Sheng et al. Biophys. J., 1990). To explore the mechanism of this inhibition, we investigated the interaction of C28R2 with troponin C (TnC) and its fragments and the effects of C28R2 on acto-S1 ATPase. In the presence of Ca^{2+}, C28R2 strongly inhibited regulated acto-S1 ATPase, whereas there was essentially no effect in the absence of Ca^{2+}. C28R2 had little effect on the ATPase activity of tropomyosin-actin/S-1. Thus the effect of C28R2 on regulated acto-S1 ATPase appears unlikely to be due to a direct interaction of the peptide with actin. Addition of TnC to C28R2 in solution induced an increase in quantum yield and a blue shift of the fluorescence spectrum of the single tryptophan in C28R2. Fluorescence anisotropy measurements showed that C28R2 bound TnC with high affinity (Ka = 6.46 x 10^6 M^{-1}) and with a stoichiometry of two C28R2/TnC. The thrombin fragment of TnC, TH_3 (residue 1-100), bound one mole of C28R2. We propose that each of the COOH-and NH_2-terminal domains of TnC contains a binding site for C28R2. The inhibitory effects of C28R2 on regulated acto-S1 ATPase and, by inference, on force development were most likely a result of binding of C28R2 to TnC and consequent interference with Ca^{2+} dependent TnI-TnC interaction. (Supported by NIH AR37701).

Th-Pos36

INTERACTION OF CALMIDAZOLIUM WITH RABBIT CARDIAC AND SKELETAL TROPONIN C. ^1C. K. Wang, ^2B. Pan, and ^1A. M. Gordon. ^{1}Dept. of Physiology and Biophysics, SJ-40, Univ. of Washington, Seattle, WA 98195 and ^{2}Dept. of Pharmacology (R-189), Univ. of Miami, School of Medicine, Miami, FL 33101

In this study we explored the interaction between calmidazolium (CDZ), one of calmodulin antagonists, and rabbit cardiac and skeletal troponin C (CTnC, STnC) by measuring the changes in fluorescence intensity and anisotropy. With excitation at 280 nm, the tyrosyl fluorescence intensity of apo-CTnC decreased by 15% at the drug/protein concentration ratio = 0.5:1. A small change in emission intensity was observed when the ratio of drug to protein approached 4:1. However, when the ratio was over 4:1, the shape of emission spectra became distorted. In the Ca^{2+}-saturated CTnC, the intrinsic fluorescence decreased at the low concentration of CDZ. As the ratio of CDZ to CTnC was beyond 10:1, the emission intensity increased with a distortion of the shape of emission spectra. Addition of CDZ to apo-CTnC-IAANS, CTnC labeled with a fluorescent probe IAANS, resulted in an increase of emission intensity with a blue shift of emission peak when CTnC-IAANS was excited at 326 nm, indicating that the probe was in a nonpolar environment. A decrease in the extrinsic fluorescence intensity was observed when the ratio of CDZ to CTnC was greater than 4:1. In the presence of Ca^{2+}, the effects of CDZ on the extrinsic fluorescence were similar, but the reduction of emission intensity occurred at higher concentration of the drug. No distortion of the shape of the extrinsic fluorescence spectra was observed in the presence of CDZ. The drug does not affect the quantum yield of the free L-tyrosine and free fluorescent probe IAANS in aqueous medium. These results suggest that the changes in the intrinsic and extrinsic fluorescence of CTnC must result from conformational change(s) induced by CDZ binding to the protein. The fluorescence anisotropy of the probe was measured isothermally as a function of medium viscosity. At the low concentration of CDZ, the anisotropy increased with increasing medium viscosity. However, in the presence of high concentration of the drug, the anisotropy became much smaller and did not follow Perrin's law, suggesting that the structure of CTnC became more disordered. It is likely that CTnC may lose its functional integrity as the drug concentration increases beyond a critical point. Effects of CDZ on STnC were similar to those obtained with CTnC, but less pronounced. (Supported in part by NIH NS08384, HL31962, and HL07090)

Th-Pos37

Ca^{2+}- and Mg^{2+}-DEPENDENT PROTEIN DYNAMICS IN MONO-CYSTEINE DERIVATIVES OF TROPONIN C (TnC) IN VITRO AND IN CARDIAC MUSCLE CONTRACTION. J.A. Putkey, S. Amed, M.Z. Zhang*, P.E. Hoar#, and W.G.L. Kerrick*#. Dept. of Biochem. and Mol. Biol., Univ. of Texas Med. Sch., Houston, TX., and Depts. of *Mol. & Cell. Pharm. and #Physiol. & Biophys., Univ. of Miami Sch. of Med., Miami, FL.

The amino acid sequence of native cardiac TnC has cysteines at positions 35 and 84. Site-directed mutagenesis was used to generate monocysteine derivatives having only Cys-35 (located in the inactive Ca^{2+}-binding site I), or only Cys-84 (located in the central helix near the N-terminal hydrophobic pocket), and these derivatives were labeled with the sulfhydryl-specific fluorescent probe IAANS. Binding of Ca^{2+} or Mg^{2+} to the high affinity sites of the TnCs gave similar fluorescence results for the monomeric forms or when incorporated in the troponin complexes. Binding of Ca^{2+} to the single low-affinity site in the monomeric protein induced an increase in the fluorescence from IAANS attached to Cys-84, while no fluorescence change was associated with IAANS labeled Cys-35. In the troponin complex, binding of Ca^{2+} to the same site induced an apparent change in the environment of Cys-84 that is similar to that of the monomeric protein as evidenced by an increase in IAANS fluorescence, and in contrast to the monomeric protein, fluorescence from IAANS attached to Cys-35 in the troponin complex showed a large Ca^{2+}-dependent decrease in fluorescence. Substitution of the endogenous TnC in skinned rat cardiac fiber bundles with the monocysteine derivatives labeled with IAANS at Cys-84 or Cys-35 showed a fluorescence increase for the Cys-84 labeled protein, but no fluorescence change for the Cys-35 labeled protein upon titration with Ca^{2+} in the presence of 1 mM Mg^{2+} and 2 mM MgATP, similar to the results for the low affinity site of the monomeric proteins. The degree of fluorescence increase was tightly coupled to Ca^{2+}-activated force. Additionally, in the absence of Ca^{2+}, rigor complexes can induce increases in the IAANS fluorescence of both the Cys-35 and Cys-84 proteins. The data demonstrate that Ca^{2+}-dependent fluorescence from IAANS attached Cys-35 is dependent on whether TnC is monomeric, or how it is associated with other subunits of troponin or other proteins in the skinned fiber, which varies depending on whether the myosin cross-bridges are cycling or in rigor. In contrast, the fluorescent response of the Cys-84 labeled protein to Ca^{2+} is the same whether TnC is monomeric, incorporated into the troponin complex, or reconstituted in skinned cardiac cells.

Th-Pos38

THE REACTIVITY OF SULFHYDRYL GROUPS OF CARDIAC TROPONIN C IN ISOLATED MYOFIBRILS. Ying-Ming Liou and Franklin Fuchs, Department of Physiology, University of Pittsburgh School of Medicine, Pittsburgh, PA 15261

We have recently shown that the reaction of the fluorescent SH reagent 7-diethylamino-3-(4'-maleimidylphenyl)-4-methylcoumarin(CPM) with the SH groups of bovine cardiac troponin C (cTnC) is accelarated by the binding of Ca^{2+} to the single regulatory site, site II (Fuchs, Liou, and Grabarek, J. Biol. Chem. 264:20344, 1989). The increased reactivity could largely be accounted for by an increased exposure of Cys-84, the latter being at the N-terminal end of the central helix, in close proximity to site II. This result was consistent with the model of Herzberg, et al, (J. Biol. Chem. 261:2638, 1986) in which it is postulated that Ca^{2+} induces a movement of helix C away from the central helix, thereby exposing Cys-84. To see whether the same reaction occurs in the intact filament system we exposed bovine cardiac myofibrils to CPM for 10 min in the presence and absence of Ca^{2+}. After terminating the reaction with DTT the myofibrils were subjected to electrophoresis on urea-polyacrylamide gels to separate the cTnC. The gels were scanned for protein content and fluorescence and the relative ratios of CPM incorporation were determined from the peak areas. In the presence of Ca^{2+} there was an approximately 2-fold enhancement in CPM incorporation. Thus it appears that Ca^{2+} induces similar structural changes in solution and in the intact myofibril. Supported by NIH (AR 10551) and AHA, PA affiliate).

Th-Pos39

EXCHANGE OF TnC BETWEEN RABBIT AND BARNACLE MUSCLE FIBERS. Y. Qian, A.M. Gordon and Z.X. Luo, Dept. of Physiology and Biophysics, Univ. of Washington, Seattle, WA 98195

Single rabbit (R) psoas and barnacle (B) (Balanus nubilus) muscle fibers were skinned and force measured at pCa's from 7.0 to 4.0. After treatment with TnC extraction solution [low Mg, low ionic strength, 5 mM K_2EDTA, 0.5 mM TFP (trifluoperazine) added, pH 7.8] for 5 min, maximum force decreased by 75%. (Results were similar without TFP but force decreased less in barnacle fibers.) If then the same species TnC was added, maximum force recovered to 85% of the original. No increase in maximum Ca activated force was observed in TnC depleted rabbit fibers either after incubation with BTnC (containing both isoforms) in a pCa 9.2 relaxing solution with Mg or in a pCa 4.0 contracting solution ($n=10$, $p>0.05$). In contrast, when barnacle fibers treated with the TnC extraction solution were incubated in rabbit fast skeletal TnC in a relaxing solution, the subsequent maximum Ca activated force increased to about 50% of the original maximum ($n=25$, $p<0.01$). This RTnC did not block the binding of BTnC since subsequent treatment with BTnC fully reconstituted the maximum Ca activated force (to 85%). Furthermore, when these barnacle fibers treated to extract TnC were incubated in RTnC in a pCa 4.0 solution, the force recovered to about 80% of the original maximum force, but after a subsequent 1 min wash in TnC free pCa 9.2 relaxing solution, the maximum force in pCa 4.0 returned to about 50% ($n=7$, $p<0.01$). These results suggest that the rabbit TnC recognition sequence may be more complex than in barnacle; and that the barnacle TnC recognition sequence may have at least two different forms in which one recognizes rabbit TnC in the presence of Mg and one only in the presence of Ca. (Supported by NIH grant NS08384.)

Th-Pos40

EVIDENCE THAT INCREASED CROSS-BRIDGES AND FORCE DECREASE THE RATE OF Ca DISSOCIATION FROM CaTn IN BARNACLE MUSCLE FIBERS.
A. M. Gordon and E. B. Ridgway, Depts. of Physiology and Biophysics, Univ. of Washington, Seattle WA 98195 and Medical College of Virginia, Richmond VA 23298.

In single aequorin injected muscle fibers from the barnacle Balanus nubilus a shortening step during the declining phase of the Ca transient decreases force and increases free Ca. We have hypothesized that this "extra" Ca comes from Ca-troponin (CaTn); the affinity for Ca being decreased by cross-bridge detachment accompanying muscle shortening because the rate of Ca dissociation from CaTn is increased (Ridgway and Gordon, 1984). Furthermore, if we assume that the peak amplitude of the "extra" Ca on shortening is proportional to the instantaneous CaTn (at the time of shortening), the time course of the peak "extra" Ca is a measure of the time course of Ca bound to Tn (Ridgway and Gordon, 1984). The hypothesis and assumptions were tested. We measured the free Ca from the aequorin signal and the bound Ca from the "extra" Ca on shortening at different times during the decline in free Ca in a twitch but while force was near its peak and thus relatively constant. These measured free and bound calciums can be fit to an apparent CaTn affinity (K_{app}). When this is done for a series of increasing forces (achieved by increasing the stimulus), the calculated K_{app} increases. If the change in K_{app} is due only to a change in the rate of Ca dissociation from Tn,

$$k_{off}=k_{off}(\text{at } F=0)[0.1+\exp(-\text{Force}(kg/cm^2)/0.3)]/(1.1).$$

Using this feedback function for k_{off}(Force), we can model the free and bound Ca and the "extra" Ca seen with a step decrease in force (to zero) during the twitch; the measured and calculated time courses and magnitudes are in good agreement. This indicates that the "extra" Ca on shortening is consistent with an increase in the rate of Ca dissociation from CaTn caused by decreased force and by cross-bridge detachment. (Supported by NIH grants NS08384, AM35597 and the Virginia Heart Assoc.)

Th-Pos41

CALCIUM BINDING PROPERTIES OF TROPONIN-C AT THE CONTRACTION THRESHOLD IN FROG SKELETAL MUSCLE FIBERS. L. Csernoch, Z. Papp, G. Szücs and L. Kovács. Dept. of Physiol., Univ. Med. School, Debrecen, Hungary.

The strength-duration (S-D) curve for the just detectable movement (checked by eye at 400X magnification) was determined in cut fibers using a single vaseline-gap voltage clamp (sarcomere length = 2.2-2.8 μm, T = 4-6 °C. Myoplasmic calcium transients, derived from antipyrylazo III absorbance changes, were measured at short (10 ms) and long (100 ms) pulse durations of the S-D curve. Though the same contractile activation was reached (threshold movement) the maximal intracellular [Ca^{2+}] increase was different with these two pulses. To characterize the calcium binding to troponin-C (Tn), we assumed, that the maximal saturation of Tn has to reach the same level in each case. The calcium binding was calculated using a first order binding site, and the rate constants (k_{ON} and k_{OFF}) were, thus, selected in order to reach a certain, presumed and equal maximal saturation on the Tn with the short and long pulses. Since the actual maximum of Tn occupancy at threshold activation is not known, different levels, from 5-95% of total sites, were used. It was found that only one k_{ON} - k_{OFF} pair exists for each and every selected maximum, that is, there is an interdependent relation between the rate constants. Moreover, the dissociation constant, calculated using the parameters determined as described above, showed a linear relationship with the reciprocal of the presumed maximal saturation. The slope and the negative of the y intercept corresponded to that intracellular [Ca^{2+}] that is measured when the calcium binding to Tn reaches its maximum. While the time-to-peak and the rising phase of the calculated waveform of the calcium-Tn complex was independent of, or showed little change with the presumed maximal saturation, in the range of 20-80% of the total sites occupied at the peak, the falling phase was prolonged for higher saturations. Supported by the MDA.

Th-Pos42

HALOTHANE DOES NOT ALTER THE BINDING OF CA^{2+} TO THE REGULATORY SITE OF CARDIAC TROPONIN C. Thomas J.J. Blanck, Emilia Chiancone, Daniela Verzilli, Gianni Colotti. Dept. of Anesthesiology and Critical Care Medicine, Johns Hopkins University, Baltimore, Md. and The C.N.R. Center of Molecular Biology, University 'La Sapienza", 00185 Rome, Italy.

The volatile anesthetic, halothane, depresses cardiac contractility in a concentration dependent manner. Its action is believed to be mediated through an alteration in the availability or recognition of Ca^{2+} by Ca^{2+} sensitive sites in the myocardium. Cardiac TnC has two cysteine residues in positions 34 and 85 which have been shown to react with DTNB (5,5'-dithiobis (2-nitrobenzoic acid)) at a rate that depends on the saturation of the low affinity, regulatory Ca^{2+} binding site.[1] We have used this reaction to monitor whether halothane at 1 mM has any effect on the binding of Ca^{2+} to this site. The rate of DTNB binding was measured as a function of Ca^{2+} concentration in the range of 10^{-7} to 10^{-3} M in the presence and absence of 1 mM halothane. The reaction rate is increased over two-fold by Ca^{2+} and the half maximal effect occurs at pCa of 4.4 and is not altered by halothane. We conclude from these data that halothane does not alter the conformation or sensitivity of the low affinity Ca^{2+} binding site in bovine cardiac TnC, and hence that cardiac TnC is probably not a primary site of the negative inotropic effect of halothane.

1. Fuchs, F., Liou, Y., Grabarek, Z. (1989), J. Biol. Chem. 253:5452-5459.

Th-Pos43

EFFECTS OF MCI-154 ON BOVINE CARDIAC TROPONIN C. Ronglih Liao and Judith K. Gwathmey. Department of Medicine (Cardiovascular Division), Beth Isarel Hospital and the Harvard Medical School, Boston, MA 02215

MCI-154 (6-[4-(4-pyridyl)aminophenyl]-4,5-dihydro-3(2H)-pydridazinone hydrochloride) is a new intropic agent reported to have direct effects on the myofilaments. The effects of MCI-154 on structural dynamics and functional properties of bovine cardiac troponin C (BCTnC) were evaluated from measurements of intrinsic fluorescence of BCTnC, which was dissolved in a buffer containing 25 mM MOPS (pH 7.2), 0.1 M KCl, 1 mM EGTA, and 1 mM DTT. The protein, containing three tyrosines and no tryptophan, was excited at 280 nm. The titration of MCI-154 to apo-BCTnC (2 μM) caused a dose-dependent increase in the intrinsic fluorescence. In the presence of 3.5 μM or less MCI-154, a normal tyrosine emission spectrum was observed. Upon increasing the [MCI-154] to the protein, a novel shape of emission spectrum with no emission peak was detected. These results suggested that MCI-154 induced conformational change(s) in the BCTnC, and thus caused an enhancement of the intrinsic fluorescence ([MCI-154] < 3.5 μM). However, when the added drug dose was above a limiting amount ([MCI-154] > 3.5 μM), the protein appears to lose its activity to a certain extent probably due to one or more types of noncovalent forces for stabilizing the protein structure, such as hydrogen bonding and hydrophobic force, being perturbed by the drug. In the presence of Mg^{2+}, an increase in intrinsic fluorescence was observed when the MCI-154 concentration was not higher than 4.3 μM. Above that concentration, a decrease of the protein fluorescence was detected, a state at which the protein activity, at least in part, might be lost. When BCTnC was saturated with Ca^{2+}, the fluorescence of BCTnC remained normal in the presence of 0.5 μM MCI-154. Beyond that point, the emission spectra became distorted. It is likely that the Ca^{2+}-induced exposure of hydrophobic patches on the protein might facilitate the effect of MCI-154. (Supported by NIH HL-39091 and HL-36797).

Th-Pos44

MYOSIN LIGHT CHAINS AND TROPONIN C: COMPARISONS OF ALL AVAILABLE AMINO ACID SEQUENCES. John H. Collins.Dept. Biol. Chem., School of Medicine, and Medical Biotechnology Center, Univ. of Maryland, Baltimore, MD 21201.

Troponin C (TNC), myosin essential light chains (ELC) and myosin regulatory light chains (RLC) evolved from a common ancestor, and contain four similar Ca-binding regions which arose by gene duplication and reduplication. Each of the regions consists of a pair of helices and a central, 12-residue Ca-binding site. Evolutionary changes in the amino acid sequences of many contemporary proteins have resulted in diverse functions in muscle, while maintaining many features of their three-dimensional structures. The purpose of this report is to assemble, evaluate, compare and analyze all the known ELC, RLC and TNC sequences. The literature was exhaustively searched in order to assemble a complete and authoritative collection. Several unpublished sequences from our own laboratory have also been included in the comparisons. The resulting information will be useful for identifying essential, conserved sequences and differences which may have led to functional specialization. An evaluation of the various natural mutants which have been tolerated and conserved throughout the course of evolutionshould be especially helpful in designing site-directed mutagenesis studies. Another important benefit of the sequence comparisons will be to note the variable distribution of amino acid residues which are potential targets for group-specific chemical modification.

Th-Pos45

RESIDUE 57 IN THE REGULATORY DOMAIN OF A MUTANT RABBIT SKELETAL MUSCLE TROPONIN-C CAN BE CROSS-LINKED TO THE INHIBITORY REGION OF TROPONIN-I. T. Kobayashi,*T. Tao,*Z. Grabarek,*J. Gergely and J.H. Collins. Dept. Biol. Chem., School of Medicine/Medical Biotechnology Center, Univ. of Maryland, Baltimore, MD 21201, & *Dept. Muscle Res., Boston Biomedical Research Institute, 20 Staniford St. Boston, MA 02114.

We have been investigating the interaction between troponin-C (TnC) and troponin-I (TnI), using site-directed mutagenesis and photocrosslinking with 4-maleimidobenzophenone (BP-Mal). Previous studies have shown that both the C-terminal domain and the N-terminal, regulatory domain of TnC can interact with the inhibitory region (residues 96-116) of TnI. In the present study, we prepared a mutant TnC (designated TnC-57) in which Ala-57 in the C helix of the N-terminal domain is replaced by Cys and the endogenous Cys-98 is replaced by Leu. The sole Cys in TnC-57 was modified with BP-Mal, and after formation of a binary complex with TnI, crosslinking between the proteins was induced by photolysis. The resulting product was purified, then cleaved with CNBr and several proteases. Peptides containing crosslinks were purified by HPLC and sequenced. We found that the benzophenone moiety of BP-Mal, attached at Cys-57 of TnC-57, is crosslinked to the segment of residues 113-121 of TnI. These results further demonstrate that both the C- and N-terminal domains of TnC interact with the inhibitory region of TnI, consistent with the hypothesis that, in a complex with TnI, TnC adopts a more compact conformation than the one seen in the crystal structure. (Supported by grants from NSF, NIH, AHA and MDA.)

Th-Pos46

BIOLOGICALLY IMPORTANT INTERACTIONS BETWEEN SYNTHETIC PEPTIDES OF THE N-TERMINAL REGION OF TnI AND TnC. S.M. Ngai, R.S. Hodges, Dept. of Biochemistry, University of Alberta, Edmonton, Alberta, Canada T6G 2H7.

Interactions between TnI and TnC play a vital role in Ca^{2+} triggered muscle contraction. Previous experiments on elucidating the molecular details of TnC-TnI interactions mainly involve fragments and/or synthetic peptides of the C-terminal inhibitory region of TnI, residues 104-115 (Grand *et al.*, 1982; Van Eyk & Hodges, 1988). Although this inhibitory site of TnI is of major importance in regulating muscle contraction, it is not the only Ca^{2+}-sensitive IC binding site. We have now focused on the interaction between TnC and the N-terminal region of TnI, which may be another regulatory site. Three TnI peptides of the N-terminal region (residues 1-40, 10-40 and 20-40) were synthesized. The effect of the N-terminal TnI peptides on the acto-S1-TM ATPase activity was investigated. The N-terminal TnI peptides bound to TnC and prevented the release of inhibition of activity induced by either TnI or the C-terminal inhibitory TnI peptide (residues 104-115) by TnC. The effect of the N-terminal peptides was Ca^{2+} dependent. The TnI peptide (1-40) was most effective in preventing the release of inhibition between the N-terminal TnI peptide and TnC. As well, the interaction was studied using HPLC methodology. These results suggest that the binding of the N-terminal TnI peptide(s) to TnC caused a conformational change in the TnC resulting in TnC no longer being able to interact effectively with the C-terminal inhibitory region of TnI.

Th-Pos47

EFFECTS OF PHOSPHORYLATION OF TROPONIN I AND/OR C-PROTEIN ON THE TENSION-pCA RELATIONSHIP OF CARDIAC MYOCYTES. P.A. Hofmann, J.W. Walker and R.L. Moss, Department of Physiology, University of Wisconsin, Madison, WI.

Phosphorylation of myofibrillar proteins by purified cAMP-dependent protein kinase (PKA) was studied in myocytes obtained from adult rat, adult pig, and fetal pig hearts. Treatment of adult rat myocytes with PKA resulted in phosphorylation of both troponin I (TnI) and C-protein. Coincident with phosphorylation of TnI and C-protein there was a decrease in the Ca^{2+} sensitivity of force generation, with no significant change in the steepness of the tension-pCa relationship (Figure). Addition of protein phosphatase 2a to myocytes previously treated with PKA resulted in a reversal of Ca^{2+} sensitivity of force to values similar to those observed prior to PKA treatment. Previous work by Saggin et al (J. Biol. Chem. 264:16299, 1989) indicates that the predominate TnI isoform in the fetal rat heart lacks the amino acids involved in the phosphorylation of TnI. In pig cardiac myocytes, it appears that neither fetal nor adult TnI is phosphorylated since the tension-pCa relationships from adult and fetal pig cardiac myocytes were not significantly affected by treatment with either cAMP-dependent protein kinase or phosphatase 2a. Consistent with this finding, PKA treatment of purified troponin from adult pigs did not phosphorylate any of the troponin subunits. These observations support the hypothesis that TnI rather than C-protein phosphorylation accounts for the decrease in Ca^{2+} sensitivity of tension observed with ß-adrenergic stimulation.

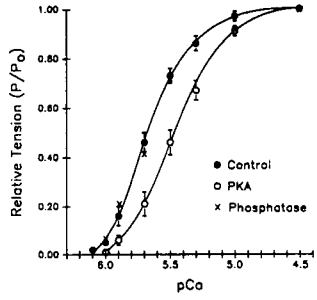

Th-Pos48

FLUORESCENCE STUDIES OF THE STATE OF TROPONIN IN THE RECONSTITUTED THIN FILAMENT. Y. ISHII & S.S. LEHRER BOSTON BIOMEDICAL RESEARCH INSTITUTE. BOSTON MA. 02114

Fluorescence probes attached to tropomyosin (Tm) monitor the "on" and "off" state change of the thin filament induced by the binding of myosin subfragment-1 (S1) (Ishii & Lehrer, Biochemistry **26** 4922, (1987); **29** 1160 (1990)). To determine what changing interaction probes on troponin (Tn) monitor, we used acrylodan (AC) labeled troponin I (TnI) in the Tn complex. The fluorescence of ACTn and ACTn-Tm was Ca^{2+}-dependent, indicating a conformational change of TnI induced by the Ca^{2+} binding to troponin C. Upon binding ACTn-Tm to actin the fluorescence changed in a Ca^{2+} dependent manner. In this reconstituted thin filament, fluorescence resonance energy transfer from tryptophan to AC on TnI was observed. The energy transfer was much less in the presence of Ca^{2+} than in its absence, consistent with Ca^{2+}-induced dissociation of TnI from actin. Binding of S1 reversed the fluorescence change caused by actin both in the presence and absence of Ca^{2+} and decreased the energy transfer in the absence of Ca^{2+}. The titration profile with S1 in the absence of Ca^{2+} showed that the AC fluorescence and the energy transfer were sensitive to both the dissociation of TnI from actin caused by competitive binding of S1 and the S1-induced state change of the thin filament. Thus, these studies indicate that the probe on TnI monitors Ca^{2+}- and S1-induced reorganization of Tn subunits in addition to the state change of the thin filament. Supported by NIH.

Th-Pos49

ISOLATION OF A RABBIT SKELETAL MUSCLE cDNA CLONE FOR TROPONIN I. Z. Sheng, T. Miller, W.L. Strauss & J.D. Potter. Dept. of Molecular & Cellular Pharmacology, U. of Miami Sch. of Med., Miami, FL 33101.

Troponin I (TnI) is the inhibitory subunit of the troponin complex, which is responsible for the regulation of muscle contraction. In order to better understand the molecular events underlying the ability of TnI to inhibit the acto-myosin ATPase activity, we have isolated a cDNA corresponding to the mRNA for rabbit skeletal muscle TnI. A cDNA library prepared from rabbit skeletal muscle mRNA was obtained from Dr. C. Brandl and Dr. D. MacLennan. Approximately 2000 recombinant clones in the vector pCD were screened on replica filters with two nondegenerate synthetic oligonucleotides corresponding to amino acid residues 1-10 and 164-170. Twenty positive clones were identified as being homologous to both probes in the primary screening, suggesting that the abundance of TnI mRNA reflects that of the protein. One clone was purified and its insert was subcloned into M13mp18 and sequenced by the chain termination method. Partial sequence information has revealed that this clone contains 76 base pairs of the 5′-noncoding region. The protein coding and 3′-untranslated sequence are currently being sequenced. To date, the translated sequence of the 5′-coding region of this cDNA has shown complete identity to the published amino-acid sequence (Wilkinson and Grand, 1978; Nature 271:31). Site-specific mutants of TnI will be expressed in E. coli and tested for their effects on the biological activity of TnI in muscle contraction. Supported by the Muscular Dystrophy Association.

Th-Pos50

THE EFFECT OF OSMOTIC COMPRESSION ON CALCIUM BINDING TO SKINNED STRIATED MUSCLE FIBERS. Yi-Peng Wang and Franklin Fuchs, Department of Physiology, University of Pittsburgh School of Medicine, Pittsburgh, PA 15261 (Intr. R.H. Connamacher).

Compression of the myofilament lattice by osmotically active agents causes an enhanced Ca^{2+} sensitivity in both skeletal and cardiac skinned fibers (Godt and Maughan, Pflugers Arch 391:334, 1981; Harrison, et al, J. Physiol. 401:115, 1988). It has been suggested that some of the length-dependent effects on Ca^{2+} sensitivity observed in skinned fibers may actually result from changes in actin-myosin spacing brought about by changes in sarcomere length. This study was carried out to determine if change in interfilament spacing at constant sarcomere length has any effect on the affinity between troponin C and Ca^{2+}. A double isotope technique was used to measure Ca^{2+} binding to detergent-extracted fibers. Filament spacing was reduced by the addition of 5% Dextran T-500. With skinned rabbit psoas fibers there was an increase in the sensitivity of the force response to Ca^{2+} without any detectable effect on the affinity of Ca^{2+} for troponin C. On the other hand preliminary data obtained with skinned bovine ventricular muscle bundles indicate that lattice compression is accompanied by a significant increase in Ca^{2+} binding. We are investigating the possible contribution of this effect to the length-tension behavior of cardiac muscle. Supported by NIH (AR-10551) and AHA, PA affiliate.

Th-Pos51

INFLUENCE OF A TIGHT-BINDING MYOSIN ANALOG, N-ETHYLMALEIMIDE S1, ON CALCIUM-SENSITIVE MECHANICAL PROPERTIES OF RABBIT SKINNED PSOAS FIBERS. D.R. Swartz and R.L. Moss, Dept. of Physiol., University of Wisconsin, Madison, WI. Tight-binding intermediates in the myosin ATPase cycle (S1-ADP and S1-rigor) show highly cooperative binding to regulated thin filaments in the absence of Ca^{2+} and have been proposed to increase the apparent calcium sensitivity of tension in skinned fibers. The influence of N-ethylmaleimide-modified subfragment 1 (NEM-S1) upon Ca^{2+} sensitive mechanical properties (tension, rate of tension redevelopment (k_{tr}) and unloaded shortening velocity) was studied in rabbit skinned psoas fibers. S1 was prepared by chymotryptic digestion of rabbit myosin and was conjugated with NEM. Skinned fibers were incubated with 5-20 μM NEM-S1 in relaxing solution for 5-20 min. During incubation, the resting tension increased to 2-10% of maximal Ca^{2+} activated tension. P_0 was not significantly altered by NEM-S1. The tension-pCa relationship of NEM-S1 treated fibers had a lower Hill coefficient and a slightly higher pCa_{50} (n_H=3, pCa_{50}=5.94) than control fibers (n_H=5, pCa_{50}=5.92). The apparent rate of tension redevelopment increased in NEM-S1 treated fibers at relative tension levels less than 0.70 and varied less with [Ca^{2+}] than control fibers. k_{tr} increased 3-10 fold at relative tension levels less than 0.50, but at higher levels of activation, k_{tr} values were similar to those from untreated fibers. V_{max} measured during maximal activation was not influenced by NEM-S1 treatment while V_{max} at low levels of activation was increased relative to untreated fibers. These observations suggest that tight-binding myosin intermediates influence the level of activation of the thin filament by Ca^{2+}, and these intermediates help to confer activation dependence to k_{tr} and V_{max}.

Th-Pos52

REGULATORY PROTEINS (TROPONIN-TROPOMYOSIN) IN DIABETIC CARDIOMYOPATHY.
Ashwani Malhotra, Frederick S. Fein, M. Cecilia Lopez, Montefiore Medical Center and Albert Einstein College of Medicine, Bronx, NY, 10467.

Cardiac myofibrils from diabetic hearts exhibit depressed Ca^{2+} Mg^{2+} ATPase activity and a downward shift of the Ca^{2+}ATPase dose response curve at different free calcium concentrations. Little is known about the role of troponin-tropomyosin (TnTm) system in the regulation of cardiac muscle in diabetic cardiomyopathy. To focus more on the regulatory proteins (TnTm), individual proteins of the cardiac actomyosin system were reconstituted under control conditions. Cardiac myosin (MY) and TnTm were purified from control (C) and chronic diabetic (D) rats. Hybridization studies were conducted by mixing cardiac C_{MY}, actin plus cardiac TnTm from C or D animals and vice versa. Actomyosin ATPase was determined in the absence of calcium (Mg^{2+} ATPase) and in the presence of 10 uM Ca^{2+}(Ca^{2+}ATPase). Mean results of 3-5 studies for ATPase activity (uM P_i/min/mg) and % inhibition by EGTA are as follows:

	$C_{MY}+C_{TnTm}$	$C_{MY}+D_{TnTm}$	$D_{MY}+C_{TnTm}$	$D_{MY}+D_{TnTm}$
Ca^{2+}ATPase	0.275	0.164	0.197	0.147
Mg^{2+}ATPase	0.056	0.053	0.049	0.056
%Inhibition	80	68	75	62

This preliminary study demonstrates a diminished calcium sensitivity in the regulation of the actomyosin system when regulatory proteins complex was recombined from diabetic hearts. Enzymatic data suggest that besides the shifts of V_1 to V_3 and depressed myosin ATPase, TnTm may be critically involved in the regulation of the actomyosin system in diabetic cardiomyopathy.

Th-Pos53

AUGMENTATION OF Ca^{2+} TRANSIENTS BY Na^+ GRADIENT REDUCTION IN ASTROCYTES AND NEURONS. M.P. Blaustein, B.K. Krueger, P.J. Yarowsky, T.D. Steele & W.F. Goldman, Depts. of Physiol. & Pharmacol., Univ. Maryland Sch. Med., Baltimore, MD.

The influence of the Na^+ gradient on resting intracellular Ca^{2+}, $[Ca^{2+}]_i$, and on glutamate- and K^+-evoked increases in $[Ca^{2+}]_i$ was measured in cultured astrocytes and in striatal neurons from rat brain. The cells were loaded with fura-2, introduced as the acetoxymethyl ester, fura-2/AM; the distribution of apparent free intracellular Ca^{2+}, $[Ca^{2+}]_{App}$, was determined by digital imaging (Goldman et al., Cell Calcium 11:221-231, 1990). In unstimulated neurons and astrocytes, $[Ca^{2+}]_{App}$ was heterogenously distributed; in most cytoplasmic areas, $[Ca^{2+}]_{App}$ was 50-100 nM, but substantially higher levels were seen in some regions. Stimulation with 100 μM glutamate or 100 mM K^+ caused transient, non-uniform increases in $[Ca^{2+}]_{App}$ to levels as high as 1 μM in both astrocytes and neurons. In some instances, cell-cell interactions in the cultures appeared to influence resting and stimulated $[Ca^{2+}]_{App}$. Addition of 1 mM ouabain to the physiolgical salt solution (PSS), or replacement of 135 mM Na^+ in the PSS by isosmolar N-methyl glucamine, for 15 min induced a small, but visible rise in $[Ca^{2+}]_{App}$. Moreover, the amplitude and duration of the transient Ca^{2+} responses to glutamate and K^+ in both neurons and astrocytes were substantially enhanced upon reduction of the Na^+ gradient. When unstimulated cells were exposed to ouabain, subsequent reduction of $[Na^+]_o$ induced a dramatic rise in $[Ca^{2+}]_{App}$. The data indicate that alteration of the plasmalemmal Na^+ gradient alters $[Ca^{2+}]_i$ in both astrocytes and neurons. Reduction of the Na^+ gradient apparently increases not only cystosolic $[Ca^{2+}]_i$, but also (perhaps more importantly) the transient rises in $[Ca^{2+}]_i$ evoked by depolarizing agents. The latter may be due to increased intracellular stores of Ca^{2+} as well as to inhibition of Ca^{2+} extrusion via the Na/Ca exchanger. These data suggest that the Na/Ca exchanger may play an important role in regulating $[Ca^{2+}]_i$ in both astrocytes and neurons, and may be a major determinant of the responsiveness of these cells to neurotransmitters and excitotoxins. Supported by N.I.H. and N.S.F.

Th-Pos54

INITIAL RATES AND KINETIC PROPERTIES OF THE Na/Ca EXCHANGER IN RAT BRAIN PRESYNAPTIC NERVE TERMINALS. Giovanni Fontana & Mordecai P. Blaustein, Department of Physiology, University of Maryland School of Medicine, Baltimore, MD.

Calcium fluxes were measured in rat brain synaptosomes in the presence and absence of external Na^+, Na_o, to determine the "initial rates" and kinetic parameters of Na/Ca exchange in mammalian neurons. Synaptosomes were equilibrated at 30°C for 15 min in physiological salt solution (PSS) that included 145 mM Na^+ and 0.2 mM Ca^{2+}. Ca^{2+} uptake was initiated by dilution with PSS containing ^{45}Ca and various concentrations of ^{40}Ca and Na^+ (N-methyl glucamine replaced Na^+ to maintain isotonicity in low-Na^+ PSS). "Initial rates" of Ca^{2+} uptake (measured at 1 sec) were:

$[Ca^{2+}]_o$ (mM)	$[Na^+]_o$ (mM)	$[Na^+]_i$	Ca^{2+} uptake (pmol/mg protein·sec, p/mgs)	$\Delta J_{Ca(Na)}$*
0.2	4.7	Normal	435 ± 63 (7)	
0.2	145	Normal	133 ± 30 (7)	302
0.2	4.7	"0"†	102 ± 36 (2)	
0.2	145	"0"†	65 ± 68 (2)	37
2.0	4.7	Normal	1544 ±185 (3)	
2.0	145	Normal	758 ± 79 (3)	786

*Ca^{2+} uptake activated by removal of Na_o. †Synaptosomes preincubated in Li^+-PSS to lower $[Na^+]_i$ to "0".

Ca^{2+} uptake was linear for 6 sec with $[Ca^{2+}]_o$ = 0.2 mM, and for 3 sec with $[Ca^{2+}]_o$ = 2.0 mM. The $\Delta J_{Ca(Na)}$ was measured as a function of $[Ca^{2+}]_o$ at 3 sec: apparent K_{Ca} = 0.9 mM; $J_{Ca(max)}$ =1325 p/mgs; Hill coefficient (N) = 0.7. Virtually all the ^{45}Ca uptake activated by removal of Na_o ($\Delta J_{Ca(Na)}$) was Na_i-dependent (Na/Ca exchange; see Table). The Na_i-dependent Ca^{2+} uptake ($[Ca^{2+}]_o$ = 0.2 mM) was inhibited by Na_o with an apparent K_{Na} = 60 mM and N = 1.9. After ^{45}Ca loading (5.8 nmol total Ca/mg protein), almost all of the Ca^{2+} efflux was Na_o-dependent (Na/Ca exchange): 860 p/mgs without FCCP; 1870 p/mgs with FCCP (to release Ca^{2+} from mitochondria and raise $[Ca^{2+}]_i$). A flux of 100 p/mgs corresponds to a change of nearly 30 μmoles of Ca^{2+}/liter cytoplasm/s. Thus, the Na/Ca exchanger in central neurons has a large capacity ($J_{Ca(max)}$) and likely plays a major role in regulating $[Ca^{2+}]_i$.

Th-Pos55

Na^+ and Ca^{2+} CURRENTS OF ADULT RAT COELIAC-MESENTERIC GANGLIA NEURONS. G.O. Carrier and S.R. Ikeda (Sponsor: K. Green). Dept. of Pharmacol. and Tox., Medical College of Georgia, Augusta, GA 30912.

Studies concerning sympathetic neuro-effector mechanisms in resistant blood vessels in adult animals have widely employed the superior mesenteric artery which is enriched highly with postganglionic sympathetic nerve fibers originating from the coeliac-superior mesenteric ganglia complex. In the present study we have examined and defined properties of voltage-gated inward currents carried by Na^+ and Ca^{2+} in acutely dissociated postganglionic sympathetic neurons of the coeliac-superior mesenteric ganglia complex of the adult rat. Voltage-gated inward currents were recorded using the whole-cell voltage-clamp variant of the patch-clamp technique. Current-clamp recordings were performed to establish the electrical viability of the neuron preparation. The average resting membrane potential was -58.0±8.0 mV. Depolarizing current pulses elicited large overshooting (51.1±2.0 mV) action potentials that had a mean threshold of -22.0±1.6 mV, amplitude of 110±1.6 mV, and a dV/dT of 149.6±6.9V/s. With Voltage- clamp recordings, step depolarizations from a holding potential of -80 mV to more positive potentials elicited a transient inward current that was followed by a sustained outward current. Isolation of the inward current by ion substitution indicated that the inward current was carried by Na^+ and Ca^{2+} ions. Inward Na^+ currents were abolished by TTX (1μm), activated at potentials positive to -60 mV, with Vh and K values of -23.8±0.59 mV and 5.87±0.12 mV, respectively and reversed at a potential close to that predicted by the Nernst equation. Na^+ current inactivation was characterized by a Vh and K equal to -71.6±0.95 mV and 7.85±0.16 mV, respectively. Inward Ca^{2+} currents were recorded using Ba^{2+} as the charge carrier and were abolished by Cd^{2+} (500μM). Ca^{2+} current were activated by step depolarization from a holding potential of -80mV to potentials more positive than -60mV, reached a maximal amplitude close to -10 mV and declined at potentials more positive than 0 mV. The N-type Ca^{2+} channel blocker ω-conotoxin (15μM) reduced the maximal Ba^{2+} current amplitude by 65% whereas the L-type Ca^{2+} channel agonist (+)202-791 (1 μm) produced a 20% increase in the maximal current amplitude. These results indicate that acutely dissociated adult coeliac -mesenteric ganglia cells are electrically excitable and contain TTX-senstive Na^{2+} channels and Ca^{2+} channels predominantly of the N-type. (Supported by HL-43242 and Am. Heart GA Affiliate.)

Th-Pos56

CALCIUM- OR BARIUM-ACTIVATED RELEASE OF CALCIUM FROM INTRACELLULAR STORES DURING THE AFTERDISCHARGE IN BAG CELL NEURONS OF APLYSIA.

S. Levy, T.E. Fisher and L.K. Kaczmarek. Dept. of Physiology, Boston Univ. Sch. Med., Boston, MA 02118 and Dept. of Pharmacology, Yale Univ. Sch. Med., New Haven, CT 06510.

Brief electrical stimulation of the bag cell neurons of *Aplysia* initiates a long-lasting period of repetitive firing of action potentials. Using calcium-sensitive microelectrodes we have previously shown that there is a transient rise in intracellular free calcium (Ca_i) during the early part of this afterdischarge (AD). A similar elevation in Ca_i occured when an AD was evoked in media in which external calcium was replaced with barium (Ba-SW) suggesting that there is an active release of calcium from intracellular stores during an AD. To further characterize these phenomenon we used calcium-sensitive electrodes to measure changes in Ca_i in bag cell neurons in primary culture. Following a train of evoked action potentials in normal seawater (NSW), the increase in Ca_i is small. In Ba-SW, the cells respond to stimulation with a prolonged action potential of 30 s or more. There is a robust increase in Ca_i peaking about 30 s after the end af the action potential and lasting several minutes. This increase is most likely caused by barium-activated release of calcium from intracellular stores. The response may be greater than that seen in NSW due to a larger influx of barium than of calcium and to a slower intracellular buffering of barium. Repeated stimuli result in diminishing increases in Ca_i. Stimulation in media containing zero external calcium results in no increase in Ca_i. These data suggest that the elevation in Ca_i during the AD is due at least in part to calcium-activated release of calcium from intracellular stores.

Supported by NSF BNS-8820001 and NIH NS-18492.

Th-Pos57

PERSISTENT Na^+ CURRENT AND Na^+-DEPENDENT K^+ CURRENT IN "GIANT" *DROSOPHILA* NEURONS.
M. Saito and C.-F. Wu, Department of Biology, University of Iowa, Iowa City, IA 52242

A culture system of giant neurons derived from cell division-arrested neuroblasts has been developed to study the genetic control of neuronal excitability in *Drosophila* (J. Neurobiol. 21: 499,1990, Biophysics J, 57: 130a, 1990, Neurosci. abstr, 281.1, 1990). We have identified in this system a persistent Na^+ current and a Na^+-activated K^+ current not previously described in *Drosophila*. The persistent Na^+ current has been shown in other species to support sustained discharge and to control the threshold potential. The persistent Na^+ current was blocked by 10^{-8} M TTX as was the transient Na^+ current. However the two currents could be separated by differences in their inactivation properties. A preconditioning pulse (-30 mV, 500 ms) inactivated the transient current to 20 % of its maximum amplitude, but did not affect the persistent current. The lack of rapid inactivation suggests that this persistent current may generate prolonged depolarization. This could be demonstrated by correlating voltage- and current-clamp data from the same neuron. After application of the K^+ channel blocker (30 mM TEA), all-or-none action potentials became broader and finally developed a long plateau potential. The plateau was eliminated by lowering Na^+ concentration. Subsequent voltage-clamp experiment confirms the presence of the persistent Na^+ current in these neurons. The persistent inward current was only observed with normal Na^+ but not with a low concentration of Na^+ in the bath.

The Na^+-activated K^+ current was decreased by inhibiting Na^+ influx with TTX or Na^+ free saline. The outward current reversed at -80 mV and was not activated by Li^+. The functional roles of the Na^+-activated and persistent Na^+ current may be revealed by mutational analysis.

Th-Pos58

CHOLECYSTOKININ ACTIVATES A VOLTAGE-DEPENDENT INWARD CURRENT IN CULTURED MAMMALIAN SYMPATHETIC GANGLION CELLS. S.R. Knoper, T.L. Anthony, D.L. Kreulen (Intro by Irwin L. Flink) Departments of Pharmacology and Internal Medicine, University of Arizona, Tucson, AZ USA.

Cholecystokinin (CCK) is a putative neurotransmitter in pathways to the prevertebral sympathetic ganglia of guinea pigs. When applied to the surface of intact ganglia or to neurons in primary culture CCK produces a prolonged depolarization (15 s to 2 min). We have evaluated the effects of applied CCK-8 on whole cell currents measured with patch clamp electrodes in 3-10 day old primary cultures of guinea pig celiac neurons. In the whole cell mode cell membrane potentials averaged -59 ± 5 mV (n=11). At holding potentials from -30 to -120 pressure application of 35-100 pmoles of CCK-8 from micropipettes produced an inward current transient the amplitude of which was voltage-dependent. The reversal potential for the inward current was -30 mV (n=2). At a holding potential of -60 mV the peak inward current averaged 365 ± 9 pA and the duration of the current was 38 ± 1 s. In a bath solution containing 105mM Na^+ $CsCl_2$, TEA and 4-aminopyridine the amplitude of the CCK-induced inward current transient was reduced 20%. Steady state inward currents required to step the membrane potential from -30 mV to -40 and -70 mV were determined before and after exposure to CCK. In the presence of CCK-8 the current required to step to -40 mV was increased by 32% whereas the current required for the -70 mV step was increased by 62% suggesting that CCK increased the inward rectification at more negative holding potentials. These experiments demonstrate that CCK depolarizes sympathetic ganglionic neurons by evoking a voltage-dependent inward current. Support: HL27781, ADCRC.

Th-Pos59

PATCH CLAMP AND COMPUTATIONAL STUDIES OF CONDUCTION IN DEMYELINATED AXONS. *Chaim T. Rubinstein*, Michael Hines*, Jin Wu, and Peter Shrager, Dept. of Physiology, Univ. of Rochester, Rochester, NY 14642, and Dept. of Neurobiology, Duke Univ., Durham, NC 27710.*

A computational model has been developed to test the minimum requirements for conduction in remyelinating nerve fibers. At the earliest stages of Schwann cell attachment transmission is successful in large axons when the Na^+ channel density in the internodes is 2 to 6% of the nodal level. The close fit between these calculations and loose patch clamp and optical experiments provides confidence in this model. Further calculations show that lateral diffusion of Na^+ channels from demyelinated nodes into internodes fails to reverse conduction block, and may actually *reduce* the safety factor for propagation. Minimal demyelination that removes only the paranodal axo-glial junctional seals slows transmission significantly, but does not result in block. Limiting internodal K^+ channels to the delayed rectifier type, the model suggested that conduction could be improved in demyelinated fibers by K^+ channel block only in the largest axons. In order to better characterize the K^+ channels in the internode, single channel currents were recorded. *Xenopus* and rat sciatic nerves were demyelinated by an intraneural injection of lysolecithin. Axons were spread apart following dissociation with collagenase. Cell-attached patches with gigohm seals were made to demyelinated internodes. Both K^+ and Na^+ single channel currents were recorded. Several Na^+ channels could be found within a patch, confirming the loose patch estimate of a significant density in the internode. In rat axons a channel with flickering block and a conductance of 200 pS in symmetrical K^+ was tentatively identified as a Ca^{++}-activated K^+ channel. Results of pharmacological block of axonal K^+ channels on conduction in demyelinated fibers will be discussed in terms of its possible therapeutic potential in demyelinating disease. Supported by NS17965 & NS11613.

Th-Pos60

VOLTAGE-SENSITIVE DYES SHOW DIVERSE RESPONSE PROPERTIES OF ELEMENTS IN OLFACTORY RECEPTOR EPITHELIUM SLICES. J.N. Brouwer, P. Farmer & R.C. Gesteland Dept. of Anat. & Cell Biol., Univ. of Cincinnati, Cincinnati, OH.

The electrical activity of constitutive elements of tissue slices can be measured optically using membrane potential-dependent fluorescent dyes. The technique is especially suited for simultaneous observation of the differences in activities of cells in tissues. When voltage changes are relatively slow, such as stimulus-evoked receptor potentials in cells of the olfactory epithelium, the sequential scan of a video camera can be used in place of a diode array as a detector. Cells in 100-μm-thick slices of olfactory epithelia of the tiger salamander *Ambystoma tigrinum* and the frog *Rana pipiens* were loaded with the styryl dye RH 414 (Molecular Probes, Inc) and observed with an inverted microscope with 40x or 63x immersion objectives. Emitted fluorescence was captured by a CCD video camera and averager. Black offset and video gain were adjusted for maximal sensitivity to brightness differences within the frame. An image analyzer was used to perform algebraic operations on the acquired images and to create pseudocolor voltage displays. Immediately prior to each stimulus the level of Ringer's solution in the chamber was reduced so vapors could reach the epithelial surface directly. Stimuli were isoamyl acetate and 2-heptanone. Odorant effects were displayed by subtracting the image taken just before from that acquired 1s after odor application. Depolarization induced by 0.6-1.2mM increases in $[K^+]_o$ decreased fluorescence intensity in most cellular elements. In the salamander, odors evoked dramatic fluorescence changes. These occurred in scattered cell-size patches and were both hyperpolarizing and depolarizing. Membrane potential changes extended from the dendritic knob to deep within the epithelium. In any particular slice only a minority of the cells were affected by the stimulus. Different odors evoked responses in different regions of the slice. The magnitude of fluorescence intensity change increased with stimulus concentration, as did the number of responding tissue elements. Responding elements were widely distributed across the slice. In the frog, odors evoked depolarizations primarily in the olfactory knob region. Only rarely were membrane potential changes seen deeper in the epithelium. It is likely that advanced optical techniques can be used to acquire odor response profiles of separate neurons. Supported by NIH grants DC00352 and DC00347, the Mark P. Herschede Medical Research Fund and the University of Cincinnati Research Challenge Program.

Th-Pos61

PROBLEMS AND SOLUTIONS IN RECORDING AND STIMULATING NEURONS WITH ONE EXTRACELLULAR MICROELECTRODE. Ian D. Hentall, Univ. of Illinois College of Medicine, Rockford, IL 61107-1897.

Electrical signals are deliberately recorded from the brain's extracellular space in studies concerning multi-neuronal activity, or specifically extracellular parameters of single-neurons, or membrane properties of neurons not readily amenable to intracellular penetration or surface clamping. To stimulate through the same microelectrode with brief (e.g. 0.2ms), rectangular pulses and observe the directly excited action potentials requires reduction of artifacts to sub-millivolt amplitudes in times <0.5ms.

The successful device initially had to overcome stimulus artifacts, component saturation, and non-ohmic conduction in electrolyte-filled micropipettes of 1-5MΩ impedance. Electronic switching between the stimulus source and the amplifier solved the first two problems, although high but acceptable switching artifacts arose. More serious were transient tip potentials (TTPs) of up to 50mV after passage of currents >1μA. TTPs were postulated to be due to ion depletion just outside the microelectrodes. They were negative when cations flowed into the tip, and reverted with time-constants also strongly present in the desired recording (0.1-1ms). They increased with the resting electrode impedance, with dilution of the external electrolyte, and with the duration and amplitude of applied current. The mobilities of the small ions in the electrolytes were not as critical. The micropipette's gross shape and glass composition were not influential. Electrode impedances rose during TTPs, e.g. about 50% in 3MΩ electrodes filled with 3M NaCl passing 2μA into 0.1M NaCl.

TTPs were subtracted by differential recording and stimulation through matched micropipettes, one in the brain and one in contiguous saline. Pressure ejection of electrolyte was found to reduce TTP amplitude considerably. With these methods, directly elicited spikes (single or multiple) could be detected 0.5ms after delivery of a rectangular stimulus pulse in the cerebellum of pentobarbital-anesthetized rats. All-or-nothing properties, thresholds, and refractoriness to a second pulse within 2-5ms verified the neuronal nature of the recorded signals. Complex, synaptically generated waveforms unable to follow high frequency stimulation were also seen.

(Supported by grant NS26116 from NINDS.)

Th-Pos62

CHARACTERIZATION OF NON-UNIFORM PROPAGATION IN A SQUID GIANT AXON AND SYNAPSE. J.M. van Egeraat, R.N. Friedman, and J.P. Wikswo, Jr., Vanderbilt University, Department of Physics and Astronomy, Nashville, TN 37235.

We used a magnetic current probe to record the intracellular action current associated with non-uniformly propagating action signals in a squid nerve. The non-uniformity either was caused by a synapse or nerve branch or was the result of an induced axial inhomogeneity such as a nerve crush, intracellular oil block or partial space clamp. The absence of a physical connection with the preparation, a key feature of the magnetic probe, allowed us to obtain multiple measurements at many different positions without the risk of damage that is associated with the use of intracellular microelectrodes.

With the probe, we studied the sequence of events following a nerve crush over a period of 3-7 hours under normal physiological conditions. We observed that the crush blocked propagation and caused a depression of the action current in the region proximal to the crush. There was a retrograde spread of the proximal depression with time, which led to the conclusion that the axon did not seal. The literature reports that other preparations do seal and, in addition, form a partition-like structure in the intracellular space that blocks propagation. We simulated this by injecting a small amount of paraffin oil into the axoplasm and verified that our crush measurements never showed any correspondence to the sealed situation. However, the action signal characteristics obtained from the crushed axon did resemble those of an action signal propagating into a partially space clamped region of an axon. This confirms that the crush can be modelled as a low-impedance pathway to the extracellular space.

Other squid preparations studied included a nerve branch and the giant synapse. By scanning the synapse we could simultaneously measure the pre- and postsynaptic action currents, separated in time by the synaptic delay of 1.0 milliseconds. This shows that the magnetic current probe may be a convenient way to study synaptic transmission.

Supported by a Grass fellowship and NIH grant 1-R01 NS 19794.

Th-Pos63

INTERNAL DIALYSIS, INJECTION OR PERFUSION OF GIANT AXONS DURING HIGH-MAGNIFICATION VIEWING BY LIGHT MICROSCOPY. Harvey M. Fishman and Kirti P. Tewari, Department of Physiology & Biophysics, University of Texas Medical Branch, Galveston, TX 77550-2779.

A method for dialyzing squid giant axons internally (Brinley and Mullins, JGP, 50:2303; 1967) was modified to observe axons under high-magnification (>200X) light microscopy during dialysis, injection or perfusion. External stimulus-response monitoring showed the state of fiber excitability in the affected region. The chamber incorporated a 1 x 3" glass slide. An isolated giant nerve fiber was finely dissected over a 5-cm length, cut to 4 cm and cannulated by placing each cut end onto collinear glass capillaries (300 μm diam.), spaced 3 cm apart, fixed by wax to separate, moveable acrylic blocks resting on the glass slide. Each cut end was secured by closing a loop of fine silk thread, placed loosely on each glass capillary prior to mounting the fiber, until each end of the fiber was firmly against the outer wall of each capillary. The fiber was stretched taut by moving the plastic blocks in opposite directions along the glass slide. A 160-μm diameter dialysis tube with porous length of 1.5 cm, delimited by dye, was moved by hand into the axon until the porous length was midway. Flow initiated through the tube exited the tip extending out of the distal cannula. For internal perfusion a uniform diameter glass capillary replaced the dialysis tube and, to clear axoplasm, the capillary tip was slowly withdrawn to the entry point. For injection the tip of a fine glass pipet was placed in the axon and the tip slowly withdrawn while injecting solution under pressure. This device enables controlled introduction of a variety of substances (e.g., fluorescent dyes, enzymes and antibodies) internally in conjunction with light microscope methods that enable continuous observation of induced modifications in structures. As an example, induced vesiculation is shown after dialysis with Ca^{2+}-containing solutions.

[Aided by ONR contract N00014-90-J-1037]

Th-Pos64

ROLE OF HCO_3^- IN THE REGULATION OF INTRACELLULAR pH (pH_i) IN RAT BRAIN SYNAPTOSOMES. Sergio Sanchez-Armass., Raúl Martínez-Zaguilan* and Robert Gillies*. Dept. de Fisiologia, Univ. de San Luis Potosi. A.P. 1521-B San Luis Potosi, Mexico and Dept. Biochemistry, Arizona Health Science Center, Arizona University*, AZ 85724.

A role for HCO_3^- in regulating pH_i in rat brain synaptosomes was suggested by Richards et.al. (B.B.Acta 803:215;1984). However, Nachshen and Drapeau found no evidence for the presence of either a $NaHCO_3/HCl$ or a Cl^-/HCO_3^- exchange systems (J.Gen.Physiol. 91:289;1988).

Rat brain synaptosomes were loaded with the pH fluorescent indicators pyranine or BCECF-AM, and their fluorescence ratios 465/405 and 500/450, respectively, were used to measure pH_i. Our results indicate that: i) HCO_3^- removal induced a fast cytosolic alkalinization (~0.1 pH units) followed by a slow acidification to a more acidic basal value (~0.1 pH units). The initial raise in pH_i was significantly reduced by DIDS or incubation in Cl^- free solution. ii) The initial recovery rate from an acid load was faster in 24 mM HCO_3^- (0.055 ± 0.009 pH units/min, n=6) than in the absence of HCO_3^- (0.0398 ± 0.012 , n=4). iii) In Cl^- depleted synaptosomes the recovery rate in HCO_3^- free solution was reduced. iv) Cl^- removal in the absence of HCO_3^-, slowly raises pH_i by ca. 0.13 pH units, suggesting that OH^- binds to the HCO_3^- site. v) The resting pH_i with or without bicarbonate was not significantly different, suggesting that HCO_3^- buffers, but does not affect pH_i. In summary, the regulation of pH_i in synaptosomes is a function of the activity of the Na^+/H^+ exchanger, operating as a H^+ extruder, and a Cl^- dependet HCO_3^- antiporter that seems to have the versatility to operate as a buffering system. Supported by SEP C89-01-0093, CONACYT P228CCOX88-0270 to SS-A and NIH R01 GM43046-01 to RJG and RM-Z.

Th-Pos65

INHIBITION OF PHOSPHORYLATION OF SYNAPTOSOMAL PROTEINS BY SNAKE VENOM PHOSPHOLIPASE A_2 NEUROTOXINS AND ENZYMES.
E. Ueno and P. Rosenberg, Sect. Pharmacol & Toxicol., School of Pharmacy, Univ. of Connecticut, Storrs, CT 06269. (Intro. by D. D. Liu, Dept. Cell. & Mol. Physiol. Yale Univ.)

Some snake venom neurotoxins such as β-bungarotoxin (β-BuTX) and notexin which inhibit neurotransmitter release in presynaptic nerve terminals possess phospholipase A_2 (PLA_2) activity. In contrast, most snake venom PLA_2 enzymes are structurally homologous to these neurotoxins but have no specific presynaptic action in vivo although they have higher enzymatic activities than the neurotoxins. To investigate their mechanism of presynaptic action we studied neurotoxin effects on protein phosphorylation. Incubation of cerebral cortical synaptosomes with ^{32}P-orthophosphate (^{32}P-Pi) at 37 ℃ for 30 min, caused phosphorylation of a wide range of proteins including most markedly proteins in the 81-86 kDa range, which is in the mol. wt. range of synapsin I. β-BuTX, notexin and PLA_2 enzymes (N. n. atra and N. nigricollis) (5-50 nM) inhibited phosphorylation (whether added during or after ^{32}P-Pi incubation) in a Ca^{2+}-dependent manner with the following order of potencies: β-BuTX>N. n. atra PLA_2≥notexin>N. nigricollis PLA_2. Using limited proteolysis with S. aureus V8 protease we found synapsin Ia and Ib in the 81-86 kDa peak and inhibition of phosphorylation by β-BuTX (15 nM) in both tail and head region phosphorylation sites. These results indicate that the inhibition of phosphorylation appears to be due to the modulation of either protein kinase or phosphatase, although it has been reported that snake venom PLA_2 neurotoxins and enzymes inhibit ATP synthesis. There is no correlation between their potencies in inhibiting phosphorylation and their levels of PLA_2 activities. Furthermore, the dramatic inhibition of phosphorylation of several synaptosomal proteins including synapsin I by β-BuTX could be at least partly responsible for its presynaptic action. (Supported by NIH Research Grant RO1NS14521 to P. Rosenberg.)

Th-Pos66

THE EFFECTS OF OKADAIC ACID (OA), A PROTEIN PHOSPHATASE INHIBITOR, ON SYNAPTIC TRANSMISSION AT THE CRAYFISH NEUROMUSCULAR JUNCTION (NMJ).
J.E. Swain, R. Robitaille, M.P. Charlton
Intro. by P.S. Pennefather

Synaptic function is dependent on cycling reactions of phosphorylation & dephosphorylation. We assayed the roles of phosphatase activity in synaptic transmission at the crayfish opener NMJ using the permeable phosphatase inhibitor OA. Excitatory post-synaptic potentials (EPSPs) evoked by electrical nerve stimulation were recorded as a measure of neurotransmitter release. OA caused a reversible, dose- & temperature-dependent increase in EPSP amplitude (156±41% @ 1 uM (n=9), 390±34% @ 10 uM (n=14)). The effect saturated at about 5 uM OA, & had a Q_{10} of 8.2.

At 10 uM, muscle input resistance increased (33.2±9.2%), but no significant change in miniature EPSP (mEPSP) amplitude occured at concentrations of OA up to 10uM. Thus OA has a presynaptic effect at 1 uM, but at 10 uM, OA acts has both pre- & postsynaptic actions.

At 10 uM, there was a clear increase in mEPSP frequency (151±4%, n=2). The presynaptic nerve action potential was reduced in duration by 119±54 usec. at 0 mV, & in amplitude by 1.3±0.5 mV. Also, the after-depolarization was decreased by OA. These effects might be masking an even larger effect of OA on EPSP amplitude.

In addition, presynaptic facilitation by serotonin (5-HT) was substantially enhanced (107±39%, n=4) in the presence of 1 uM OA, as if OA augments the phosphorylation caused by 5-HT. Finally, facilitation (3 pulses @ 100 Hz) decreased by 20±11% @ 1 uM OA, and by 51±3% @ 10 uM OA), but there was no effect of OA on facilitation decay. Supported by the MRC of Canada, & the Savoy Foundation for Epilepsy.

Th-Pos67

CONTROL OF ACTION POTENTIAL DURATION AND CALCIUM INFLUX BY A CA-ACTIVATED CHLORIDE CONDUCTANCE IN AtT-20 PITUITARY CELLS
Stephen J. Korn, Arthur Bolden, and Richard Horn
Neurosciences Department, Roche Institute of Molecular Biology, Nutley, NJ 07110

Perforated patch recording and fluorescent measurement of $[Ca]_i$ were combined to study the effect of a Ca-activated chloride current (I_{Cl}) on action potentials (APs) in AtT-20 pituitary cells. These action potentials are typically 2-4 s in duration. The calculated equilibrium potential for Cl (E_{Cl}) was manipulated by alterations in either $[Cl]_i$ or $[Cl]_o$. Setting E_{Cl} more positive increased the duration of APs. Spontaneous APs were not inhibited by setting E_{Cl} negative to firing threshold, although the long-duration plateau was abolished. Voltage clamp experiments showed that Cl conductance was greater than that of Ca or K during the AP plateau. Niflumic acid (≥30 μM) blocked the AP plateau and I_{Cl} without effect on I_{Ca} or I_K. Ca transients, measured in fura-loaded cells, were not affected by niflumic acid (NFA) in voltage clamped cells. Ca transients were temporally associated with spontaneous APs and were blocked by NFA. The duration of these transients in the absence of electrical recording suggests that $[Cl]_i$ is ~45 mM. NFA (≤100 μM) had little effect on either basal or stimulated release of adrenocorticotrophic hormone, suggesting that secretion is not tightly coupled to the transient nature of APs or Ca influx.

Th-Pos68

A MODEL FOR SYNCHRONOUS NEURAL ACTIVITY IN THE VISUAL CORTEX

Ch. Kurrer, B. Nieswand, K. Schulten,
(Intro. by Michael Glaser)
Beckman Institute and Department of Physics
University of Illinois at Urbana-Champaign, Urbana, IL 61801

We modeled the onset of synchronous neural spiking activity in the visual cortex, which has been observed in recent multielectrode recordings by Singer and Gray (PNAS,86,pp.1698, March 1989). The synchronicity of the spiking of neurons is believed to play an important role in visual information processing tasks such as the figure-ground separation.

In our model, we describe the neuron by nonlinear dynamics as an excitable system, and then consider large populations of weakly coupled neurons. Constant background noise is responsible for stochastic firing activity in the neuron population. External excitation of a subpopulation of these neurons will change the firing pattern of those neurons from stochastic to synchronized periodical activity.

After presentation of the mechanism responsible for the onset of synchronized activity, we discuss an application which shows, how this synchronized activity might be used for information processing in the visual cortex.

Th-Pos69

BIOCHEMICAL AND STRUCTURAL ANALYSIS OF LIPID MEMBRANES FROM THE TEMPORAL GYRUS AND CEREBELLUM OF ALZHEIMER'S DISEASE BRAINS.

R.P. Mason, L. Shajenko, T.E. Chambers, H.J. Grazioso, W.J. Shoemaker and L.G. Herbette. Departments of Radiology, Psychiatry, Medicine, the Travelers Center on Aging and Biomolecular Structure Analysis Center. University of Connecticut Health Center, Farmington, CT 06032.

The pathogenesis of Alzheimer's disease (AD) is not well understood. AD is characterized by neuropathological lesions including abundant neuritic (or senile) plaques in the cerebral cortex. The core of the neuritic plaque is composed of β-amyloid, a small polypeptide which is cleaved from the β-amyloid precursor protein (APP), a membrane bound protein. Perturbation in neural membrane structure has been implicated in the abnormal cleavage of the APP and release of the hydrophobic β-amyloid from the membrane. We used small angle x-ray diffraction and biochemical analysis to study lipid extracts from unfractionated homogenates of gray matter in affected (temporal gyrus) and non-affected (cerebellum) regions of AD and control (C) brains. Lipid and protein analysis of seven AD and six age-matched controls showed that the phospholipid to protein mass ratio was unchanged but the cholesterol to phospholipid (C:Pl) mole ratio decreased by 26% ($p < .005$, Wilcoxan two-sample rank test) in the AD temporal gyrus (AD:0.49 ±0.11 versus C:0.66 ±0.05, mean ±S.D.). By contrast, the C:Pl mole ratio in the cerebellum did not change significantly (AD:0.50 ±0.09 versus C:0.45 ±0.09). Small angle x-ray scattering studies on reconstituted lipid membranes showed significant differences ($p < .001$, Student's t-test) in the bilayer width (D-space) and electron density profiles in the temporal gyrus. The D-space was 58.68 ±0.43 Å for AD membranes and 62.61 ±1.22 Å for control samples (mean ±S.D., $n=3$). There were no significant structural differences in the cerebellum of AD and control samples. These data suggest that membrane cholesterol content, which was highly preserved in the control samples, was significantly reduced in only the affected regions of AD brains (e.g., the temporal gyrus). These changes in membrane lipid composition and structure may be related to the pathobiology of AD. [Supported by American Health Assistance Foundation, John A. Hartford Foundation, and AHA-CT Affiliate].

Th-Pos70

OPTICAL MEASUREMENTS OF PRESYNAPTIC CALCIUM DURING SYNAPTIC ENHANCEMENT. K.R. Delaney, W.G. Regehr and D.W. Tank, AT&T Bell Laboratories, Murray Hill NJ 07974. (Intro. by Yuan-chin Ching)

We have used fura-2 imaging to compare the time course of decay of calcium accumulations in presynaptic terminals with the time-course of decay of synaptic enhancement after brief tetanic stimulation.

At the crayfish neuromuscular junction, the decay of synaptic enhancement following intense synaptic stimulation contains exponential components known as augmentation (5-7 sec) and post-tetanic potentiation (>60 sec). We have measured presynaptic calcium beginning 1-2 seconds after tetanic stimulation and observe exponential components for the decay of calcium accumulation identical to those for the decay of the synaptic enhancement. During this period there is a linear relationship between the level of presynaptic calcium and the amount of enhancement. This linear relationship continues to hold when the decay times and calcium levels are modified by exogenous buffer injection or tetanus frequency, suggesting a causal relationship between presynaptic calcium level and degree of enhancement.

We have performed similar measurements in presynaptic terminals of mammalian neurons (see Regehr and Tank for methods). For both mossy fiber synapses onto hippocampal CA3 pyramidal cells and parallel fiber synapses onto cerebellar purkinje cells the decay of accumulated calcium is well fit by an exponential decay with two time constants following tetanic stimulation. For mossy fiber inputs to CA3 neurons the time constants of decay of presynaptic calcium accumulations are similar to those reported for the decay of tetanically-induced short-term enhancement of synaptic transmission (Griffith, 1990, J. Neurophysiol. 63(3) 491), suggesting that the linear relationship between residual calcium and synaptic enhancement may hold at these synapses as well.

Provided such a linear relationship is universal, optical measurement of presynaptic calcium decay may provide an indirect measurement of the kinetics of short term synaptic plasticity, allowing this putative substrate for short-term memory to be easily and extensively mapped in the mammalian brain.

Th-Pos71

SELECTIVE LOADING OF PRESYNAPTIC TERMINALS AND NERVE CELL PROCESSES BY LOCAL PERFUSION OF FURA-2 IN MAMMALIAN BRAIN SLICE W.G. Regehr & D.W. Tank AT&T Bell Labs, Murray Hill NJ 07974.

We have developed a method for filling presynaptic terminals and cell dendrites in adult brain slices with the fluorescent calcium indicator fura-2 by localized perfusion of the acetoxymethyl (AM) ester derivative. The method provides labeling selectivity, similar to that produced by intracellular microinjection of fura-2, with the simplicity of bath application of membrane-permeant AM esters. When applied to mossy fiber tracts in hippocampal region CA3 and parallel fiber tracts in cerebellum the method produced distinct presynaptic terminals well labelled with fura-2 without concomitant postsynaptic labelling, allowing optical measurements of calcium concentration in individual presynaptic terminals. Application of the method to CA1 pyramidal cells produced intracellular loading of apical dendrites with fura-2. Dendritic calcium changes produced by Schaffer collateral stimulation were similar to those determined from cells filled with fura-2 by intracellular microinjection. The local perfusion method appears to be general, and should provide a means to fill projecting axons and dendritic processes in many areas of the brain with fluorescent indicators, allowing optical measurements of ion concentration dynamics to be performed in brain slice that were previously impractical.

Th-Pos72

ARACHIDONIC ACID INCREASES CYTOPLASMIC CALCIUM IN CULTURED OLIGODENDROCYTES. Betty Soliven, Timothy Shandy, and Deborah J. Nelson (Intro. by M. Haas). The University of Chicago, Dept. of Neurology, Chicago, IL 60637.

Changes in $[Ca^{2+}]_i$ play a role in modulating a variety of cellular functions. Measurements of cytoplasmic Ca^{2+} were performed with the fluorescent Ca^{2+} indicator fura-2 (5 μM) in cultured rat and mouse spinal cord oligodendrocytes (OLGs). Perfusion with 70 mM K^+ failed to increase $[Ca^{2+}]_i$, consistent with the absence of voltage-gated Ca^{2+} channels in these cells. In contrast to astrocytes, adult spinal cord OLGs also appear to lack the receptors for various neuroligands linked to Ca^{2+} mobilization such as carbachol, bradykinin, norepinephrine. However, perfusion with arachidonic acid (5-50 μM) (n=7) elicited a concentration-dependent increase in $[Ca^{2+}]_i$ to 3-5 times the baseline level in these cells. The response consisted of a transient phase followed by slower and a more sustained phase. Perfusion with normal bath solution (n=6), 1% ethanol(n=2), other fatty acids (n=4) such as myristic acid, oleic acid had no effect on intracellular Ca^{2+}. In Ca^{2+}-free media (Ca^{2+} omitted, 11 mM EGTA), the response was diminished, but not completely abolished, suggesting the involvement of both calcium influx as well as intracellular calcium mobilization. These findings bear relevance to various inflammatory conditions in which increased arachidonic acid and/or its metabolites may alter calcium-dependent functions of OLGs; prolonged and excessive elevation of intracellular Ca^{2+} following exposure to inflammatory mediators could result in OLG demise. (Supported by MS Society grant RG-2195-A-2 and NIH grant PO1 NS24575).

Th-Pos73

ELECTRICAL RESONANCE IN VESTIBULAR AND AUDITORY HAIR CELLS OF THE ALLIGATOR LIZARD. R.A. Eatock and M. Saeki, University of Rochester, Physiology Department, Rochester, NY 14642.

The hair cells of several auditory and vestibular organs show electrical resonances whose frequencies closely match their mechanical best frequencies (BF's), which are in the range 10-1000 Hz. To examine the role of electrical resonance in tuning outside the 10-1000 Hz range, we are studying the whole-cell currents and voltages of isolated vestibular and auditory hair cells of the alligator lizard. The vestibular cells are primarily from the lagena, which probably detects linear accelerations below 10 Hz. The auditory cells are from a region of the lizard cochlea with BF's between 1 and 4 kHz; tuning in this region may depend on micromechanical resonance (T.F. Weiss and R. Leong, Hearing Res. 20, 157, 1985).

The vestibular cells have large inactivating outward currents which are partly inactivated at -60 mV, and smaller inwardly rectifying and noninactivating outward currents. In current clamp mode, the voltage responses to depolarizing current steps fall to steady-state from an initial peak, suggesting a heavily damped resonance. The auditory cells have large inwardly rectifying currents that activate near -70 mV. Voltage steps above -50 mV activate a non-inactivating outward current. In both cell types, N-shaped steady-state I-V relations suggest a Ca-activated K current. In auditory hair cells, depolarizing current steps evoke damped ringing below 300 Hz. If such resonances contribute to the cells' acoustic tuning, sensitivity should be enhanced for acoustic stimuli at the frequency of the electrical resonance. Instead, the acoustic tuning curves show single resonances between 1 and 4 kHz (T. Holton and T.F. Weiss, J. Physiol. 345, 205, 1983). Thus, the electrical resonance of isolated hair cells is not always consistent with their mechanical tuning *in vivo*.

Supported by NIH 8 R29 DC00414-03.

Th-Pos74

A NON-INVASIVE METHOD FOR RECORDING ACTION POTENTIALS OF TASTE CELLS MAINTAINED IN THE TONGUE.

P. Avenet and B. Lindemann (Intro. by Kurt Beam), II Dept. of Physiology, Univ. of Saarland, D-6650 Homburg/Saar, Germany

Transient currents of 10 ms duration and up to 100 pA amplitude were recorded from single taste pores of taste buds maintained in the tongue of the rat. The monophasic time course and the amplitude of these currents suggest that they are driven by action potentials arising in the receptor cells and that they are conducted by the apical membrane of these cells.
Glass micropipettes of 150 μm tip diameter were positioned onto a fungiform papilla under a dissecting microscope and a loose seal of 50 MOhm was obtained by applying suction. The pipette holder, specially designed, allowed us to simultaneously apply taste stimuli to the taste pore and to record the response of the taste cells, while maintaining the seal. When the pipette was perfused with a low Na, saliva-like solution, spontaneous outward current transients occasionally occurred. When perfusing the pipette with solutions containing salty taste stimuli (200 mM NaCl), a strong increase in the spike rate of the receptor cells ensued. The maximal rate was on the order of 2/s. It was maintained for 10-15 s and was followed by an adaptive decrease to about 0.2/s. Different responses were seen with acid stimulation.
The simplicity of this non-invasive recording procedure allows one to observe the response of receptor cells to chemical stimuli, as reflected by the receptor spike rate, while the cells remain undamaged in their natural environment.
(Supported by the Deutsche Forschungsgemeinschaft through SFB 246, project C1).

Th-Pos75

MODULATION OF POTASSIUM CURRENTS BY SWEETENERS IN HAMSTER TASTE CELLS.

T.A. Cummings, P. Avenet, S.D. Roper and S.C. Kinnamon, Department of Anatomy and Neurobiology, Colorado State University, Ft. Collins, CO 80523 and Rocky Mountain Taste and Smell Center, University of Colorado Health Sciences Center, Denver, CO 80262.

Cyclic nucleotides have been implicated in sweet taste transduction (Striem et al., Biochem. J. 260:121-126, 1989; Béhé et al., J. Gen. Physiol., in press), yet the precise mechanisms involved remain unclear. In this study we have used the whole cell patch clamp technique to investigate the membrane currents of receptor cells in taste buds isolated from fungiform papillae of the hamster, a species which responds strongly to sweet stimuli. When the pipette contained K^+ as the principal cation, most taste cells exhibited large, transient Na^+ currents followed by more sustained K^+ currents in response to depolarizing voltage pulses. When pipette K^+ was replaced by NMDG and the bath contained 100 mM Ba^{++}, voltage-activated L-type Ca^{++} currents were also observed in about half of the taste cells. The artificial sweeteners saccharin and aspartame (20 mM), when bath applied, caused a reversible reduction in voltage-activated K^+ current in about half of the taste cells. The response was variable in magnitude, ranging from 20% - 60% block in different taste cells. The response was mimicked by bath application of 0.5 mM 8-cpt cAMP. In the presence of the nucleotide or the K^+-channel blocker TEA, saccharin caused no further reduction in K^+ current. These data are consistent with the hypothesis that receptor potentials in response to sweeteners are mediated by a cAMP-induced closure of K^+ channels.
Supported by NIH grants DC-00766, DC-00244, and DC-00378.

Th-Pos76

INVARIANT TIME COURSE OF TRANSMITTER RELEASE PREDICTED BY SIMULATIONS OF A CALCIUM DIFFUSION MODEL

Walter M. Yamada & Robert S. Zucker, Molecular & Cell Biology Dept., Univ. of California, Berkeley, CA 94720

When transmitter release is evoked by paired depolarizing pulses at crayfish neuromuscular junctions, the time course of release is unaffected by changes in pulse amplitude and external calcium concentration, and is similar for both pulses, but is sensitive to temperature (Parnas et al., *Biophys. J.* 55:859-874, 1989). The time course of calcium concentration changes at presynaptic release sites ($[Ca^{++}]_i$) was calculated by solving the diffusion equation for calcium influx from arrays of calcium channels opened by the pulses. These simulations showed different changes in $[Ca^{++}]_i$ for the two pulses, and for pulses of different amplitudes and external calcium levels, suggesting that the time course of release is not determined by the time course of $[Ca^{++}]_i$. When calcium was made to bind rapidly to a receptor, and multiple occupied receptors triggered release by a final slow step, the changes in time course of release with pulse amplitude or external calcium level, and between the two pulses, were reduced to the point of being experimentally undetectable. The temperature sensitivity of release arises from the temperature sensitivity of the slow exocytotic step. Our simulations differ from previous simulations arriving at opposite conclusions (*op. cit.*) in the following respects: 1) The calcium unbinding rate was increased from 0.4 to 10 ms^{-1}, reducing calcium affinity from 0.8 to 20 μM and decreasing binding time constant at 2 μM $[Ca^{++}]_i$ from 0.7 to 0.09 ms. This desaturation of transmitter release restored its high sensitivity to changes in external calcium. 2) The interval between pulses was increased from 5 to 15 ms, to match experimental protocols. 3) Pulse amplitudes were chosen so that larger pulses release twice as much transmitter as smaller pulses, to match experimental protocols.
Supported by NIH grant NS 15114.

Th-Pos77

Na/Ca EXCHANGE REGULATES PRESYNAPTIC CALCIUM LEVELS.

K. Zipser, G.J. Augustine & J. Deitmer. Univ. Kaiserslautern, Univ. Chicago, Univ. Southern California & MBL, Woods Hole.

We have used single-cell fluorimetry and ion substitution to examine the role of Na/Ca exchange in regulating presynaptic Ca concentration ($[Ca]_i$) at the squid giant synapse. Microinjected fura-2 and BCECF were used to measure $[Ca]_i$ and presynaptic pH (pH_i), respectively. Replacement of external Na with Li or NMG caused a large and reversible rise in resting $[Ca]_i$, into the uM concentration range. This rise in $[Ca]_i$ is due to an influx of Ca because it was abolished by removal of external Ca. The rise in resting $[Ca]_i$ caused by Na removal is not secondary to a change in pH_i, because pH_i acidified less than 0.05 units during Na removal while acidifying pH_i by as much as 0.3 units (via exposure to 50 mM acetate) had little effect on $[Ca]_i$. Trains of presynaptic action potentials (10-60 Hz, 1-10 s) caused a rise in $[Ca]_i$ into the uM range. Following stimulation, $[Ca]_i$ decayed with at least two components: a fast phase of approx. 10 s duration and a slow phase of more than 100 s duration. Eliminating external Na dramatically slowed the slow phase of $[Ca]_i$ removal, but had little effect on the fast phase. This effect of Na removal also was not secondary to presynaptic acidification, because pH_i decreased by less than 0.02 units during stimulation and acidification by 0.3 units did not slow the slow phase of Ca removal. We conclude that Na/Ca exchange is present in the squid presynaptic terminal and is important both in maintaining resting $[Ca]_i$ and in causing the slow phase of Ca removal following a Ca load. Supported by a Kuffler Fellowship and DFG grant 7/1 to JD and NIH NS-21624 to GJA. We thank PTI for the loan of their Deltascan microspectrofluorimeter.

Th-Pos78

CAN STOCHASTIC VARIATION ACCOUNT FOR THE DATA USED TO SUPPORT THE SUBUNIT HYPOTHESIS FOR TRANSMITTER RELEASE?
W. B. Ferguson and K. L. Magleby, Dept. of Physiology and Biophysics, University of Miami School of Medicine, Miami Fl. 33101.

Magleby and Miller (1981. J. Physiol. 311:267-287) have previously suggested that stochastic variation can give rise to the observations used to support the subunit hypothesis. However, it has been argued that this conclusion is invalid because the experimental data were inadequate. In order to overcome this problem we have examined experimental data that has been recently used to support the subunit hypothesis (Erxleben and Kriebel 1988. J. Physiol. 400:659-676) to test if stochastic variation can account for the data. We find that the apparent regularly spaced peaks in the histograms of number of events versus the amplitude of miniature end-plate currents (MEPC) derived from the experimental data are consistent with the expected stochastic variation for a single gaussian distribution of MEPC amplitudes. The expected stochastic variation for no subunits was determined by assuming a single gaussian distribution could describe the MEPCs. (Gaussian distributions typically give excellent descriptions of the classical MEPC amplitudes). Thirty to forty percent of the histograms from the gaussian distribution appeared to show peaks similiar or better than the experimental histograms used to support the subunit hypothesis. Furthermore, the effects of combining bins were similiar for simulated and experimental data. The experimental effects of physostigmine on the spacing between the apparent peaks could be mimicked by increasing the mean and standard deviation of the gaussian distribution. Approximately 95% of the peaks in the histograms of experimental data fell within the 95% confidence intervals for the gaussian distribution that appeared to fit the data, consistent with random variation. In conclusion, while our findings can not rule out the subunit hypothesis, they do suggest that the recent data used to support the hypothesis appears consistent with stochastic variation. Supported by grants from the NIH (AR32805), MDA and Markey foundation.

Th-VCR1

ROLE OF RESIDUAL CALCIUM IN TRANSMITTER RELEASE AT THE SQUID GIANT SYNAPSE. D. Swandulla, M. Hans, K. Zipser & G.J. Augustine (Intro. by L. Byerly). Max Planck Institute, Goettingen, FRG Univ. Chicago, Univ. Southern California & MBL, Woods Hole.

We have combined digital imaging and electrophysiology to correlate presynaptic Ca concentration, $[Ca]_i$, with evoked transmitter release at the squid giant synapse. Trains of presynaptic action potentials (50 Hz for 1-10 s) produced changes in $[Ca]_i$ that were largest in portions of the terminal that secrete transmitter. When measured within 10 um of the release sites, $[Ca]_i$ gradually accumulated during a train and reached peak levels on the order of 1 uM. Following a train, $[Ca]_i$ decayed slowly over tens of s. During such trains two forms of synaptic plasticity were observed. Under conditions of high release rates (e.g. 11 mM external Ca), synaptic depression developed during the train and, following the train, decayed with a time constant of approx. 5 s. With low release rates [as in low (approx. 1 mM) external Ca], depression was eliminated and an underlying tetanic potentiation (TP) of release was observed. TP increased evoked release by up to 3-fold and decayed with a time constant of approx. 3 s. To evaluate the role of the residual $[Ca]_i$ signal in depression and potentiation, we microinjected EGTA into the presynaptic terminal. EGTA eliminated the slowly-rising $[Ca]_i$ signal produced by trains of action potentials but did not block evoked release, thus acting as a high-pass filter for $[Ca]_i$ signals. EGTA injection blocked TP, but had no obvious effect on synaptic depression. We therefore conclude that residual $[Ca]_i$ is responsible for TP, but not synaptic depression. Supported by a Kuffler Fellowship to DS and NS-21624 to GJA.

Th-Pos79

SPIKE BROADENING IN MAMMALIAN AND AMPHIBIAN NERVE TERMINALS: DIFFERENT PROPERTIES AND DIFFERENT CONDUCTANCES.
A.L. Obaid and B.M. Salzberg. Dept. of Physiology, University of Pennsylvania School of Medicine, Philadelphia, PA 19104-6085.

Secretion from a variety of vertebrate nerve terminals increases non-linearly with firing frequency. This facilitation may be related to the temporal broadening of the terminal action potential (Gainer et al. *Neuroendocr.* 43: 557-636, 1986; Bourque *J. Physiol. (Lond.)* 421:247-262, 1990) that, in the rat neurohypophysis (Jackson et al. *Neurosci. Abstr.* 16: 1013, 1990) enhances Ca^{2+} entry. Such Ca^{2+}-currents may help to define the shape of the terminal action potential, directly, or indirectly through the activation of a Ca^{2+}-dependent K^+ conductance. The latter, however, would tend to shorten the spike. We have examined these issues in neurosecretory terminals of frog (*Xenopus laevis*) and mouse (CD-1) neurohypophyses using voltage-sensitive dyes and optical measurement of membrane potential.

The shape of the terminal action potential in the frog is dramatically altered by organic (ω-conotoxin, FTX) and inorganic (Cd^{2+}, Ni^{2+}, Mn^{2+}, etc.) blockers of Ca^{2+} currents, while in the mouse it is not. In particular, the afterhyperpolarization in the frog reflects a very prominent G_{KCa}, while we find no evidence for this conductance in the mouse. However, secretion from mouse neurohypophysial terminals does depend upon Ca^{2+} entry.

The action potential in the amphibian neurohypophysis also exhibits a different pattern of broadening from that observed in the mammal. In the frog, the spike width reaches its maximum value by the second spike in a train, and then, gradually declines. The broadening increases with frequency up to 30 Hz (150 %). In the mouse, by contrast, the spike broadening is progressive during the train. These differences may be related to differences in the mechanisms of release: in the mammal, Ca^{2+} required for secretion may derive primarily from intracellular stores, triggered by Ca^{2+} entry, and requiring only small transmembrane currents; in the amphibian, much of the activator Ca^{2+} may come from the extracellular space *via* voltage gated Ca^{2+} channels.. The prominence of G_{KCa} in the frog could explain why spike broadening does not progress throughout the train.

Supported by USPHS grant NS16824.

Th-Pos80

PROBING THE TRANSMEMBRANE TOPOGRAPHY OF THE BOVINE HEART MITOCHONDRIAL PORIN.

Vito De Pinto[1], Friederich Thinnes[2], Thomas Link[3] and Ferdinando Palmieri[1] (Intro. by K.W. Kinnally)

[1]Department of Pharmaco-Biology, University of Bari, Bari, ITALY, [2]Max-Plank-Institut for Experimental Medicin, Göttingen, GERMANY and [3]Medical Biochemistry, University of Frankfürt, FRANKFÜRT, GERMANY

We have investigated the transmembrane topography of the mitochondrial porin from bovine heart by means of proteases and antibodies raised against the amino terminal region of the protein. The antiserum raised against the 19 amino terminal residues of porin purified from human lymphocytes reacted with bovine heart mitochondrial porin in Western blots and with the membrane-bound bovine heart porin in ELISA assays. ELISA showed that the amino terminal region of the protein is not embedded in the lipid bilayer but is exposed to aqueous compartments. Intact mitochondria and mitochondrial membrane fractions were subjected to proteolysis by several proteases. Comparison of cleavage patterns of membrane-bound porin in intact or in freeze/thawed mitochondria, in which the internal side of the outer mitochondrial membrane was accessible, showed no difference, thus indicating as the most likely a parallel arrangement of porin in the membrane. The computer search for amphipathic β-strands in the sequence of human porin showed that 16 β-strands can span the phospholipid bilayer. The computer analysis allowed us to draw a possible scheme of the transmembrane arrangement of the mammalian mitochondrial porin.

Th-Pos81

LIPOPHILES WITH DIVERSE STRUCTURES ARE ADDITIVE IN PRODUCING UNCOUPLING OF HEART CELLS **Brian N. Minnich** and **Janis M. Burt**, Dept. of Physiology, University of Arizona, Tucson.

As previously shown, anesthetics such as halothane and ethrane, and fatty acids such as decanoic and oleic, uncouple neonatal rat myocytes in a dose and time dependent manner. We have suggested these and other lipophilic substances produce uncoupling by a common mechanism that involves destabilization of the channel through a disordering effect at the channel-membrane interface. If this is true, combinations of these compounds should be more effective in producing uncoupling than any of the compounds in isolation. We tested this hypothesis using dual whole cell voltage clamp and dye injection techniques. In the presence of extracellular calcium, 2, 1.5, and 1 mM halothane reduced junctional conductance, g_j, by 100, 49, and 13% in 90 ± 10, 133 ± 12, and 107 ± 17 sec, respectively. These values are not different from those obtained in the absence of extracellular calcium. Similarly, 2, 3 and 4 mM ethrane reduced g_j by 40, 46, and 99% in 150 ± 8, 120 ± 11 and 98 ± 11 sec, respectively. The dose dependence of ethrane's uncoupling effect was shifted significantly to the left by 1mM halothane, such that 2, 3 and 4 mM ethrane reduced g_j by 62, 100 and 100% in 113 ± 11, 100 ± 9, and 100 ± 13 seconds, respectively. Decanoic acid (DA) caused complete uncoupling at a concentration of 1 mM. 750 μM DA had no detectable effect on coupling. When combined with 1 mM halothane, 750 μM DA reduced g_j by 69% in 180 ± 12 sec. Oleic acid (OA) completely uncouples heart cells at aqueous concentrations greater than 5 μM in 11 minutes or less. Oleyl alcohol (OAl), the alcohol analog of OA, requires 95 minutes to reduce the incidence of coupling to 25% at its aqueous solubility limit of 50 μM. 1 μM OA approximately mimics the uncoupling time of 50 μM OAl. In combination, these agents reduced the incidence of coupling to 25% in 75 min. The membrane concentration of OA associated with complete uncoupling is on the order of 1-10 mM, the same concentration range at which general anesthetics are known to produce anesthesia. This concentration corresponds to approximately 1 OA molecule for every 100 phospholipid molecules or 1 OA molecule for every protein molecule in the membrane. Thus it is likely that OA causes uncoupling through direct interaction with the channel. The additivity of these various compounds in producing uncoupling supports our hypothesis of a common mechanism of action of these uncoupling agents. Further, the data are consistent with this mechanism involving direct interaction of the lipophiles with the channel. Since all of these compounds are known to disorder membranes in the C9-C18 region, the interaction of the lipophiles with the channel may destabilize through a disordering effect directly on the channel or at the channel-membrane interface. Supported by: PHS HL31008

Th-Pos82

TRIORGANOTIN COMPOUNDS INHIBIT THE MITOCHONDRIAL INNER MEMBRANE ANION CHANNEL (IMAC). Mary F. Powers and Andrew D. Beavis, Dept. of Pharmacology, Medical College of Ohio, Toledo, OH 43699.

IMAC catalyses the electrophoretic transport of a variety of anions through the inner mitochondrial membrane. It is regulated by matrix Mg^{2+} and H^+ and appears to have two mercurial reactive sites on the cytosolic side which also modulate activity (A.D. Beavis, Eur. J. Biochem. 185, 511-519 (1989)). Both mercurials and N-ethylmaleimide react at the first site increasing the IC_{50} values for Mg^{2+} and H^+. Reaction at the second site inhibits transport to an extent which is dependent on the species of both the anion and the mercurial. This second effect is reversed by cysteine.

For many years it has been known that low concentrations of tributyltin inhibit the F_1F_o-ATPase and that higher concentrations catalyse electroneutral Cl^-/OH^- exchange. We have now shown that tributyltin is also a potent inhibitor of IMAC. Unlike inhibition by mercurials, inhibition by triorganotins appears to be complete for all anions. The following doses inhibit malonate uniport 95%: tributyltin (0.8 nmol/mg), triphenyltin (0.8 nmol/mg), tripropyltin (1.2 nmol/mg), triethyltin (64 nmol/mg), trimethyltin (4700 nmol/mg, 0.47 mM). Slightly higher doses are required to inhibit Cl^- and NO_3^- transport. Because the inhibitory concentrations appear to be inversely related to hydrophobicity, we believe they probably bind to a site located in the hydrophobic phase of the membrane.

An interesting feature of this inhibition is that mercurials, such as p-chloromercuribenzenesulfonate substantially increase the inhibitory concentration. This effect is not reversed by cysteine nor induced by N-ethylmaleimide, consequently it appears that a third mercurial reactive site may be involved.

This research was supported by NIH Grant HL 36573.

Th-Pos83

INCORPORATION OF CATION AND ANION CHANNELS FROM STRIPPED ROUGH MICROSOMES ISOLATED FROM RAT LIVER HEPATOCYTES INTO PLANAR LIPID BILAYERS. N. Morier and R. Sauvé. Groupe de Recherche en Transport Membranaire, Université de Montréal, Montréal, Québec, Canada .

It has been proposed that the release and\or re-uptake ofCa^{2+} from IP_3-sensitive internal Ca^{2+} stores in stimulated non-excitable cells is compensated by an opposite charge movement in order to maintain electroneutrality. We have therefore investigated the presence of ionic channels in stripped rough ER (RER) membranes by incorporating ionic channels from RER vesicules into lipid bilayers (PG in decane, 25mg/ml). We found that the fusion of RER vesicules with BLM was enhanced in presence of GTP in accordance with Paiement et al. (BBA 1983, 898:6-22). Three types of channels were observed namely: a voltage-dependent, DIDS sensitive-anionic channel of 180pS in asymetrical 450/50 mM KCl solutions, and two voltage-dependent, TEA- insensitive cationic conductance of 20pS and 90pS recorded in symetrical 450 mM KCl solutions. The 90pS channel activity appeared DIDS and GTP-insensitive but was blocked by Ba^{++} (10mM). The involvement of ionic channels in the Ca^{2+}-uptake and IP_3-Ca^{2+} release processes was also investigated using FURA-2. Results obtained on crude microsomal fractions showed an uptake of Ca^{2+} (≈960 nM) upon addition of ATP and a 13% release by 5uM IP_3 of the Ca^{2+} sequestred. The effects of anionic and cationic channel blockers on Ca^{2+}-released by IP_3-from crude and highly ER enriched liver microsomes will be discussed. This work was supported by FRSQ and MRC.

Th-Pos84

FLUORESCENCE ASSAY FOR ACTIVITY OF A CATION TRANSPORT CATALYST FROM RAT LIVER MITOCHONDRIA. Ranjana Paliwal and Joyce J. Diwan, Biology Dept. & Center for Biophysics, Rensselaer Polytechnic Institute, Troy, NY 12180.

A protein fraction obtained from rat liver mitochondrial membranes by affinity chromatography on immobilized quinine, an inhibitor of K^+ transport, has been reconstituted into phospholipid vesicles by detergent dialysis. The fluorophore 8-amino-1,3,6-naphthalene trisulfonate (ANTS) was trapped inside the vesicles by freeze-thawing. External ANTS was removed by sequential passage through columns of Bio-Rad P-6DG and Bio-Beads. Quenching of the ANTS fluorescence by externally added Tl^+, a K^+ analog, provided a measure of cation entry. The fluorescence was more rapidly quenched when vesicle membranes contained the affinity-purified protein. The data indicate that the quinine affinity column eluate contains a protein which mediates transport of Tl^+. These results are consistent with patch clamp data showing ion channel activity in vesicles reconstituted with the affinity column eluate (Costa & Diwan, Biophys. Soc. Abstr., 1991). Some inhibitors of ion channels in mitochondria and other systems, amiodarone, charybdotoxin, and glybenclamide, were found not to affect the quenching of ANTS fluorescence by externally added Tl^+. MgATP at 0.5 mM also failed to affect uptake of Tl^+ by the reconstituted vesicles. SDS PAGE of the affinity-purified fraction has indicated the presence of protein bands at 97, 77, 57, 53, and 31 kDa. Amino acid sequence analysis has shown that the 53 kDa band is aldehyde dehydrogenase, an enzyme unlikely to have a role as an ion channel (Diwan et al., FEBS Lett., in press). Experiments underway are aimed at determining which of the other protein bands in the affinity column eluate is (are) responsible for the observed cation transport activity. In some studies, preparative SDS PAGE is being used to separately purify each of the proteins of the affinity column eluate.
(Supported by USPHS grant GM-20726).

Th-Pos85

PATCH CLAMP ANALYSIS OF A PARTIALLY PURIFIED ION CHANNEL FROM RAT LIVER MITOCHONDRIA. German Costa and Joyce J. Diwan, Biology Department. and Center for Biophysics, Rensselaer Polytechnic Institute, Troy, NY 12180.

A protein fraction was isolated from detergent solubilized rat liver mitochondrial membranes on immobilized quinine, an inhibitor of K^+ transport. SDS PAGE of the affinity purified fraction indicated protein bands at 97, 77, 57, 53, and 31 kDa. These proteins were reconstituted into phospholipid vesicles by detergent dialysis. The vesicles were then enlarged to a diameter of 10 μm or larger by partial dehydration and gentle rehydration. The resulting vesicles were of suitable size for patch clamp analysis. Patch clamp data recorded using a Dagan 8900 patch clamp amplifier were analyzed using software developed by John Dempster. Patch clamp recordings of excised patches at 30 mv, using a symmetrical solution of 150 mM KCl, 5 mM HEPES, and 0.01 mM $CaCl_2$, showed the presence of a 140 pS channel. This channel favored the open configuration at positive voltages in the inside out mode. A 40 pS channel was less frequently observed and has not been further characterized yet. Control vesicles prepared in the same fashion but without protein showed no channel activity. The results are consistent with fluorescence quenching studies indicating that vesicles reconstituted with the quinine affinity column eluate are permeable to the K^+ analog Tl^+ (Paliwal and Diwan, Biophys. Soc. Abstr., 1991). Current experiments include characterization of the selectivity and voltage dependance of the observed channels. Experiments are also underway to determine which polypeptides in the quinine affinity column eluate are responsible for the ion channel activity. Special thanks to Dr. Kathleen Kinnally for her technical advice and to Dr. Kinnally and Dr. Henry Tedeschi for use of the patch clamp facilities. (Supported by USPHS grant GM-20726).

Th-Pos86

SINGLE-CHANNEL ANALYSIS OF THE EFFECT OF EXTERNAL pH ON THE BRADYKININ-EVOKED Ca^{2+} RISE IN ENDOTHELIAL CELLS. D. Thuringer, A. Diarra and R. Sauvé. Groupe de Recherche en Transport Membranaire. Dépt. de Physiologie. Montréal, Qué. H3C 3J7.

We have used the patch-clamp technique in order to investigate, via the activation of calcium-activated potassium channels ($K(Ca^{2+})$ channels), the effects of extracellular pH (pHo) on the bradykinin-stimulated Ca^{2+} increase in bovine aortic endothelial cells (BAE). In cell-attached experiments, the external application of bradykinin (BK) caused a transient activation of the $K(Ca^{2+})$ channels. Increasing pHo from 7.3 to 9 maintained the channel activity which was not inhibited by withdrawing BK. However, this channel activation process could be blocked either by removing external Ca^{2+}, or by adding a calcium channel blocker such as La^{3+}, or by depolarizing the cells using high K^+ external solution. These results indicate that the Ca^{2+} influx triggered by BK contributes in maintaining the agonist-evoked Ca^{2+} response in high pHo conditions. Changes in pHo did not affect significantly pHi measured fluorimetrically with the H^+ indicator dye BCECF. In addition, increasing pHi by the external application of NH_4Cl at physiological pHo, caused a rapid decline in the $K(Ca^{2+})$ channel activity triggered by BK. In Fura-2-loaded cells, alkaline pHo had no effect on the time course of the Ca^{2+} response to BK in external Ca^{2+}-free conditions, suggesting that the Ca^{2+} extrusion process is not affected by pHo. Our results show that the BK-evoked Ca^{2+} influx which is required to reload internal Ca^{2+} stores, is controled by a mechanism depending on extracellular H^+ ions. This work was supported by MRC, F. Cino del Duca and HSFC.

Th-Pos87

SIMULTANEOUS MEASUREMENT OF INCREASED Ca_i AND SECRETION IN SINGLE, RAT MELANOTROPHS EVOKED BY PHOTOLYTIC RELEASE OF CAGED Ca^{2+}. P. Thomas & W. Almers (Intro. by W. Nonner), Dept. Physiology & Biophysics, U. Washington, Seattle, WA 98195.

To investigate the relationship between intracellular $[Ca^{2+}]$ (Ca_i) and exocytosis we combined flash-photolysis of the caged Ca^{2+} compound DM-nitrophen (DM-n) with determinations of membrane capacitance (C_m, a measure of secretion) in single melanotrophs. Using fura-2, we measured the amplitudes of the rapid jumps in Ca_i elicited by such photolytic release. Photolysis of DM-n by the Ca^{2+}-measuring system was minimized by using brief, low intensity, excitation flashes. Photolysis was achieved by intense (50-244 J) flashes from a Chadwick-Helmuth xenon lamp. When cells were dialysed with 10 mM Ca^{2+}-free DM-n, a 244 J flash raised Ca_i by 10-20 nM and no secretion was observed. In contrast, when cells were dialysed with 10 mM 50% Ca^{2+}-saturated DM-n, a 66 J flash raised Ca_i from ~150 nM to ~1.5 μM; this increase was accompanied by rapid and extensive secretion (see figure). Such experiments will allow closer examination of the regulation and modulation of Ca^{2+}-induced secretion in melanotrophs and other cells.

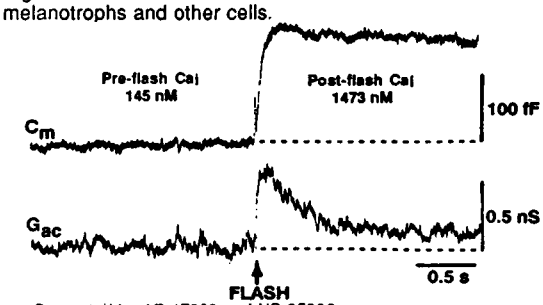

Supported by AR-17803 and NS-25996.

Th-Pos88

EXTERNAL ELECTRIC FIELDS ALTER INTRACELLULAR CALCIUM DISTRIBUTION. R.S. Bedlack, M.-d. Wei, H.M. Smilowitz, and L.M. Loew, Departments of Physiology and Pharmacology, UConn. Health Center, Farmington, CT 06030.
Small endogenous electric fields have been implicated in the control of embryonic development and cell differentiation. Applied fields have also been shown to elicit directed motility or process outgrowth in a number of cells in culture. The mechanism by which these small fields are transduced by the cell are not completely understood, but the membrane is a likely initial site. This is because the voltage across the cell drops essentially completely across the high resistance of the membrane, affecting a large electric field amplification which varies in a complex way along the cell surface. We have been able to use voltage sensitive dyes to map the cell surface distribution of membrane potential induced by external fields via digital fluorescence microscope imaging. Suggestions of the involvement of intracellular calcium as a second messenger in the transduction of the electric field response have emerged from several studies on field-directed motility. Accordingly, we chose to investigate the possibility of changes in intracellular calcium distribution upon exposure to external fields by dual-wavelength ratiometric microscope imaging of fura-2 fluorescence. Our results show that gradients of calcium concentration do, indeed, develop during exposure to fields of 10-15 V/cm over periods of 30 min. Interestingly, the direction of the gradient depends on the cell line. In particular, the neurites and growth cones of N1E-115 neuroblastoma cells show increases in intracellular calcium directed toward the cathode. A model which rationalizes these results involves the electromigration of voltage-dependent calcium channels. (Supported by USPHS grant. GM35063)

Th-Pos89

Localization of the endoplasmic reticulum in living sea urchin eggs and demonstration of its calcium uptake and release properties. M. Terasaki, L.A. Jaffe*, C. Sardet# and T.S. Reese. Lab of Neurobiology, NINDS, NIH, Bethesda, MD, *Dept. of Physiology, Univ. of Connecticut Health Center, Farmington, CT, and #Station Marine, CNRS, Villefranche-sur-mer, France.

The fluorescent dicarbocyanine DiI was microinjected into sea urchin (L. pictus) eggs in a saturated 2-8 picoliter droplet of oil and then observed by laser scanning confocal microscopy. Within 30 min, DiI spread throughout the ER membranes in the egg, staining two distinct but interconnected domains: a dense system of connected cisternae in the interior, and a tubular network adjacent to the plasma membrane. Other organelles, such as cortical vesicles, were not stained. Since diffusion of DiI is confined to continuous bilayers, these results provide evidence that the ER is a single continuous compartment in the cytoplasm. DiI-injected eggs proceeded normally through fertilization and cleavage. When examined in time lapse images of z-series, the ER was seen to concentrate at the poles and line up along the astral microtubules during mitosis; breakdown and reformation of the nuclear envelope were also clearly observed. The distribution and organization of ER membranes is potentially significant because the ER may support Ca transport as well as protein and lipid synthesis. Ca transport properties of the cortical ER were demonstrated by loading fluo-3 AM into the ER of isolated cortices of eggs of the sea urchin A. punctulata. There was a rapid decrease in the fluorescence signal in 1 μm IP3 and re-perfusion with ATP caused a recovery in the signal; this finding shows that the cortical ER is a site of IP3-induced Ca release as well as ATP-dependent Ca uptake (we have not determined the degree to which ER of the interior also transports Ca). Thus, the egg ER membranes form a single compartment which possesses structural and perhaps functional domains, including the Ca transport functions. This interconnected, physiologically active membrane system could thus serve to coordinate large regions of cytoplasm by 1) transmission of signals from plasma membrane to the interior via the cortical ER 2) establishing intracellular ion gradients through regional differences in uptake and release 3) coupling bulk cytoplasmic movements via contacts with microtubules (Terasaki et al., JCB 103 1558) or actin filaments (Kachar and Reese, JCB 106 1545) and 4) regulating metabolic and synthetic processes that occur within its membranes.

Th-Pos90

INTRACELLULAR CALCIUM OSCILLATIONS IN HUMAN PERIPHERAL T CELLS ARE TRIGGERED BY THE T CELL RECEPTOR COMPLEX. Stephen D. Hess and Michael D. Cahalan, Dept. of Physiology and Biophysics, University of California, Irvine CA 92717.

When stimulated with phytohemagglutinin, Jurkat leukemic T cells display oscillations in the concentration of intracellular calcium ($[Ca^{2+}]_i$). We have extended these results by using normal human T cells and cross-linking the T cell receptor with monoclonal antibodies to more accurately mimic the *in vivo* parameters of antigen presentation. T cells purified from human blood were loaded with fura-2 AM and fluorescence ratios monitoring $[Ca^{2+}]_i$ were obtained by alternately exciting the dye at 350 and 385 nm. Cross-linking anti-CD3 monoclonal antibodies bound to the T cell receptor complex elicited a rise in $[Ca^{2+}]_i$ in approximately 64% of the cells; 13% of cells displayed oscillations in $[Ca^{2+}]_i$. In other experiments a conjugate CD3/CD4 antibody (kindly supplied by Dr. Jeffrey Ledbetter) resulted in elevated $[Ca^{2+}]_i$ in 69% of the cells, and 21% of the cells oscillated. In the cells that oscillated after addition of the CD3/CD4 antibody, the latency to the first peak in $[Ca^{2+}]_i$ was 180 ± 65 sec (mean ± S.D. of 70 cells from 3 experiments) at room temperature (22°C). The period of the subsequent oscillations was 130 ± 55 sec. The oscillations in $[Ca^{2+}]_i$ appear to depend upon membrane potential and Ca^{2+} influx, since $[Ca^{2+}]_i$ decreases and the oscillations cease in the presence of high external K^+ or low Ca^{2+} Ringer. Our results indicate that $[Ca^{2+}]_i$ oscillations occur in normal human T cells in response to mitogenic stimulation by the CD3/T cell receptor complex. Supported by grants from Pfizer Inc and NIH (GM 41514).

Th-Pos91

HYPOOSMOTIC STRESS GENERATES CALCIUM TRANSIENTS IN MOUSE THYMOCYTES. Paul E. Ross. Dept. of Physiology and Biophysics, UCI, Irvine, CA 92717.

Lymphocytes are capable of regulating cellular volume in the face of osmotic gradients. These experiments address a possible role of intracellular calcium concentration ($[Ca^{2+}]_i$) during the regulatory volume decrease upon hypoosmotic challenge. $[Ca^{2+}]_i$ in individual mouse thymocytes was monitored by video imaging of fura-2 fluorescence-ratios at 350/385 nm. All experiments were performed at 37°C with continuous chamber superfusion. During exposure to stepwise dilutions of Ringer solution, $[Ca^{2+}]_i$ transients were elicited in an threshold-like manner with individual cells responding at particular osmolarities. $[Ca^{2+}]_i$ transients in 17% of the cells were initiated by exposure to 70% Ringer; responses were recruited in 50% of the cells by exposure to 60% Ringer. During the transient, $[Ca^{2+}]_i$ peaked rapidly at μM levels and subsequently declined, with a time course well-fitted by a double exponential function (average time constants of 17.3 and 340 seconds, n = 125). Futhermore, multiple transient calcium spikes can be elicited with stepwise decreases in superfusate concentration below threshold level; many thymocytes show a graded amplitude of the response with larger calcium transients occurring at lower osmolarities. The rise in $[Ca^{2+}]_i$ appears to be due primarily to transiently induced Ca^{2+} influx, since cells do not respond in hypoosmotic solutions containing zero added calcium. We suggest that Ca-activated K^+ channels may contribute to the volume regulatory mechanism during osmotic challenges beyond a threshold level. Supported by NIH grant # NS14609.

Th-Pos92

IS SLOW WAVE GENERATION AND PROPAGATION IN COLONIC SMOOTH MUSCLE RELATED TO SPATIO-TEMPORAL PATTERNS OF $[Ca^{2+}]_i$? E.A. Mayer, R. Torres, X.P. Sun, A. Kodner, G. Sachs. Dpts. of Medicine and Physiology, UCLA; and CURE VA Wadsworth Medical Center, Los Angeles, Ca. 90073.

Colonic smooth muscle generates spontaneous oscillations in membrane potential. They propagate as slow waves along the intestine, and their frequency (10-35 c·s-1) is not affected by agonists. To determine the intracellular mechanisms underlying this electrical behaviour, we used digital video imaging techniques to study subcellular changes in $[Ca^{2+}]_i$ in freshly dispersed, FURA-2/AM-loaded myocytes from the longitudinal muscle layer of the rabbit colon. **Results**: In resting and stimulated cells, gradients of high $[Ca^{2+}]_i$ were found in the subplasmalemmal space and in one cell pole. These $[Ca^{2+}]_i$ gradients showed temporal and spatial variations in the form of $[Ca^{2+}]_i$ oscillations and Ca^{2+} waves respectively. $[Ca^{2+}]_i$ oscillations in unstimulated cells (n=60) were independent of extracellular $[Ca^{2+}]$ ($[Ca^{2+}]_o$) and had a frequency of 12.6±1.1 c·min^{-1}. Baseline $[Ca^{2+}]_i$ was 171±13 nM and mean oscillations amplitude was 194±12 nM. Ca^{2+} waves originated in the cell pole with high $[Ca^{2+}]_i$, were independent of $[Ca^{2+}]_o$ and propagated along the subplasmalemmal space with a velocity of 23±3 um s^{-1} (n=10). $[Ca^{2+}]_i$ changes induced by carbachol, substance P and membrane depolarization (126 mM KCl) were partially dependent on nifedipine-sensitive Ca^{2+} influx, and were encoded into agonist-specific patterns of changes of baseline $[Ca^{2+}]_i$ and oscillation amplitude, but not into their frequency. **Conclusion**: 1. Colonic myocytes generate spatiotemporal variations in $[Ca^{2+}]_i$ by intracellular mechanisms. 2. Agonists modulate the amplitude of oscillations, involving Ca^{2+} influx through voltage-sensitive Ca^{2+} channels. 3. The observed spatiotemporal pattern of $[Ca^{2+}]_i$ regulation may be responsible for slow wave generation and propagation in this tissue.

Th-Pos93

CALCIUM EFFLUX FROM EARLY EMBRYOS OF THE HYDROZOAN *PHIALIDIUM GREGARIUM*. Ellis B. Ridgway and Gary Freeman, Department of Physiology Medical College of Virginia, Richmond Va 23298 and Department of Zoology Univ. Texas, Austin TX 78714.

We have measured the efflux of labeled calcium from the early embryos of the hydrozoan *Phialidium gregarium*. A large number (50 to 100) of cleavage stage (16 to 32 cell stage) *Phialidium* embryos were loaded with 45-Ca^{++} by two KCl depolarizations separated by a 14 minute recovery period. The efflux of calcium was then followed (for 100 to 150 minutes) by perfusing the embryos with 180 microliters per minute of filtered sea water (FSW) and measuring the counts appearing in the perfusate. The calcium efflux into normal FSW can be fit by the sum of 3 exponentials, suggesting 3 compartments, and the counts remaining in the embryos at the conclusion of the experiment suggest a fourth non-exchanging or very slowly exchanging compartment. Efflux from the two fastest compartments have rate constants of 2 and 0.6/min. and probably represent escape from extracellular regions and/or extracellular binding sites in the extensive jelly coat. The slow exponential efflux with a rate constant of 0.01/min. is probably from an intracellular store. This efflux is unlikely due to sodium-calcium exchange because removing sodium from the perfusing SW has no effect on the efflux. Raising external calcium from 10 to 50 mM also has virtually no effect on the slow calcium efflux, but 50 mM cobalt inhibits it by roughly 35%. Lowering the temperature from 13 to 1 degree centigrade reduces the efflux by about 50%, suggesting the involvement of a calcium pump. About 60% of KCl loaded calcium is virtually unexchangeable during the roughly 2 hrs of the experimental period. Depolarizations induced by KCl can, however, induce a massive calcium efflux which includes much of the otherwise unexchangeable calcium. Supported NSF grants DCB-8904333 and DCB-8904377, and a grant from the Virginia Heart Association.

Th-Pos94

RYANODINE SENSITIVITY OF CAFFEINE-INDUCED INTRACELLULAR CALCIUM RELEASE IN CULTURED EMBRYONIC MOUSE CORTICAL NEURONS. T.D. Tsai and M.E. Barish. Division of Neurosciences, Beckman Research Institute of the City of Hope, Duarte, CA 91010.

We are investigating the role of Ca release from cytoplasmic stores in regulating the intracellular Ca ion concentration ([Ca]i) of embryonic cortical neurons. In muscle, peripheral neurons and other cells caffeine will elicit release Ca from sarcoplasmic reticulum or homologous structures, and this process can be blocked by ryanodine.

Cultures of cortical neurons were prepared from embryonic day 14-16 mice, and were studied after 1-21 days in culture. [Ca]i was measured using the Ca-sensitive dye fura-2 and a video-interfaced fluorescence microscope. In resting unstimulated neurons, application of caffeine (10 mM) elicited a transient increase in [Ca]i in a varying percentage of morphologically-identified neurons. Responses were seen in both Ca-containing and Ca-free external solutions. Acute predepolarization (50 mM K) or glutamate stimulation (100-300 μM), or incubation in a low concentration of glutamate (0.3 μM), increased the proportion of responding cells and the amplitudes of their responses. Repetitive [Ca]i responses (1/5 min) to caffeine were reduced or blocked by ryanodine (0.1-100 μM) in a use- and concentration-dependent manner; with successive applications of caffeine [Ca]i response amplitudes declined more rapidly at higher ryanodine concentrations. As neurons matured the numbers of responding cells and the amplitudes of their responses to caffeine increased, but no change in the sensitivity of caffeine responses to ryanodine was observed. (Supported by NIH, AHA and BRI/CoH).

Th-Pos95

Ryanodine Increases $[Ca^{2+}]_i$ in Rat Descending Colonic Epithelial Cells. L. Reinlib and N. Kraus-Friedman, Div. Intramural Clin. & Biol. Research, NIAAA, Bethesda, MD 20892 and Dept. Physiol. & Cell Biol. Univ. Texas Sch. Med., Houston, TX 77030.

Epithelial cells from rat descending colon were prepared and loaded with Fura-2 (free acid form) using a novel scrape permeabilization technique. The preparations exhibited 75% viability as determined by exclusion of the nuclear stain, propidium iodide. $[Ca^{2+}]_i$ was studied in viable single cells with a microfluorometry system. Morphologic and histologic examination indicated the preparation to be free of non-epithelial cells, including smooth muscle. The cells were perfused in a Dvorak Stottler chamber with Ringer's-HCO3, 10 mM glucose, 10 mM HEPES, pH 7.40 (37°C) and $[Ca^{2+}]_i$ was continuously monitored using excitation wavelengths 345 and 379 nm. Addition of carbachol (100μM) elevated $[Ca^{2+}]_i$ 132 ± 25 nM (n=10 cells) above basal, which was similar to reported measurements in T84 cultured colonic cells (Reinlib et al., Am. J. Physiol. 257: G950; 1989). Ryanodine (200 μM) perfusion increased $[Ca^{2+}]_i$ in 7 of 9 cells studied from the basal level of 102 ± 11 nM to 133 ± 18 nM (n=7) within 60 seconds. Thirteen minutes after ryanodine administration, $[Ca^{2+}]_i$ was still elevated at 128 ± 19 nM. These preliminary data raise the possibility that ryanodine binding sites are present in epithelial cells. (Supported by NDDK 36916).

Th-Pos96

DIFFERENTIAL LOCALIZATION OF RYANODINE RECEPTORS IN THE AVIAN BRAIN. P.D. Walton, Y. Ouyang*, T.J. Deerinck*, M.H. Ellisman*, J.A. Airey, J.L. Sutko. Pharmacology, Univ. of Nevada Reno, NV, 89557; *Neuroscience, U.C. San Diego, La Jolla, CA, 92093.

The avian brain possesses ryanodine binding protein(s) that are biochemically and immunochemically similar to the two ryanodine receptor (RR) isoforms in avian skeletal muscle (Ellisman et al. 1990, Neuron, 5:135-146). Anti-avian skeletal muscle foot protein monoclonal antibodies, 110F (anti-alpha), 110E (anti-beta), and 34C (anti-alpha/beta), were used to investigate the pharmacology and cellular distribution of the multiple RR isoforms in the avian brain. 110F and 110E each immunoprecipitated a distinct RR homotetramer from the avian cerebellum. Both of these RRs have native and subunit mol. wts. of ~2000 kDa and ~500 kDa respectively, and both bind [^{3}H]ryanodine. Only a single RR isoform (beta) was observed in the remainder of the brain. Immunolocalization experiments were conducted using laser-scanning confocal light microscopy to determine the differential distributions of the RR isoforms in avian cerebellum. RR isoform specific intracellular distributions were observed in cerebellar Purkinje neurons. The alpha RR is localized to the soma and dendrites of all Purkinje neurons, whereas the beta RR appears mainly in the neuronal soma, near the plasma membrane, of a subset of alpha positive Purkinje neurons. Electron microscopic analysis demonstrated that the RRs are localized to intracellular membranes in the soma and dendritic shafts, a higher concentration was present at dendritic branch points, but no RR immunoreactivity was present in dendritic spines. Therefore, in contrast to the mammalian brain, which appears to have only one RR isoform, the avian cerebellum possesses two isoforms of the RR that have distinct cellular and intracellular distributions.

Th-Pos97

CAFFEINE- AND RYANODINE-SENSITIVE CALCIUM STORES IN DOG CEREBRUM AND CEREBELLUM. L. G. Mészáros and P. Volpe, Univ. Texas Med. Branch at Galveston, Dept. Physiol. Biophys., Galveston, TX 77550

A number of physiological evidence suggests that, in addition to the well characterized inositol 1,4,5-trisphosphate-sensitive Ca-store, another one sensitive to Ca^{2+} and drugs such as caffeine also exists in neurons. Our results reported here and derived from studies on brain microsomal vesicles indicate the presence of a caffeine-, extravesicular Ca^{2+} and ryanodine-sensitive Ca^{2+} store in both the cerebral and the cerebellar membrane fractions and also describe some of the relevant properties of the store.

In particular, the presence of a high affinity ryanodine binding site with similar characteristics in both cerebrum (CBM) and cerebellum (CBL) fractions was demonstrated (CBM: B_{max}=446 fmol/mg; K_d=9 nM; n (Hill coeff.)=0.95 - CBL: B_{max}=650; K_d=12; n=1.8). The kinetic parameters of Ca^{2+}- and caffeine-induced Ca^{2+} release were also determined: the rate constants of Ca^{2+} release from both CBM and CBL vesicles when previously actively loaded with Ca^{2+} reached the value of 100 s^{-1} as measured by stopped-photometry of arsenazo III absorbance changes. The effect of inhibitors and activators of both ryanodine binding and Ca^{2+} release known from studies on sarcoplasmic reticulum (SR) was also investigated. It was found that except the lowered ruthenium red sensitivity as compared to SR, the properties of both the ryanodine binding and the Ca^{2+} release process of CBM and CBL, in many aspects, resemble those in striated muscle SR. Supported by NIH grant GM 40068.

Th-Pos98

Ca^{2+} DEPENDENCE OF Ca^{2+} RELEASE CHANNEL ACTIVITY IN THE SARCOPLASMIC RETICULUM OF CARDIAC AND SKELETAL MUSCLE. **Seiko Kawano and Roberto Coronado.** Department of Physiology, University of Wisconsin, School of Medicine, Madison, WI,

Ca^{2+} release from sarcoplasmic reticulum (SR) is the key step for E-C coupling in both cardiac and skeletal muscle. To elucidate the properties of Ca^{2+} release from SR, we examined the dependence of opening of ryanodine receptor channel on intra cellular Ca^{2+} using planar lipid bilayer techniques. The SR vesicles were purified from bovine heart and rabbit skeletal muscle. Cs^+ (500 mM) was used as the charge carrier. In both preparations, the Ca^{2+} release channel was activated with > 10 nM Ca^{2+} in the cis side (cytoplasmic side). The slope conductance of heart channel(602 pS) was smaller than that of skeletal one(723 pS). The open probability(P_o) increased with raising calcium concentration and reached a peak around 10 uM. However, at higher Ca^{2+} >~10 uM, P_o decreased and became null at 1 mM Ca^{2+}. Thus the curve of P_o-Ca^{2+} relationship formed a bell-shaped configulation. The max. P_o value of heart was 5-6 times higher than that of skeletal channel at each calcium concentration. ATP increased max. P_o values and shifted the P_o-Ca^{2+} curves to the left in the both preparations. Millimolar Mg^{2+} completely blocked the channel activity at the ranges between 10 nM and 10 uM Ca^{2+} in the presence of 5 mM ATP. At more than 0.1 mM Ca^{2+}, 1 mM Mg^{2+} failed to block this channel. The blocking effect of Mg^{2+} was concentration dependent in the presence of 5 mM ATP and 1 uM Ca^{2+}. The half-maximal blocking occured at pMg^{2+} 4.4. From these results, it is suggested that the ryanodine receptor channel has at least two calcium sensitive sites(the activation site and the inactivation site) on the cytoplasmic face. These Ca^{2+} sensitive sites are modulated by ATP and Mg^{2+}.

Th-Pos99

INOSITOL 1,4,5-TRISPHOSPHATE-GATED CHANNELS IN CEREBELLUM AND SMOOTH MUSCLE: PRESENCE OF MULTIPLE CONDUCTANCE STATES. J. Watras, I. Bezprozvanny, and B.E. Ehrlich. Departments of Medicine and Physiology, University of Connecticut, Farmington, CT 06030

The mechanism by which inositol 1,4,5-trisphosphate ($InsP_3$) induces calcium (Ca) release from the reticulum of canine cerebellum and aortic smooth muscle was examined. Reticular membrane vesicles used in these experiments accumulated Ca in the presence of ATP, and then released ~30 % of the accumulated Ca upon addition of micromolar concentrations of $InsP_3$. When these membrane vesicles were incorporated into planar lipid bilayers, $InsP_3$-gated Ca channels were observed. Up to four current amplitudes were observed at a given voltage, yielding conductances of 20, 40, 60, and 80 pS. Thus, the cerebellar $InsP_3$-gated calcium channel exhibits four conductance levels which are multiples of a unit conductance step. Moreover, examination of the single channel records showed both openings directly to each of the current levels as well as rapid transitions between current levels. Similar results were obtained with reticular membranes isolated from aortic smooth muscle. These four conductance steps may reflect the interaction among the four $InsP_3$ receptors thought to comprise the $InsP_3$-gated Ca channel in these tissues. Examination of the $InsP_3$ dependence of channel opening or Ca release from vesicles, however, yielded Hill coefficients of 1-1.3. Thus, we hypothesize that it takes only one molecule of $InsP_3$ to open the channel to any of the four conductance levels. The observation that the conductance of the $InsP_3$-gated Ca channel assumes four levels which are multiples of a unit conductance suggests that the number of interacting $InsP_3$ receptors in one complex can vary from one to four and supports the hypothesis that the channel is a tetramer.

Supported by NIH grant HL-33026. BEE is a Pew Scholar in the Biomedical Sciences.

Th-Pos100

INOSITOL 1,4,5-TRISPHOSPHATE-GATED CALCIUM CHANNELS IN CEREBELLUM AND SMOOTH MUSCLE: EFFECTS OF POLYANIONS. J. Watras, I. Bezprozvanny, K. Ondrias, and B.E. Ehrlich. Depts of Med. and Physiol., Univ. of CT, Farmington, CT 06030

The mechanism by which polyanions inhibit the inositol 1,4,5-trisphosphate ($InsP_3$)-gated calcium (Ca) channel in reticular membranes from cerebellum and aortic smooth muscle was examined. Heparin, for example, is a polysulfated compound which acts as a potent competitive inhibitor of $InsP_3$-induced Ca release from vesicles with $K_{0.5}$ = 4 ug/ml and blocks $InsP_3$-gated Ca channels in bilayer experiments. The Hill coefficient of heparin inhibition in vesicle release experiments was 2.7, suggesting that cooperative binding of heparin to three $InsP_3$ receptors in the Ca channel complex closes the channel. Several other polysulfated compounds (dextran sulfate (40 kDa or 500 kDa) and polyvinyl sulfate (~100 kDa)) also yielded Hill coefficients of 2.5-3.2 for the inhibition of $InsP_3$-induced Ca release. In contrast, low molecular weight (5 kDa) heparin and dextran sulfate yielded much lower Hill coefficients for the inhibition of $InsP_3$-induced Ca release (0.8-1.4). We hypothesize that small polyanions (<15 kDa) are binding to single receptors of the tetrameric $InsP_3$-gated channel complex. The cooperativity of binding of the large polyanions (>15 kDa) suggest that the receptors are in close association and that binding of one large polyanion affects binding of additional polyanions to contiguous $InsP_3$ receptors. Note that a variety of other polyanions (de-N-sulfated heparin, chondroitin sulfates, glucosamine disulfates, polygalacturonic acid, all at 50 ug/ml) were without effect on the $InsP_3$-induced Ca release. Moreover, these effects of the polyanions were not a general property of all Ca release channels because in skeletal muscle sarcoplasmic reticulum large polyanions such as heparin and polyvinyl sulfate opened the Ca release channel. Supported by NIH grant HL-33026. BEE is a Pew Scholar in the Biomedical Sciences.

Th-Pos101

CALCIUM BINDING PROPERTIES OF THE MITOCHONDRIAL CALCIUM TRANSPORTING GLYCOPROTEIN. G. Mironova, Zh. Utesheva, T. Sirota. (Intro. by K.D. Garlid) Institute Biological Physics of Acad. Sci. USSR, Pushchino, USSR, 142292

One of the ways to study the molecular mechanism of calcium transport in mitochondria is to isolate, identify and reconstitute the protein responsible for transport. We isolated a 40 kDa calcium-transporting glycoprotein from beef heart mitochondria (Mironova et al., J. Bioenerg. Biomembr. 14, 213-225, 1982). Reconstitution of this glycoprotein into lipid bilayers shows that the protein forms calcium-selective, ruthenium red-sensitive conductance channels. Data presented here indicate that the calcium-transporting glycoprotein is a complex consisting of the glycoprotein itself and a low-molecular weight peptide component. A technique was elaborated to divide the complex into constituents. It was found that the channel-forming part of the complex is the peptide. Pronase treatment of this component eliminates its calcium transporting properties. The glycoprotein component is unable to transport Ca^{2+} and probably fulfills a regulatory function. The glycoprotein-peptide complex contains calcium binding sites with high affinity (K_d = 3.8 x 10^{-6} M) and low affinity (K_d = 4.3 x 10^{-5} M), whereas the separated glycoprotein component contains only sites with high affinity for calcium (K_d = 5.8 x 10^{-6} M). A model for the glycoprotein-peptide complex functioning in the electrophoretic transport of calcium in mitochondria is suggested. Supported in part by NIH grants HL 36573 and HL 43814.

Th-Pos102

THE STABILITY OF A LAC REPRESSOR MEDIATED "LOOPED COMPLEX" IS DIMINISHED BY THE ACTIVATOR PROTEIN CAP. Dennise Dalma-Weiszhausz, Elizabeth Jamison, Amy Pickar & Michael Brenowitz, Department of Biochemistry, The Albert Einstein College of Medicine, Bronx, NY 10461.

The binding of wildtype Lac repressor (LacI) to two sites that are separated by 11 helical turns on a fragment of linear DNA was investigated by quantitative footprint and mobility-shift titration studies. The results of this analysis showed that ~65% of the molecules present in solution are looped complexes at pH 7.0, 100 mM KCl and 20° C when the binding sites on the DNA are saturated with protein. However, Lac repressor binding to this DNA was only moderately cooperative; a cooperative free energy of -1.0 kcal/mol was calculated from the individual-site loading energies. Reconciliation of these experimental observations could only be obtained when the titration data were analyzed by a model in which Lac repressor tetramers dissociate into dimers in solution. This result is consistent with the determination by high-pressure fluorescence techniques of the dimer-tetramer dissociation free energy of Lac repressor [Royer, C.A., Chakerian, A.E. & Matthews, K.S. (1990) *Biochemistry 29*, 4959-4966]. The proportion of looped complexes present in solution is dependent on the dimer-tetramer association constant. Quantitation of the DNase I hypersensitivity observed in footprint titrations in bands located between the two binding-sites and the resolved "looped" and "tandem" complex bands in the mobility-shift titrations allowed an assessment of the dimer-tetramer association constant to be made. When the dimer-tetramer association constant of -10.6 kcal/mol reported by Royer et al. (1990) is assumed, the titration data demand that tetramers bind DNA with much greater affinity than dimers; a result inconsistent with the destabilization of tetramers by operator observed in the dimer-tetramer dissociation studies. Analysis of the titration data subject to the assumption that the DNA-binding affinity of dimers and tetramers are identical yields a value of free energy of dimer-tetramer association, ΔG_{ass}, of -13.2 ± 0.5 kcal/mol and a free energy describing loop formation, ΔG_{loop}, of +12.0 ± 0.3 kcal/mol. Since the intrinsic free energies of Lac repressor binding to the DNA sites is -13.7 ± 0.2 kcal/mol the result is a looped complex that is only twenty fold more stable than the DNA-tetramer complex containing only a single protein-DNA interaction. A value for the cyclization probability, or "j-factor", for this complex of 1×10^{-9} was calculated from ΔG_{loop}. This value corresponds to that predicted for a DNA fragment of approximately 17 helical turns; significantly longer than the 11 turn spacing between the two protein binding sites.

The distance of the centers of the two LacI binding sites from the center of the CAP site are 1.8 and 10.0 helical turns, respectively, on this DNA. The presence of saturating concentrations of CAP had no effect on either ΔG_{loop} or on LacI binding to the distal site. However, saturating concentrations of CAP *decreased* the binding of LacI at the proximal site by 1.3 ± 0.2 kcal/mol, thereby decreasing the stability of the complex. These results differ from the reported cooperative interaction of CAP and LacI where the center to center distance of the CAP and LacI binding sites are 6.9 helical turns apart [Hudson, J.M. & Fried, M.G. (1990) *J. Mol. Biol. 214*, 381-396]. (Supported by NIH Grant GM 39929).

Th-Pos103

COMPARISON OF OPERATOR-SPECIFIC AND NONSPECIFIC DNA BINDING OF THE LAMBDA *cI* REPRESSOR: PH AND [KCL] EFFECTS. R. Batey and D.F. Senear, Department of Molecular Biology & Biochemistry, University of California, Irvine, CA 92717.

The effects of proton activity and KCl concentration on the non-specific interactions of the cI repressor and DNA, and on the site-specific repressor-O_R interactions were compared, in order to asess their roles in site specificity. Non-specific binding was studied using a nitrocellulose filterbinding assay. Filterbinding proves advantageous in this case, due to the relatively weak non-specific binding under the conditions used, and aggregation of repressor at high concentration. By using large DNA fragments (>1000 bp), binding was monitored in a represssor concentration range well below the half-saturation point, where aggregation does not occur. The data provide estimates of the intrinsic ΔGs for non-specific binding, but not for cooperativity. Salt effects on the cooperative repressor-O_R interactions were studied using DNase footprint titration. The ΔGs for binding and for cooperativity were determined between 25 mM and 300 mM KCl, from individual site isotherms resolved for the binding of repressor to each site of O_R and to reduced valency mutants. The proton-linked effects on repressor-O_R interactions have been published (Senear, D.F. & Ackers, G.K. (1990) *Biochemistry 29*, 6568-6577). Above neutral pH, the proton linkages to specific and non-specific binding are similar. Significant differences below neutral pH implicate at least one protein group with a pK_a near 6 that plays a role in discriminating between operator and non-operator DNA, as well as between the three operator sites. The [KCl] dependence of the non-specific binding free energy, of the operator specific binding free energies, and of the pairwise cooperative free energies all define a transition near 0.1 M KCl. A transition in repressor structure or conformation provides the simplist single explanation for this. Above this transition point the slopes, $d\ln k/d\ln[KCl]$, are significantly greater for binding to O_R1 and O_R2 than to O_R3, but are the same for O_R3 and non-specific DNA. The data were analyzed subject to the simplifying assumption that the dimer dissociation is independent of [KCl]. The results for the (weak) repressor binding to O_R3 and to non-specific DNA are nearly independent of this assumption. The expectation that repressor dimers are preferentially stabilized by increasing [KCl] leads to even larger differences in KCl effects between the three operator sites. These facts indicate the importance of ion binding and release to the ability of the repressor to discriminate between the three operator sites, but suggest similar overall modes of binding to operator and non-operator DNA.

Th-Pos104

THERMODYNAMIC STUDIES ON CRO REPRESSOR-DNA INTERACTIONS

Yoshinori Takeda[1], Philip D. Ross[2] and Courtney P. Mudd[3]; [1]Laboratory of Molecular Biology, NCI-FCRF, PRI, Frederick, MD 21701, [2]Laboratory of Molecular Biology, NIDDK, NIH, Bethesda, MD 20892, [3]Biomedical Engineering and Instrumentation Branch, DRS, NIH, Bethesda, MD 20892

Using a computer controlled highly sensitive pulsed-flow microcalorimeter, we have determined the changes in enthalpy and heat capacity for Cro-DNA association reactions. (1) The ΔH upon the formation of the specific Cro repressor-OR3 operator DNA complex (OR3 operator is the highest affinity binding site for Cro repressor) is endothermic below 15° and exothermic above 15°. ΔCp = -282 cal/mol/deg. (2) The ΔH accompanying the formation of the nonspecific DNA complex is slightly positive and ΔCp is zero. (3) The ΔCp's for the formation of other specific DNA complexes fall in between. We have observed a linear correlation between the specific DNA binding affinity ΔG and heat capacity change ΔCp. (4) In order to understand what forces govern the Cro-DNA association reaction, we have studied the effects of single amino acid and/or single base substitution mutations on ΔG, ΔH, TΔS and ΔCp. Studies suggest that both specific and nonspecific Cro-DNA association reactions are entropy-driven. The stability of the specific complex is governed mainly by the specific H-bonds and van der Waals contacts, while charge interactions and hydrophobic effects, make only a moderate and minor contribution.

Th-Pos105

DNA-induced Dimerization of *Escherichia coli* Rep Helicase.

Kinlin Chao[1] and Timothy M. Lohman[1,2] 1. Biochem. & Biophysics, Texas A & M Univ., College Station, TX 77843 2. Biochem & Mol. Biophysics, Wash. Univ. School of Medicine, St. Louis, MO 63110

Escherichia coli Rep protein, a helicase, unwinds duplex DNA with an apparent 3' to 5' directionality, in an ATP-dependent reaction. In order to probe the mechanism of unwinding, the effect of DNA binding on the assembly state of the Rep protein was studied using small-zone gel filtration chromatography, chemical crosslinking of the protein, and indirectly by nitrocellulose filter binding. In the absence of DNA, Rep protein is a monomeric species of 73 kD up to a concentration of 8 μM, even in the presence of ATP, ADP-Mg^{2+}, or ATPγS-Mg^{2+}. However, upon binding ss oligodeoxynucleotides [$p(dT)_n$, n=12,14,16, 20], Rep protein forms a crosslinkable species with an apparent molecular weight (M_{app}) of 155±5 kD, which is consistent with a dimer. From the dimethylsuberimidate crosslinking studies, we show that the dimerization does not result from two Rep monomers bound contiguously to a single oligodeoxynucleotide for n<16. In addition, a duplex DNA in the form of a hairpin (16 bp duplex region) also induces dimerization of the Rep protein. Formation of the crosslinked Rep dimer increases its binding affinity for DNA. Based on equilibrium binding studies, we have determined that the Rep dimer has two non-equivalent DNA binding sites. The binding of one DNA molecule (D) to a Rep monomer (P) can induce the dimerization to form P_2D. The crosslinked Rep dimer is active in ATP hydrolysis and maintains its ability to unwind M13 RF DNA completely, hence we propose that the DNA-induced Rep dimer is the functionally active helicase. (Supported by NIH GM 30498).

Th-Pos106

Thermodynamics of Charged Oligopeptide-Nucleic Acid Interactions.

David P. Mascotti* and Timothy M. Lohman, Washington Univ. School of Medicine, Dept . of Biochemistry and Molecular Biophysics, St. Louis, MO 63110 and *Texas A&M Univ., College Station, TX 77843.

Stability of protein-nucleic acid complexes is the net result of several factors. One major factor for nearly all proteins and many other ligands which interact with nucleic acids is electrostatics and the resulting release of counterions associated with the nucleic acid. To examine the contribution of electrostatic effects to the stability of protein-nucleic acid complexes, we have measured the equilibrium binding affinities (K_{obs}) of a series of cationic peptides of the general type: B-W-B_p-NH_2 (where B = Lys or Arg, W = Trp and p = 1 to 8) to various ss- and ds-polynucleotides as functions of monovalent salt ([MX]), pH, and temperature.

$LogK_{obs}$ decreases linearly with increasing log[M^+] for all peptide-nucleic acid interactions studied, and the magnitudes of the slopes are proportional to the charge of the peptide (oligoarginines and oligolysines give identical slopes) (Mascotti and Lohman, *P.N.A.S. 87* (1990) 3142). The proportionality constant is higher for double-stranded DNA than for single stranded homopolynucleotides, reflecting the higher charge density of duplex nucleic acids. We have previously shown a negligible preferential anion interaction with these peptides, thus the derivative ($\partial logK_{obs}/\partial log[M^+]$) is primarily a measure of preferential cation release from the polynucleotide. Our thermodynamic analysis indicates that these salt effects are predominantly entropic in nature.

We find that the peptides are not required to be fully protonated for binding, based on the small $\Delta H°$ (< ±5 kcal/mole) and the form of the pH dependence of K_{obs}. From dissection of the thermodynamics of polynucleotide binding to a series of oligolysines containing one or two tryptophans as a function of the peptide length, most of this favorable $\Delta H°$ can be attributed to the interaction of the tryptophan residue with the polynucleotides. However, for interactions with poly(U), the favorable $\Delta H°$ due to tryptophan interaction is nearly compensated by an unfavorable $\Delta S°$, hence the tryptophan contribution to $\Delta G°$ is very small. For peptide interactions with poly(A) and poly(C), $\Delta H°$ becomes more positive with increasing peptide charge. Oligoarginines display a more favorable enthalpic contribution upon binding ss-polynucleotides relative to oligolysines, presumably due to hydrogen bonding between the arginine sidechains and the backbone phosphates. Systematic model studies such as these will facilitate interpretation of more complex protein-nucleic acid thermodynamics. (Supported by NIH GM39062)

Th-Pos107

ENERGETICS OF SUBUNIT INTERACTIONS IN BACTERIOPHAGE λ cI REPRESSOR: LINKAGE TO PROTONS, TEMPERATURE, AND KCl

Kenneth S. Koblan and Gary K. Ackers Department of Biochemistry and Molecular Biophysics, Washington University School of Medicine, St. Louis, MO 63108

Cooperative binding of the bacteriophage λ cI repressor dimer to specific DNA sites of the operator regions O_R and O_L controls the developmental state of the bacteriophage. A common feature of this and other gene regulatory systems is the linkage between reversible protein oligomerization and DNA binding. In this study, we have employed large zone analytical gel chromatography to determine the effects of proton activity, temperature and monovalent salt on the monomer-dimer assembly reaction of the λ cI repressor. We find a large negative enthalpy (ΔH) change for dimer formation at all conditions studied. There is a small proton linkage to the reaction in the acidic range and a large dependence on the monovalent salt concentration over the range studied (1-200 mM). These results suggest a specific ion binding event upon formation of the dimer interface. Implications of these findings to the mechanism of site specific DNA binding will be discussed.

Th-Pos108

TRANSCRIPTION TERMINATION FACTOR RHO FUNCTIONS AS A DIMER WHICH MUST RELEASE POLYNUCLEOTIDE COFACTOR DURING THE ATPase REACTION CYCLE

Steven E. Seifried, Yan Wang, and Peter H. von Hippel. Institute of Molecular Biology, University of Oregon, Eugene, OR 97403.

Transcription termination factor rho from *E. coli* has been shown to assemble as a trimer of dimers. Each dimer of identical protomers will function as an ATPase. The phosphohydrolase activity requires the occupation of a polynucleotide binding site on each monomer. Affinity for both cofactor sites in the dimer is determined by the base composition of the polymer; cytosines provide greatest free energy of binding, uracil provides moderate affinity, and purines do not contribute to binding. It has been stated that activation of the ATPase activity occurs if a 2' hydroxyl is contained within the nucleic acid bound in at least one of the adjacent cofactor sites.

ATPase functional assays with homopolymers, random copolymers, and designed oligonucleotides show that release of polymer from one of the two cofactor sites within the dimer is required for the continuation of the ATPase reaction cycle. Polymers of deoxycytosine can generate a low but significant ATPase rate. Competition experiments with ribo-polymers show the offrate of poly(dC) from a single polymer binding site to equal the measured poly(dC)-stimulated ATPase rate. Therefore the 2' hydroxyl of the ribose sugar increases the offrate of the polymer from an activated enzyme state. Additionally, base sequence can affect the offrate of an oligomer, and therefore the turnover rate of the ATPase cycle. The RNA bind-release cycle, driven by ATPase, is coupled to 3-D geometric elements to generate translocation of rho on nascent transcript.

Th-Pos109

ECORI ENDONUCLEASE BINDING TO 26-MERS RESULTS IN A CONFORMATIONAL CHANGE OF THE DUPLEX BEYOND THE BINDING SITE REGION. A. M. Bobst*, J. M. Rosenberg‡, and E. V. Bobst*, *Department of Chemistry, University of Cincinnati, Cincinnati, OH 45221, and ‡Department of Biological Sciences, University of Pittsburgh, PA 15260.

Deoxyuridine analogs spin labeled in position 5 with 5-atom tethered six- and five-membered nitroxides were enzymatically incorporated sequence specifically within 26-mers containing an EcoRI binding site. The spin labeled analogs are located symmetrically beyond the binding site. The labeled 26-mers with the structure

5'-CCACCCCCGCGAATTCGCGGGGGLGG
GGLGGGGGCGCTTAAGCGCCCCCACC-5'

have L-A base pairs either in position 3,24 as shown above, or positions 5,22 or 8,19. None of the EPR spectra of the above labeled 26-mers display Heisenberg spin exchange as is to be expected from the distance between the two labels in any of the three 26-mers. Also, the lineshape of the spectra of the uncomplexed 26-mers shows no L-A base pair position dependence. The spectra correspond, as reported earlier for the 5,22 L-A labeled 26-mer (FEBS Lett. 228, 33 [1988]), to spectra of polynucleotide duplexes with L-A base pairs incorporated at random. This further corroborates the motional model (Biochemistry 22, 5563 [1983]) which assumes that spin labels covalently attached to the C-5 position of dU with non-rigid tethers reflect local base dynamics, i.e., the spectra are not affected by the global dynamics of the labeled system. Saturation of the EcoRI binding site with stoichiometric amounts of EcoRI endonuclease in the absence of Mg^{2+} results in spectral changes which are L-A position dependent. Even though the formation of the 26-mer-EcoRI complex significantly increases the molecular mass of the spin labeled system, the EPR lineshape changes suggest that the L-A base pairs only reflect local structural and dynamic changes. Computer simulations of the spectra suggest that the probe motion is slightly reduced with L-A in position 8,19. However, only the probe geometry undergoes a change with L-A located in either positions 3,24 or 5,22. Thus, we present experimental evidence that the binding of EcoRI endonuclease to its binding site results in conformational distortions of the DNA extending beyond the binding site. Supported in part by NIH GM 27002.

Th-Pos110

ISOTOPIC EXCHANGE OF THE PURINE 8-CH GROUP AS A PROBE OF DNA RECOGNITION BY THE HELIX-TURN-HELIX MOTIF.

K. E. Reilly, R. Becka and G. J. Thomas, Jr., Div. Cell Biol. and Biophys., School of Basic Life Sciences, University of Missouri, Kansas City, MO 64110

Rates of deuterium exchange of purine 8-CH groups in DNA are determined by the local secondary structure and by interactions involving 7-N sites which line the major groove.[1] Raman optical multichannel analysis (ROMA) may be employed to differentiate exchange rates of adenine and guanine residues and to kinetically discriminate purines in inequivalent microenvironments of DNA.[2] We have refined and extended the ROMA method for applications to lambda operator recognition by the helix-turn-helix (HTH) motif of lambda repressor. The 8-CH exchange profile of the lambda operator O_R1 in aqueous solution has been obtained both in the absence of interacting protein, and in the presence of half-molar, equimolar and excess concentrations of the DNA-binding HTH domain (residues 1-102). The observed kinetics reveal participation of specific major groove sites of the cognate operator in binding by the HTH domain. The ROMA results extend structural studies of co-crystalline repressor-operator complexes by demonstrating specific binding of repressor to a recognition operator in aqueous solution. The Raman dynamic probe also complements equilibrium Raman studies and has the potential for application to other nucleic acid-protein complexes. It enables monitoring of purine-specific interactions in a biologically relevant medium without chemical modification of the complex or its constituents.

1. Benevides & Thomas, Biopolymers 24, 667 (1985); ibid. Biochemistry 27, 3868 (1988).
2. Lamba et al., Biopolymers 29, 1465 (1990).

Supported by NIH Grant AI18758.

Th-Pos111

RECOGNITION OF LAMBDA OPERATORS O_R1 AND O_R3 BY THE HELIX-TURN-HELIX MOTIF: INVESTIGATION IN SOLUTION BY LASER RAMAN SPECTROSCOPY.

J. M. Benevides, M. A. Weiss and G. J. Thomas, Jr., Div. Cell Biol. and Biophys., School of Basic Life Sciences, University of Missouri, Kansas City, MO 64110.

We describe laser Raman studies of lambda operator sites O_R1 and O_R3 and their interactions with the DNA-binding domain (helix-turn-helix, HTH) of lambda cI repressor. Spectra of the two operators exhibit significant differences in bands diagnostic of backbone torsions and in purine and pyrimidine ring modes sensitive to base-stacking configurations. The results reflect sequence-dependent variations in B-DNA structure probably originating at interstrand purine/purine steps which differ in the two recognition operators. Repressor binding, which involves hydrogen bond formation and hydrophobic contacts in the major groove, induces subtle changes in Raman bands of interacting DNA groups, including sequence-specific perturbations to backbone phosphodiester geometry at AT-rich domains, hydrophobic interaction at thymine 5-CH_3 groups and hydrogen bonding to guanine 7N and 6C=O acceptors along the major groove. Repressor binding also induces alterations of furanose ring pucker, yet within the C2'-endo family. Remarkably, these perturbations differ between the aqueous O_R1 and O_R3 complexes of repressor, indicating that HTH binding in solution determines the precise DNA conformation. As expected in ligand recognition, local differences are observed in the orientations and interactions of repressor side chains; but repressor secondary structure is not altered significantly. The results demonstrate distinguishable modes of interaction of the lambda repressor DNA-binding domain with operators O_R1 and O_R3 in aqueous solution. This application provides a prototype for future Raman studies of other DNA-binding motifs at physiological conditions.

Supported by NIH Grant AI11855.

Th-Pos112

UV LASER CROSSLINKING AS A PROBE OF SPECIFIC PROTEIN-DNA INTERACTIONS: E.M. Evertsz, W.L. Kubasek, R.G. Brennan and P. H. von Hippel. Inst. of Molecular Biology, U. of Oregon, Eugene, OR 97403, U.S.A.

UV laser crosslinking can be used to investigate structural and dynamic aspects of the conformations of the protein and nucleic acid components involved in specific protein-DNA interactions. The efficiency of crosslink formation reflects both the geometry of the contacts between specific functional groups within these species and the dynamics of the equilibria between conformations involving different binding contacts. As a model for "static" interactions of specific geometry we have examined the crosslinking efficiency of cro protein complexed with its specific DNA operator sequence, and have compared the results with those of an x-ray crystallographic study of the same system (Brennan et al., PNAS in press.). We find that cro protein can be crosslinked to its operator with ~ 17% efficiency by one 5 ns laser pulse at 266 nm, while the efficiency of crosslinking cro to a nonspecific DNA sequence of the same length is <1%. In contrast, E. coli cAMP-binding protein (CAP) crosslinks very inefficiently to its operator sequence (even less efficiently than to nonspecific DNA). The results of these experiments will be discussed in terms of the specific protein environments of the thymidine residues (which comprise the major sites of crosslinking under these conditions) within these specific and nonspecific complexes.

To calibrate the use of UV laser crosslinking as a probe of the dynamics of DNA-protein complexes, we also describe experiments on the protein (and DNA) concentration dependence of crosslinking efficiency between non-interacting proteins and DNA in solution. These experiments show that the half-life of the thymidine free radical formed by UV laser activation is < 0.5 μsec, and thus that crosslinks form only between species that are actually in intimate physical contact at the instant of irradiation.

Th-Pos113

BINDING OF d(pCGCGGATCCGCG) TO BamHI RESTRICTION ENDONUCLEASE STATICALLY AND DYNAMICALLY QUENCHES A SINGLE LIFETIME SPECIES. Jay R. Knutson*, Denise Porter*, and Preston Hensley†, *Laboratory of Cell Biology, NHLBI, NIH, Bethesda, MD., †Macromolecular Sciences Department, SmithKline Beecham Pharmaceuticals, King of Prussia, PA.

BamHI, a type II restriction endonuclease containing three trp, requires only Mg^{++} as a cofactor. It specifically cleaves double stranded DNA at the palindrome G*GATCC. Time-resolved and steady-state fluorescence were employed to characterize the binding of a DNA to the active site. Decay associated spectra (DAS) were obtained by global analysis of decay curves taken at 5 nm intervals from 310-450 nm with laser excitation at 293 nm. The DAS revealed a blue shifted, 1.8 ns species and a redder, 3.8 ns component. The former provided 35% of the intensity, the latter 65%. Addition of 10 mM $MgCl_2$ yielded DAS with unchanged lifetimes and a small redistribution of intensity (to 40%/60%). A tight complex with substrate altered only the long lifetime (reduced 15% to 3.3 ns). The intensity of this DAS was reduced 30%, however, implying both static and dynamic effects in this component-specific quench. Time resolved anisotropy of the native, Mg^{++}, and DNA-complexed states was acceptably fit with a single correlation time, ϕ (little segmental motion seen). The average ϕ_s were 22, 22 and 20 ns, respectively. The lack of increase in the last instance suggests an altered shape. KI quenching results indicate a greater K_{SV} for the redder component, suggesting one trp is solvent exposed. (We thank I. Schildkraut and Wm Jack of New England Biolabs for providing Bam HI).

Th-Pos114

SYMMETRY OF DNA BEND IN cAMP RECEPTOR PROTEIN-DNA COMPLEX

Tomasz Heyduk and James C. Lee
University of Texas Medical Branch, Department of Human Biological Chemistry and Genetics, Galveston, Tx 77550

Protein induced DNA bending is one of the distinctive features of the complex formed between E. coli cAMP receptor protein (CRP) and its specific site on DNA. It has been proposed that the induced bend is asymmetric and plays an important role in the mechanism of activating the transcription by CRP.
In this study the symmetry of CRP induced DNA bend was monitored by fluorescence resonance energy transfer (FRET) measurements. A 26 bp DNA fragment was labeled with fluorescent acceptor at the 5' end either upstream or downstream from the binding site. Distances between protein trp residues and the acceptors on these two DNA samples in the protein-DNA complex were compared at several salt concentrations. Under all conditions within experimental error the distances between the upstream or downstream end of DNA and CRP are the same. This distance is salt dependent therefore the structure of CRP-DNA complex depends on salt concentration as well. The extent of DNA bend was estimated by measuring the change in FRET between fluorescent donor and acceptor attached to the ends of the same DNA molecule upon formation of a complex with CRP. The measured end to end distance changes from about 86 Å in free DNA to about 75 Å in CRP-DNA complex. Such a change corresponds to a CRP induced DNA bent of about 48 Å in radius.

Th-Pos115

SYNTHESIS AND PURIFICATION OF FLUORESCENTLY LABELED OLIGONUCLEOTIDES. D.J. Scothorn, C.E. Cobb, W.L. Taylor, J.M. Beechem, & A.H. Beth, Molecular Physiology & Biophysics, Vanderbilt Univ., Nashville, TN 37232.

Fluorescence spectroscopy provides a highly sensitive method for observing and quantitating interactions between DNA and proteins. For such studies, it is often desirable to end-label DNA with an exogenous fluorophore which will "report" binding interactions and/or serve as a defined marker for measuring intermolecular distances in a DNA-protein complex. Several procedures have been published for end-labeling oligonucleotides and some methods for HPLC purification have been reported. However, labeling often involves multi-step synthetic procedures and if the target oligonucleotide is >50 bp in length, purification procedures are tedious and provide comparatively low yields. In the present work we report a single-step labeling procedure which can be adapted to produce highly purified oligonucleotides of essentially any desired length. In this method, the 5′ terminal phosphate of a synthetic 15 base oligonucleotide was specifically labeled with dansyl cadaverine using 1-ethyl-3,3-dimethylaminopropyl carbodiimide (EDC) as the coupling agent (Chu et al., (1983) Nucleic Acids Res. 11, 6513). The labeled 15-mer was readily purified by RP-HPLC in high yield. The labeled 15-mer was then annealed to a complementary unlabeled 60-mer corresponding to the internal control region for Xenopus transcription factor IIIA (TFIIIA) and then elongated with Klenow fragment to form a specifically labeled double-stranded 60 bp oligo corresponding to bases +40 to +99 of the 5S RNA gene. Dansyl cadaverine was chosen for use in initial studies since it contains a single primary amino group for coupling to the 5′ phosphate of the 15-mer and the fluorescence properties of the dansyl moiety are appropriate for energy transfer studies, both as an acceptor from intrinsic Trp residues and as a donor for extrinsic fluorescein labels. However, any fluorophore having an aliphatic primary amino group and which does not react with EDC can be coupled to a phosphorylated oligo by this method.

Th-Pos116

PHOSPHORESCENCE AND OPTICALLY DETECTED MAGNETIC RESONANCE STUDIES OF QUINOLINE PEPTIDE-NUCLEIC ACID COMPLEXES

Thomas V. Alfredson, Alan Lim, and August H. Maki, University of California, Dept. of Chemistry, Davis, California U.S.A. 95616
and
Michael J. Waring, Cambridge University, Dept. of Pharmacology, Tennis Court Road, Cambridge, U.K.

Low temperature phosphorescence and optical detection of triplet state magnetic resonance (ODMR) spectroscopic investigations of the biosynthetic quinoline analogues of echinomycin, a bisintercalating quinoxaline antibiotic (1), have been carried out in order to examine the role of aromatic stacking interactions of the peptide chromophores upon binding to nucleic acids. Both the monoquinoline analogue (1QN), which contains one quinoxaline moiety and one quinoline moiety attached to a cyclic octadepsipeptide, and the bisquinoline analogue (2QN), which contains two quinoline moieties attached to the peptide ring, have been examined in complexes with synthetic and natural DNAs. Spectroscopically observed perturbations of the triplet state properties of these peptides such as the phosphorescence emission spectrum and lifetime, ODMR spectrum, zero-field splitting (zfs) energies, and triplet sublevel kinetics were investigated upon peptide binding to polymeric DNAs and model duplex oligonucleotides. For echinomycin and 2QN, the reduction in zfs D parameter upon binding to polymeric DNA targets correlates with previously measured binding constants (2) and, furthermore, plots linearly with the $-\Delta G^{\circ}$ values of these complexes. The zfs D-value reduction of the heterocycle thus can be interpreted as a measure of the contribution of the aromatic stacking energy to the stability of the peptide-DNA complex. Further results bearing on the dynamics of the quinoline triplet state of these peptides will be presented.

(1) Alfredson, T.V. and Maki, A.H., *Biochemistry, 29* (1990) 9052-9064.
(2) Fox, K.R., Gauvreau, D., Goodwin, D.C., and Waring, M.J., *Biol. J., 191* (1980) 729-747.

Th-Pos117

FLUORESCENCE STUDIES OF ENDONUCLEASE V: A MODEL SYSTEM FOR TRYPTOPHAN-DNA AND PROTEIN-DNA INTERACTIONS. Katherine A. Atkins[¶], R. Stephen Lloyd[¶], and Joseph M. Beechem[§], Vanderbilt University, Depts. of Biochemistry[¶] and Molecular Physiology and Biophysics[§], Nashville TN 37232.

T4 Endonuclease V is a 16 kD DNA repair enzyme that excises ultraviolet light induced pyrimidine dimers from DNA. EndoV has a single tryptophan and recent crystallographic work reveals that the tryptophan interacts directly with DNA bases of the major groove [Morikawa et.al., 10th Intnl. Biophys. Congress, P2.2.95, 1990]. Thus, EndoV represents an ideal case for examining the interaction of tryptophan with DNA. The tryptophan fluorescence was found to be greater than 90 percent quenched upon addition of DNA to EndoV. This quenching was used to measure the binding of Endo V to dimer-containing and non-target DNA. There is a slight blue shift upon binding to DNA. Heat denaturation profiles for this protein were very unusual, in that upon unfolding, the tryptophan emission spectra shifts dramatically to the blue (λ_{em} 360nm ⇒ 340nm). Thermal unfolding studies in the presence of DNA yield the same blue shift, although with an abrupt increase in the fluorescence at the transition temperature caused by the release of the protein from the DNA. The unfolding temperature for the protein-DNA complex was found to be approximately five degrees higher than for the protein alone. Time-resolved fluorescence experiments are being performed to further examine these transitions. Stopped-flow kinetic studies are also being performed to determine the kinetics of the DNA binding reaction and of the folding transition. From these studies, the role of tryptophan intercalation in the energetics and biological function of this DNA repair enzyme are being investigated. KAA is supported by an NSF graduate fellowship. JMB is supported by the Lucille P. Markey charitable trust. JMB is a L. P. Markey scholar in biomedical science.

Th-Pos118

FLUORESCENCE STUDIES OF THE SINGLE TRYPTOPHAN CONTAINING PROTEIN TRANSCRIPTION FACTOR IID (TFIID).
Gina M. Perez Howard, P. Anthony Weil, Joseph M. Beechem, Vanderbilt University, Dept. of Molecular Physiology and Biophysics, Nashville TN 37232.

TFIID is a eukaryotic 16 kD protein involved in the polymerase II transcription process and represents the very first protein (of a multi-protein complex) to bind DNA for transcription. Binding occurs at the TATA box, just upstream of the startpoint. The fluorescence properties of TFIID are being examined, in hopes of establishing a sensitive method to quickly monitor binding, and also to determine the structural changes induced in both the protein and DNA upon complex formation. The fluorescence emission spectra of the protein in solution is very blue shifted (λ_{max} = 325nm). Upon binding to DNA, the fluorescence intensity is quenched approximately 70% with a small red shift of 5nm. The kinetics of the DNA binding process have been examined and are highly complex. There is a large segment of the fluorescence change which occurs in the sub-second time scale, as well as much slower transitions which are very temperature dependent, rangeing in time-scale from as short as 5 minutes at 37°C, to as long as 12 hours at 4°C. At temperatures between 4 and 15°C, there is an initial period where the fluorescence intensity actually *increases* before becoming quenched. At temperatures above 15°C this process occurs too fast, and is no longer observable with standard mixing experiments. Stopped-flow binding studies are now being performed in order to characterize the intial fast binding reation. There is a very large shift in the emission spectra upon either thermal or guanidine unfolding (λ_{max} 325 ⇒ 360nm). This exceptionally large shift allows very subtle structural transitions along the folding pathway to be observed. Quenching studies (using KI) reveal that in the absence of DNA, quenching yields linear Stern-Volmer plots. However, upon binding to DNA two very distinct populations of tryptophans are observed.

JMB is a L. P. Markey scholar in biomedical science.

Th-Pos119

THE SITE SELECTIVITY OF ANTHRACYCLINE DRUGS
Camille J. Roche, Donald M. Crothers, Gary A. Sulukowski, David Berkowitz Samuel J. Danishefsky; Chemistry Department, Yale University, New Haven, CT., 06511.

Daunomycin is an antitumor drug that has been used for the treatment of leukemia. Its antitumor activity has been correlated with binding to DNA and interferring with DNA and/or RNA synthesis. The site selectivity of the drug on a random sequence DNA is not fully known. To clarify this issue, a series of oligonucleotides were synthesized that contain specific binding sites for daunomycin. The binding of daunomycin to these oligonucleotides was characterized by optical methods. In addition, daunomycin analogues were synthesized that differed in the substituents on the sugar ring. When these analogues were compared with daunomycin, it was found that the sugar ring conferred some specificity to the binding and altered the order of preference for the series of oligonucleotides. The order of preference implies that the sugar aids in the binding, possibly by interactions in the minor groove. These results will be discussed.

Th-Pos120

INTERACTION OF HMG2 SUBFRACTIONS WITH DNA
Azra Rabbani,and Soheila Kashanian.Institute of Biochemistry and Biophysics, University of Tehran, Tehran, IRAN

High mobility group (HMG) proteins are a group of non-histone chromosomal proteins designated as HMG1, HMG2, HMG14, and HMG17. Calf thymus HMG2 consists of at least four subfractions which differ in their isoelectric points. Total HMG2 binds to DNA and gives a soluble complex. In this study the interactions of four HMG2 subfractions defined as A,B,C,and D with DNA was investigated. The fractions were purified on CM Sephadex C25 column pH 8.8 and the DNA protein complexes were analysed by thermal denaturation (Tm) studies. Results obtained from derivative melting profiles showed that fractions did not behave similarly. HMG2A and C did not change the Tm of DNA at any ratios used. HMG2D was the only subfraction capable of changing the melting profile of DNA in a concentration dependent manner. At low ratios (1:0.5) the complex underwent a transition below the temperature at which DNA alone melts but at higher concentration (1:4) it stabilized DNA against thermal denaturation. HNG2B differed completely from other subfractions. It made an insoluable complex with DNA even at very low concentrations. Its binding to DNA resembled to the binding of histones to DNA. The results suggest that subfraction D of HMG2 is a helix stabilizing-destabilizing protein and together with subfraction B may play an important role in genome structure and function.

Th-Pos121

STRUCTURE-FUNCTION RELATIONSHIPS AND DIPHTHERIA TOXIN NUCLEASE ACTIVITY.
Donald G. Lewis, Stephen L. Lessnick, Jeffrey B. Lyczak, Lawrence T. Nakamura and Bernadine J. Wisnieski (Intro. by Can Bruce), Department of Microbiology and Molecular Genetics, University of California, Los Angeles, CA 90024

The nuclease active site of diphtheria toxin (DTx) appears to be distinct from the site at which NAD binds and ADP-ribosylation of elongation factor 2 (EF-2) occurs. Because both activities are associated with the A domain of DTx, the question of the location of a second catalytic site needs to be addressed. Structure-function studies thus far support the findings [Science 246,1165 (1989)] that led us to propose an intrinsic nuclease activity. New data indicate the co-elution of nuclease activity, ADPr-transferase activity and toxin during anion-exchange chromatography. Recently we have begun to assess the basis of the divalent cation requirement of DTx nuclease activity. In addition to exploring the effects of divalent cations on structure by intrinsic fluorescence, ESR, and other structural assays, we have initiated studies to examine toxin-DNA interactions with the goal of gaining some insight into the location of the DNA binding site and the mechanism of cleavage. The results of these studies will be presented with a discussion of toxin structure-function relationships and biological activity. [Supported by NIH Grant GM22240; S.L.L. held a Short Term Training Program Grant for Excellence in Research, UCLA School of Medicine, Office of the Dean]

Th-Pos122

INSIGHT INTO SPECIFICITY AND UNCOATING FROM INVESTIGATIONS OF THE INTERACTION OF THE AVIAN RETROVIRAL NUCLEOCAPSID PROTEIN WITH NUCLEIC ACIDS. Joyce E. Jentoft, Josephine Secnik, & Qi Wang. Department of Biochemistry, Case Western Reserve University, Cleveland, OH 44106.

Retroviral nucleocapsid proteins (NC) are small, multi-functional RNA binding proteins. As the isolated protein the NC apparently dissociates from the RNA before the transcription complex associates with the nuclear membrane, yet it stimulates the first stage of reverse transcription; within the virion it performs a histone-like packaging function. These varied functions have been characterized using fluorescence spectroscopy. Mononucleotide binding was studied by displacement and subsequent quenching of the fluorescence of the extrinsic probe bis-ANS. Mononucleotides displaced bis-ANS with a K_{app} of 10^{-6} M, essentially independent of base composition, as expected for the histone-like, non-specific binding activity of NC. Unexpectedly, no difference in binding was observed for, e. g., AMP and dAMP, suggesting that any ability the NC has to distinguish between RNA and DNA must be based on recognition of different *structural* forms. Consequently, polynucleic acid binding was studied, by following the increase in anisotropy of the intrinsic fluorescence of NC. Single stranded poly(A) and poly(dA) were found to bind more tightly to NC than double stranded poly(rA:rU) and poly(dG:dC), indicating that the NC binding site selectivley accommodates single stranded nucleic acids. A mechanism for dissociation of the NC-RNA complex is suggested by the observation that subcellular concentrations of ATP are capable of dissociating the NC-poly(A) complex. (Supported by GM 36948 and AR 20618.)

Th-Pos123

DETERMINATION OF THE ROLE OF THE SINGLE PHOSPHORYLATION ON THE NUCLEOCAPSID PROTEIN OF AVIAN RETROVIRUS. Craig A. Gelfand, Qi Wang, and Joyce E. Jentoft. Department of Biochemistry, Case Western Reserve University, Cleveland, OH 44106.

Structural and functional comparisons have been made between the nucleocapsid protein (NC) of avian myeloblastosis virus and the wild-type recombinant NC. The viral form of AMV NC is phosphorylated at Ser 40, a modification that is not present on the recombinant protein. Structural stability is monitored from the circular dichroism and the intrinsic fluorescence of NC as a function of urea concentration. The function of the proteins is assessed by following the anisotropy of the intrinsic fluorescence of NC as a function of added long chain nucleic acids. Mononucleotide binding can be similarly evaluated by monitoring the loss of anisotropy in competition experiments with long chain nucleic acids. Comparison of the two NC forms is a prerequisite for future studies of recombinant single amino acid mutant forms, which will similarly lack the phosphate. The structural and functional advantages, if any, of the phosphorylation are of particular interest since very few retroviral species bear this NC modification. (Supported by grants GM 36948 and AR 20618.)

Th-Pos124

THE USE OF BINDING SITE NEIGHBOR-EFFECT PARAMETERS TO EVALUATE THE INTERACTIONS OF LIGANDS WITH A LINEAR LATTICE. A. R. Wolfe & T. Meehan, Dept. of Pharmacy, UCSF, San Francisco, CA 94143-0446. A method for modelling ligand-DNA binding has been developed involving binding site "neighbor-effect" parameter(s) (NEPs), which are statistical analogues of cooperativity parameters. Binding site overlap and cooperativity between adjacent bound ligands are taken into account. This allows the conditional probability approach of McGhee & von Hippel (JMB, **86**, 469, 1974) to be extended from the case of symmetric ligands to more complex cases involving asymmetric ligands on isotropic and anisotropic lattices. The general equation for the isotherm is $\nu/L_F = S_F K_{\bar{F}}$, where ν is the ratio of bound ligands to lattice residues, L_F is the free ligand concentration, S_F is the fraction of binding sites that are free, and $K_{\bar{F}}$ is the association constant of the average free site. The neighbors of a site are the moieties adjacent to its ends. For symmetric ligands there is one NEP (ε). ε is the ratio, at a given ν, of the average binding affinity of a free site when the status (bound or free) of one of its neighboring lattice residues is *unspecified* (left to chance) to the affinity when this neighbor is *free*, holding the site's other neighbor constant. $K_{\bar{F}}$ is $K_I\,\varepsilon^2$, where K_I is the affinity of an isolated site. For a site n residues long, S_F is $f\,ff^{n-1}$, where $f = 1-n\nu$ is the fraction of residues that are free and ff is the probability that a free residue is bordered on a given side by another free residue. ff is $1/(1+\chi/\varepsilon)$, where χ is ν/f, ε is $(1-\chi+[(1-\chi)^2+4\chi\omega]^{1/2})/2$, and ω is the cooperativity parameter. ε varies from one to ω as ν goes from zero to saturation. Binding of asymmetric ligands to an isotropic lattice is described by three ω's and two NEPs. The last case involves four ω's, two K_I's, four NEPs, and a bound ligand orientation parameter (q); also, n may differ depending on the orientation of the ligand relative to the lattice. Values for the NEPs and q are obtained by solving five simultaneous equations.

Th-Pos125

NEW DATA ON THE CONFORMATION OF FREE AND BOUND NUCLEOSIDES 5'-TRIPHOSPHATES OBTAINED BY ROESY EXPERIMENTS.

ANDRE François, CHAMPEIL Philippe & NEUMANN Jean-Michel.

Dpt de Biologie Cellulaire et Moléculaire, Centre d'Etudes Nucléaires de Saclay, 91191 Gif-sur-Yvette Cedex, France.

Recent NMR techniques can provide new data about intramolecular interactions of small biological compounds, and solute concentrations can be significantly decreased in order to minimize the influence of intermolecular interactions. We show in this study that ROESY experiments (2D nuclear Overhauser enhancement in the rotating frame) give a precise conformational description of various nucleotides such as ADP, ATP, AMPPCP and AMPPNP, commonly used as ATPase substrates. Our data indicate that, whereas ADP exhibits a conformational flexibility similar to that known for the nucleosides 5'-monophosphates (i.e. similar proportions of the *syn* and *anti* domain), a particular base conformation is favored when a third phosphate group is present: ***high anti*** orientations are predominant and are accompanied by a folding of the triphosphate chain towards the base. Such conformational features are observed whatever the presence or absence of magnesium ions and the base-phosphate stacking is experimentally related to intramolecular interactions [André et al., *J. Am. Chem. Soc.* 112, 6784-6789 (1990)].

Such a feature of adenylyl nucleotides is meaningful as regards their conformation when bound to an enzymatic active site. For ATP bound to sarcoplasmic reticulum Ca^{++}-ATPase, ROESY spectra indicate that *anti* base orientations are preferred to ***high-anti*** conformations and that the triphosphate chain is predominantly extended. This could suggest that the opening of the triphosphate chain of ATP is involved in related enzymatic mechanisms.